Properties of Paleogene Clays

TNO Publiek › TNO 2025 R12312
21 November 2025

Energy & Materials Transition
www.tno.nl
+31 88 866 42 56
info@tno.nl

TNO 2025 R12312 – 21 November 2025

Properties of Paleogene Clays

Author(s)	S. Nelskamp, A. Pascarella, A. Kaliar, S. Aksay, E. Peters, J. Wollenweber
Classification report	TNO Publiek
Title	TNO Publiek
Report text	TNO Publiek
Number of pages	103
Number of appendices	8
Sponsor	Ministerie van Infrastructuur en Waterstaat
Project name	COVRA; Characterisation Paleogene Clays
Project number	060.65900

Samenvatting

Dit rapport[1] biedt een uitgebreide regionale screening van Paleogene klei-eenheden in de Nederlandse ondergrond, in de context van hun mogelijke geschiktheid voor de geologische berging van radioactief afval. De studie wordt gecoördineerd door COVRA, in opdracht van het Ministerie van Infrastructuur en Waterstaat. Het primaire doel is het actualiseren en integreren van geologische, mineralogische en petrofysische data om de afsluitende werking (hydraulische weerstand) en de permeabiliteit van de belangrijkste Paleogene klei-eenheden te beoordelen. De studie wijst geen specifieke bergingslocaties aan, maar belicht de belangrijkste fysisch-chemische processen en klei eigenschappen die relevant kunnen zijn voor toekomstige locatiekeuze.

De belangrijkste resultaten van het onderzoek zijn:

- Herziene kaarten van de diepte en dikte van alle belangrijke Paleogene klei-eenheden (de Laagpakketen van Wintelre, Boom, Asse, Ieper, Engelschhoek, De Wijk en Liessel).
- Een petrofysische en mineralogische karakterisering op basis van geïntegreerde boorgat- en kerngegevens. Uit deze analyses blijkt dat een hoog smectietgehalte (>50% van de kleifractie) en een hoog schalie volume (Vshale >0,8) positieve indicatoren zijn voor lage permeabiliteit en een goede hydraulische weerstand. Porositeit en permeabiliteit variëren daarnaast met diepte, mineralogie en facies. Diepere en dikkere kleipakketten vertonen over het algemeen een lagere permeabiliteit, wat gunstig is voor de hydraulische weerstand. Daarentegen zijn glauconiet-rijke intervallen minder gunstig vanwege de potentieel grotere korrelgrootte en daarmee verhoogde permeabiliteit.
- Een analyse van aanwezige geologische breuken en scheuren op basis van de interpretatie van seismische data. In deze analyse zijn op meerdere schaalniveaus breuken en scheuren geïdentificeerd, waaronder polygonale breuken die veel voorkomen in fijnkorrelige sedimenten. Polygonale breuken zijn kleinschalige breuken die een gerangschikt zijn in polygonen (lengte van 1-2 km met een verzet van 10-70 m). Hoewel deze lokaal de verticale permeabiliteit kunnen verhogen, blijken dikke kleipakketten (>100 m) met dergelijke structuren in bestaande gasvelden nog steeds effectief als afdichting. De afwezigheid van grootschalige doorsnijdende breuken is positief voor de effectiviteit van de klei als afdekkende laag.
- Een regionale beoordeling van de hydraulische weerstand, waarbij overdrukdata, de aanwezigheid van olie- en gasvelden en “gas shows” (aanwezigheid van gas boven de achtergrondwaarde gezien tijdens het boren), en incidenten tijdens het boren als indirect bewijs zijn gebruikt. Goede indicatoren voor een lage permeabiliteit zijn overdruk onder of binnen de kleilagen, de aanwezigheid van gasvelden onder een kleilaag, en de aanwezigheid van zwellende, plastische kleien. Daarentegen wijzen gas shows die over een grotere diepte optreden op lokale heterogeniteit en de noodzaak van zorgvuldige locatie-specifieke beoordeling.

[1] Deze samenvatting is gemaakt met hulp van CoPilot van Microsoft en door de auteurs gecontroleerd op juistheid en compleetheid.

De studie toont aan dat meerdere factoren gecombineerd moeten worden om de geschiktheid van een locatie te evalueren daar geen enkele parameter op zichzelf de geschiktheid garandeert. Polygonale breuken vormen een onzekerheidsfactor bij de beoordeling van de afsluitcapaciteit vanwege de onzekerheid over hun invloed op de hydraulische weerstand. In het algemeen varieert de geschiktheid van de Paleogene kleien aanzienlijk binnen Nederland, als gevolg van hun afzettings- en diagenetische geschiedenis en lokale faciesverschillen. Nieuw verkregen data uit lopende projecten, zoals het SCAN-boorprogramma, kunnen relevante informatie bieden voor toekomstig onderzoek. De Paleogene kleien in de Nederlandse ondergrond tonen veelbelovende eigenschappen voor het langdurig insluiten van radioactief afval, maar locatie-specifieke evaluaties op basis van alle van belang zijnde processen en eigenschappen zijn essentieel. Voortgaande gegevensverzameling en integratie daarvan met bestaande gegevens draagt bij aan het verkleinen van onzekerheden, en daarmee aan het ondersteunen van besluitvorming binnen de nationale strategieën voor radioactief afvalbeheer.

Summary

The report[2] provides a comprehensive regional screening of Paleogene clay units in the Dutch subsurface, in the context of their potential suitability for the geological disposal of radioactive waste. The study is coordinated by COVRA, commissioned by the Ministry of Infrastructure and Water Management. The primary goal is to update and integrate geological, mineralogical, and petrophysical data to assess the sealing capacity and permeability of key Paleogene clay units. The study does not identify specific disposal sites but highlights the main physical and chemical processes and clay properties that could be relevant for a future site selection process.

The main results of the study consist of:

- Updated maps of the depth and thickness of all major Paleogene clay units (Wintelre, Boom, Asse, Ieper, Engelschhoek, De Wijk, Liessel Members).
- A petrophysical and mineralogical characterisation based on integrated well log and core data analyses. These analyses show that high smectite content (>50% of clay fraction) and high shale volume (Vshale > 0.8) are positive indicators for low permeability and good sealing capacity. In addition, porosity and permeability vary with depth, mineralogy, and facies. Deeper and thicker clay intervals generally show lower permeability, which can be favourable for containment. On the other hand, Glauconite-rich intervals are less favourable due to potentially larger grain size and therefore the possibility of increased permeability.
- An analysis of the geological faults and fractures based on the interpretation of seismic data. Faults and fractures were identified at multiple scales, including polygonal faults, which are small-scale (1-2 km in length with a throw of 10-70 m) features that are common in fine-grained sediments. While these can locally increase vertical permeability, thick clay intervals (>100 m) with such features are effective as seals in existing gas fields. However, the absence of large-scale through-going faults is a positive indicator for containment.
- A regional assessment of the sealing capacity in which overpressure data, the presence of hydrocarbon fields, gas shows (presence of gas recorded during drilling above the background level), and drilling event records were used as indirect evidence for sealing capacity. Indicators for good sealing capacity and low permeability are overpressure below or within the clay units, the presence of gas fields below the clays units, or the widespread identification of swelling clays. However, stacked gas shows indicate local heterogeneity and the need for careful site-specific assessment.

The study shows that multiple characteristics need to be combined to assess the suitability for the disposal of radioactive waste, since no single parameters guarantees the required characteristics. The presence of polygonal faults is still an uncertain factor when assessing sealing capacity. In general, the suitability of the Paleogene clays varies significantly across the Netherlands due to their depositional and diagenetic history and local facies changes. Newly acquired data from ongoing projects such as the SCAN drilling program can provide relevant data for future studies. The Paleogene clays in the Dutch subsurface present

[2] This summary was written with the help of CoPilot from Microsoft and cross-checked for correctness and completeness by the authors.

promising characteristics for long-term radioactive waste containment, but site-specific, multi-parameter assessments are essential. Continued data acquisition and integration will further reduce uncertainties and support robust decision-making for national waste management strategies.

Contents

1 Introduction

1.1 Aim of the study and framing

The decision-making process of the Dutch government on the final disposal of radioactive waste foresees an assessment of different potential geological disposal options. These potentially include Paleogene clay units and salt deposits (COPERA program, 2020-2025). Part and an initial step of this assessment is the collection of new geoscientific information and integration and consolidation of already available data to address the feasibility of the disposal of radioactive waste. For this reason investigations of these geological units has been conducted, coordinated by COVRA, which is the organisation with the practical responsibility of handling Dutch radioactive waste, including the collecting, processing and disposal of all radioactive waste in the Netherlands. This work received funding from the Ministry of Infrastructure and Water Management.

The results of this study will provide an update of geological, mineralogical and petrophysical information on Paleogene clay units in the Dutch subsurface. The main focus is on the Wintelre Member of the Veldhoven Formation (formerly Veldhoven Clay Member), The Boom Member of the Rupel Formation (formerly Boom Clay Member or Rupel Clay Member), The Asse Member, Ieper Member, Engelschhoek Member (formerly Dongen Clay Member), and De Wijk Member (formerly Basal Dongen Tuffite Member) of the Dongen Formation, and the Liessel Member (formerly Landen Clay Member) of the Landen Formation. Previous studies looking at the Paleogene units for disposal potential either focussed mainly on the Boom Member (OPERA, 2010-2017, Verhoef et al. 2017) or merit an update (CORA, 1995-2001, Commissie Opberging Radioactief Afval, 2001).

The aim of the study is a regional screening of these Paleogene Clay members, focussing on processes influencing sealing capacity and permeability. The identification of these processes is relevant for the safety of radioactive waste disposal, limiting fluid flow through, and out of the potential disposal units. Regional depositional trends influencing mineralogy, fluid flow and large-scale diagenesis as well as burial-related processes can be identified using publicly available information such as well logs, seismic data, core measurements, fluid composition and pressure as well as drilling incidents. The results of this study do not aim at pinpointing a suitable location for a disposal facility but rather highlight the main physical and/or chemical processes that need to be taken into account when looking for favourable geological properties and -units in the future.

The following topics are addressed in this study:

- Section 2: Maps of the depth and thickness of the listed Paleogene clay units are updated based on well data.
- Section 3: The petrophysical logs of a selection of wells, core measurements and XRD data are studied for clay content, mineralogical composition, porosity and permeability.
- Section 4: For three case study areas, an analysis of seismic data is performed to better understand faults in clay. The three case study area are selected based on availability of seismic data and presence of oil or gas fields which have a Paleogene clay seal; they are not chosen because they seem suited as potential disposal areas.

- Section 5: Analysis of regional data from previous studies which provide information on sealing behaviour of clays such as overpressure, presence of oil and gas and drilling events.
- Section 6 and 7: Discussion of the findings and recommendations

Before these topics are addressed, the Paleogene clays are introduced and previous work is briefly summarised.

1.2 Geological setting Paleogene clays

In the following part the geological setting of the Paleogene clays is described from the older/deeper units towards the younger/shallower units. The descriptions are to a large part based on the descriptions published in the Stratigraphic Nomenclature of the Netherland (TNO-GDN 2025[3]) as well as the Paleogene – Neogene chapter of the Geology of the Netherlands (Munsterman et al. 2025).

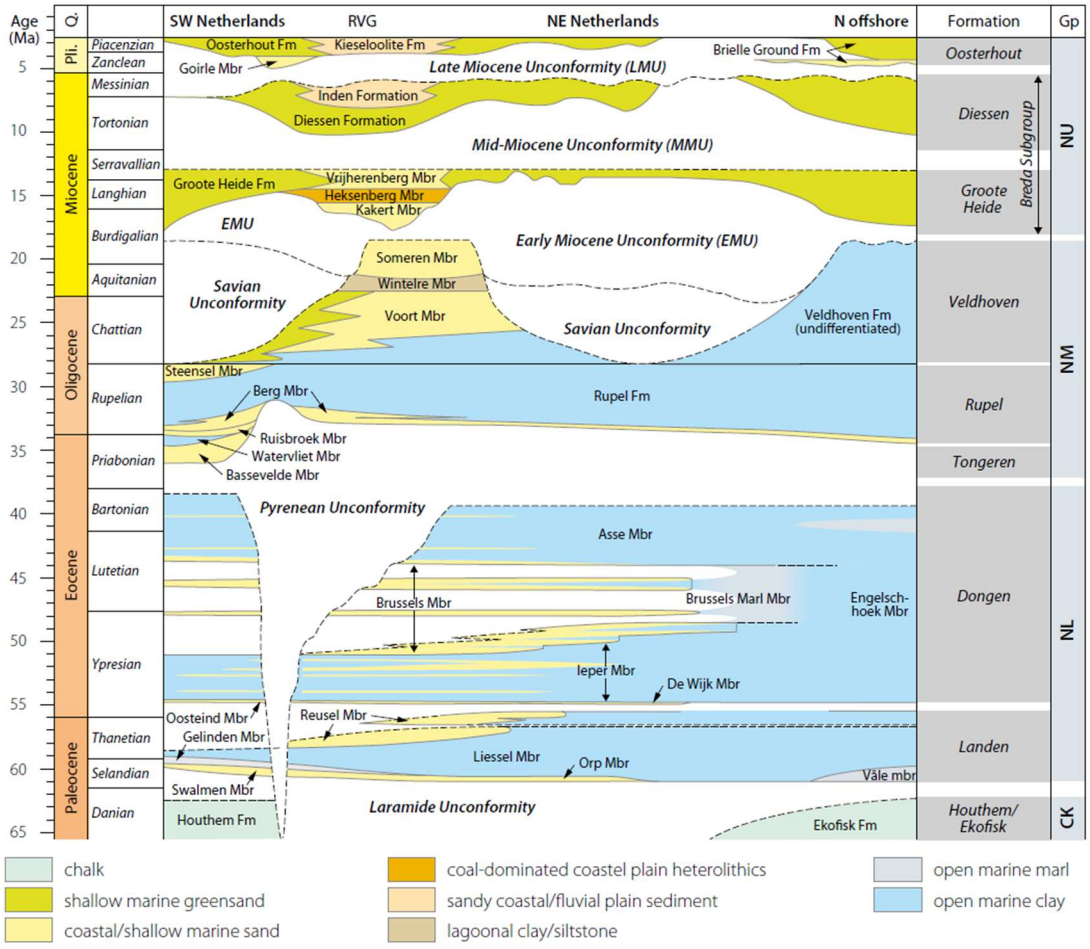

Figure 1.1 Stratigraphic chart, Geology of the Netherlands (Munsterman et al. 2025)

The Paleogene clay sediments were deposited in the North Sea Basin at the boundary between land and sea with the coastal line mainly located in the southern and southwestern part of the Netherlands. The shift of the coastal line was controlled by the interaction between tectonic and climatic processes as well as sediment supply, influencing

[3] https://www.dinoloket.nl/en/stratigraphic-nomenclature

the sedimentary facies of the deposits. The North Sea Basin developed as a post-rift thermal sag basin, deep marine sediments dominating during the early Paleogene. By the late Paleogene to Miocene the basin shallowed, resulting in the deposition of mostly shallow marine to coastal sediments (Figure 1.1).

1.2.1 Liessel Member

The Liessel Member, formerly known as the Landen Clay Member, is part of the Landen Formation of Late Paleocene (Thanetian) age. It consists of generally dark green, hard, flaky clay with high glauconite content with additions of pyrite and mica. At the base of the unit it contains more carbonate. In the south of the Netherlands, close to the paleo-coast line as well as close to other structural highs the unit is more sandy to silty and can also act as an aquifer. It was deposited in an open marine environment and is present in most of the Dutch on- and offshore.

1.2.2 De Wijk Member

The De Wijk Member, formerly known as Basal Dongen Tuffite Member, is the lowermost unit of the Dongen Formation of early Eocene (Ypresian) age. It consist of tuffaceous clay and silt alternating with dark-grey and red-brown clay. Volcanic ashes from magmatic activity related to the opening of the North Atlantic Ocean have also been identified. The more silty areas can also act as aquifers with medium to good permeability. It was deposited in marine conditions and is present in the northern onshore as well as the offshore of the Netherlands.

1.2.3 Ieper Member

The Ieper Member is of early Eocene (Ypresian) age and consists of dark-grey, green and brown, slightly calcareous clays with intercalated glauconitic sands towards the top. It shows significant regional and horizontal differences in composition and can be roughly subdivided into two parts. The lower part contains pyrite and is not calcareous while the upper part is usually more sandy and calcareous and contains glauconite. Close to the coast line the unit is generally more silty to sandy. It was deposited in an open marine environment and is present in most of the Dutch on- and offshore. The depositional thickness is strongly influenced by (salt)-tectonic processes in the northern part of the Netherlands.

1.2.4 Asse Member

The Asse Member is of middle to late Eocene (Lutetian to Bartonian) age and consists of dark green-grey to blue-grey, plastic clay. The upper part as well as the area close to the coast line of the formation is more sandy to very sandy. The unit was deposited in an open-marine shallow water environment and is present in most of the Dutch on- and offshore with the exception of the area of the Jurassic rift basins (WNB, CNB, RVG and BFB) due to uplift and erosion during the Pyrenean inversion.

1.2.5 Engelschhoek Member

The Engelschhoek Member, formerly known as Dongen Clay Member, is the distal equivalent of the Brussels Sand and Brussels Marls Members and consists of marine clays. It is defined in the areas where the Brussels Sand and Marl Members are absent and a distinction between the Ieper and Asse Members cannot be made.

1.2.6 Boom Member

The Boom Member, formerly known as Boom Clay or Rupel Clay Member, is of early Oligocene (Rupelian to early Chattian) age. It consists of pyrite rich clays with carbonate concretions alternating with silt layers and occasional bituminous bands. The clays become more silty towards the base and the top. The Boom Member was deposited in a middle to outer neritic marine setting with occasional anaerobic conditions. It is present in most of the Dutch on- and offshore. A more detailed description is given in the context of the OPERA project by Vis & Verweij (2014).

1.2.7 Wintelre Member

The Wintelre Member, formerly known as Veldhoven Clay Member, is of late Oligocene (Chattian) age. It consists of grey to greenish-grey clays that become more silty to the top. It was deposited in an inner-neritic marine environment and is present in the southern part of the Dutch onshore.

1.3 Previous work

The Paleogene clays in the Netherlands have been studied for over 50 years. The CORA study from the 1990's (Simmelink et al., 1996) resulted in the first digital maps of thickness and depths of the clay units of Paleogene age in the Dutch subsurface (onshore). The work builds on previous maps from the 1980's. Included in this study were the Oosterhout Formation, Breda Subgroup, Boom Member, Asse Member, Ieper Member and Liessel Member. The focus was on identifying where the formations are shallow (< 500 m) or deep (> 500 m) and where they are thicker than 100 m.

Within the OPERA project (2010-2017) a large range of studies was conducted into the safe disposal of radioactive waste, of which a large number on the Boom Member in the Dutch subsurface. The most relevant studies in the context of this report are:

- Vis and Verweij, 2014: geological and geohydrological characterisation
- Koenen and Griffioen, 2014: mineralogical and geochemical characterisation
- Wiseall et al., 2015: summary of the thermal, hydraulic, mechanical and biological properties and behaviour (based on data from the underground research laboratory in Mol, Belgium)
- Verweij et al., 2016b: the expected future conditions in terms of temperature and hydraulic conditions
- Griffioen et al., 2017: geochemical interactions and groundwater transport

The results of the OPERA studies will be discussed where appropriate throughout the report. Based on the OPERA studies, a special issue of the Netherlands Journal of Geosciences was published of which the following two papers will be used extensively: Verweij et al (2016a) published a summary of spatial distribution of the porosity and permeability of the Boom Mb and Vis et al. (2016) focused on the geometry and depositional environment.

Ten Veen et al. (2013) studied the presence of shallow (< 1 km) gas in unconsolidated sediments of Cenozoic age in the Southern North Sea delta (in the A and B blocks). As part of this study, the sealing properties of clays in this depth interval were studied as well as their continuity. To estimate the capillary seal capacity, a grain size analysis was conducted to calculate porosity, permeability, pore throat size and ultimately capillary seal capacity. The relationships by Yang and Aplin (2010) were used, which for permeability are mainly based

on clay content (fraction < 8 µm, based on Laser Particle Sizer Helos KR Sympatec) and void ratio. Despite limitations of the methods such as an underestimation of the clay content, the predictions of capillary seal capacity did line up reasonably well with observations. An update of this study was performed in the context of the GEODE[4] project and resulted in published maps and fact sheets for the different shallow gas occurrences in the Dutch offshore (Ecclestone et al. 2021).

A number of TKI projects[5] were executed from 2015 to 2023 on wellbore sealing using naturally occurring ductile materials. Of interest for the current research are two non-public TKI reports on the presence and distribution of ductile formations in the Dutch subsurface (Geel, 2016) and a shale classification for sealing capacity and database inventory (Hoving et al., 2019). Relevant information on properties of Paleogene clays from these reports are public and included in this study. Corina et al. (2021) present a summary of the experimental findings on geomechanical properties of bentonite, which can provide useful information for fault behaviour in ductile shales.

The SCAN[6] project is focused on characterizing relatively poorly known parts of the subsurface for geothermal energy production. In this framework 2D seismic lines have been acquired and several research drillings are being conducted. For Paleogene clays the most relevant wells are ORO-01 and SVG-01 both in Noord-Brabant. In ORO-01, cores have been collected in the Boom and Asse Members. In addition to the core measurements of porosity and permeability which have been used in Chapter 3, geomechanical measurements were done. These include tri-axial tests with increasing confinement and a Mohr-Coulomb analysis. The results show that the Asse Mb is stiffer (higher cohesion and uni-axial compressive strength) than the Boom Mb[7]. In well SVG-01 cores have been collected in the Wintelre Mb (2 cores) and in the Boom Mb (1 core). Similar measurements as in ORO-01 are planned for these cores as well[8].

A number of detailed mapping projects in the southern part of the Dutch onshore were executed since 2014. The focus of these so-called H3O projects[9] is on the mapping of shallow, middle deep as well as deep hydrogeological units (aquifers or reservoirs) for the purpose of groundwater modelling, heat storage or geothermal energy. In the context of these studies the Paleogene units were mapped through a combination of seismic interpretation and modelling using information from shallow as well as deep wells. These maps are available for the individual study areas and give a very detailed view of the thickness, depth and distribution. Due to the different focus (aquifers instead of aquitards) as well as the different mapping approach these maps were not included in this project but can be seen as additional, more detailed information within the H3O areas.

Information from several other studies and publications was used for this study. Where relevant, these sources are listed in the individual chapters of this report. An overview of all studies used for this report is given in Appendix A.

[4] www.geodeatlas.nl
[5] Topconsortium voor Kennis en Innovatie (TKI)
[6] https://scanaardwarmte.nl/
[7] Geomechanics report available in ORO-01 page on NLOG (Dutch Oil and Gas Portal, www.nlog.nl)
[8] https://scanaardwarmte.nl/onderzoeksboring-in-stad-van-gerwen/
[9] H3O programme - Geologische Dienst Nederland

1.4 New naming convention for the North Sea Supergroup

In 2020 a new classification and naming scheme was adopted for the North Sea Supergroup. This was done to reflect new understandings of the internal structure of these sediments and to harmonize the naming conventions of the shallow and deep models. In Table 1.1) the new as well as the old names of the formations and members of the Middle and Lower North Sea Groups are shown. In the context of this report it is attempted to use the new classification as much as possible, however, some older datasets can still use the old scheme and will be used in this project.

Table 1.1 Overview of the old as well as new naming convention for the Middle and Lower North Sea Groups.

Group	Abbrev.	Formation	Old abbrev.	New abbrev.	Old members	Old abbrev.	New members	New Abbrev.
Middle North Sea	NM	Veldhoven (Oligocene to Miocene)	NMVF	NMVE	Someren	NMVFS	Someren	NMVESO
					Veldhoven Clay	NMVFO	Wintelre	NMVWI
					Voort	NMVFV	Voort	NMVEVO
		Rupel (Oligocene)	NMRF	NMRU	Rupel Clay	NMRFC	Boom	NMRUBO
					Vessem	NMRFV	Berg	NMRUBE
Lower North Sea	NL	Dongen (Eocene)	NLFF	NLDO	Asse	NLFFB	Asse	NLDOAS
					Brussels Marl	NLFFM	Brussels Marl	NLDOBM
					Brussels Sand	NLFFS	Brussels Sand	NLDOBR
					Ieper	NLFFY	Ieper	NLDOIE
					Dongen Clay	NLFFC	Engelschhoek	NLDOEN
					Basal Dongen Sand	NLFFD	Oosteind	NLDOOO
					Basal Dongen Tuffite	NLFFT	De Wijk	NLDOWY
		Landen (Paleocene)	NLLF	NLLA	Reusel	NLLFR	Reusel	NLLARE
					Landen Clay	NLLFC	Liessel	NLLALI
					Gelinden	NLLFG	Gelinden	NLLAGE
					Heers	NLLFS	Orp	NLLAOR
					Swalmen	NLLFL	Swalmen	NLLASW

1.5 Report structure

In Chapter 2 the methods as well as the results of the update of the mapping of the clay units is presented. Chapter 3 introduces the methods and results of the log analyses for selected wells in the Dutch on- and offshore. Chapter 4 presents the method and results of the seismic analyses for the case study areas. Chapter 5 gives an overview of the more regional processes as seen from previous studies on overpressure, hydrocarbon fields and shows, and drilling events and integrates the results from chapters 3 and 4 into this regional picture. Chapter 6 closes with a discussion of the results. Chapter 7 summarises the conclusions and gives recommendations for further research.

2 Mapping

2.1 Methodology

The main scope for this work package was to get an overview of thickness, depth and distribution of the Paleogene clays. In this paragraph we discuss the datamining procedure and the workflow used for the creation of the thickness and depth maps. The maps were created in Petrel in a workflow using the kriging interpolation algorithm. For these maps also the faults at the Base of the Lower North Sea Group of the HIKE fault database[10] collected in the context of the GeoERA project were used.

For datamining the usual working method is to select all wells onshore and offshore with sub-selections per relevant stratigraphic interval. Datamining consists of all public available well data as found on NLOG[11]. Well data from shallow wells as well as the DAPGEO well was included in the data gathering process as well. For the depth and thickness maps, the DGMv5[12] depth grids of the Upper and Lower North Sea Groups were used as a basemap.

The general sub-selection criteria per stratigraphic interval are:

1. Are aquitard top and bottom interpretations correct and consistent (do they comply with the regional picture?) For this criterion also the DGMv5 grid was used as a guide for the regional trend.
2. Are anomalous thicknesses explainable (e.g. due to vicinity to a fault) → keep the well, otherwise reject and/or adjust

This method is similar to the ThermoGIS data selection procedure[13] where data is undergoing quality control while being selected and gridded. This is an interactive method.

The datasets of the wells are true vertical depth point data with top, base and thickness and with their anomaly code. An anomaly code gives information about the structural features encountered in the various stratigraphic units. For example is there a fault, an unconformity or is the end of drilling depth reached in the stratigraphic unit considered. The latter means that only the minimal thickness and not the full thickness a the stratigraphic unit (in this case the clay layer) is known. The wells are selected based on their anomaly code and the wells with faults at the top or base of the unit as well as off-chart anomalous thicknesses are skipped per aquitard for the calculation.

Based on these anomaly codes, not all wells are used for the thickness and depth maps, but all are equally important to define the distribution polygons. Distribution polygons of the aquitards give the maximum map extent and are not necessarily constrained by faults.

In addition to the well data the extent of the clays of interest is used, which is a combination of various sources. Polygons from the Stratigraphic Nomenclature of the Dutch Subsurface[14], previous H3O projects and the previous CORA project (Simmelink et al. 1996) were collected

[10] HIKE European Fault Database | GeoERA
[11] Boreholes, Stratigraphy | NLOG
[12] DGM-deep V5 on- and offshore | NLOG
[13] Areal extent, gross thickness and depth | ThermoGIS
[14] Stratigraphic Nomenclature | DINOloket

and used as a base polygon. The resulting distribution polygon was, where applicable updated with new insights. This is the case in areas with newly drilled wells such as the SCAN-wells and geothermal wells.

2.2 Results

Thickness maps, top and base maps were created for all the clays of interest in true vertical depth (TVD; Appendix B).

The results will be discussed from older (deeper) to younger (shallower) stratigraphic unit. The overall thickness of the clays may vary a lot and is strongly influenced by the structural elements as presented in Figure 2.1.

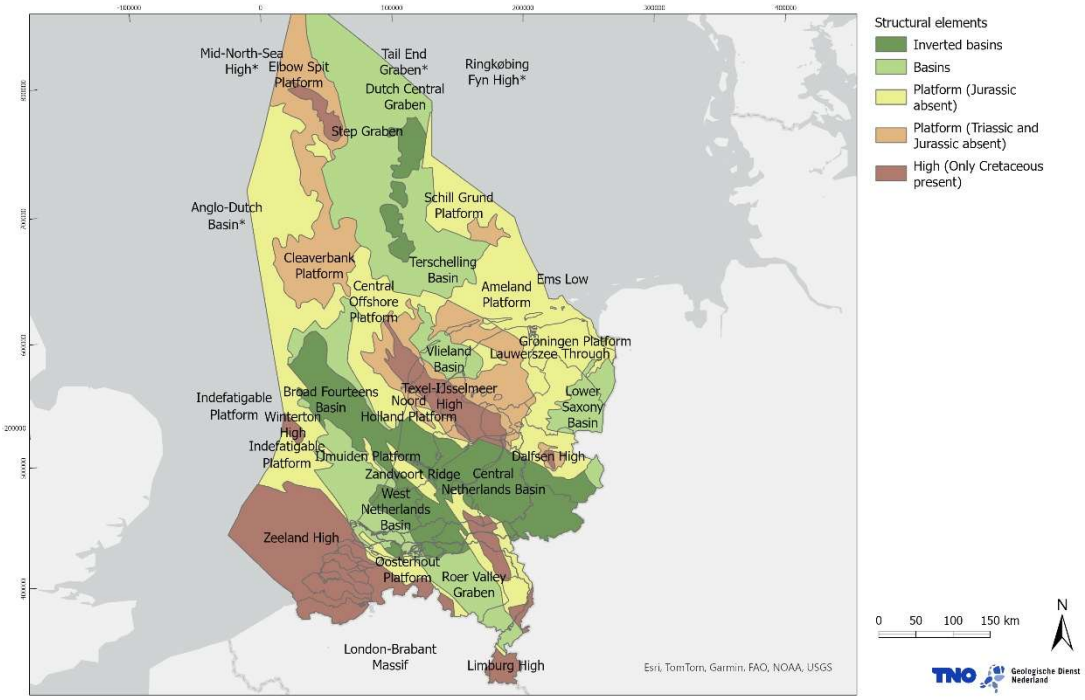

Figure 2.1 Structural elements map of the Netherlands showing Mid and Late Cimmerian (Jurassic and Early Cretaceous) basins, highs and platforms. The main basement highs are formed by crystalline basement and Palaeozoic rocks, generally without Rotliegend (modified after De Jager et al. 2025).

2.2.1 Liessel Member - Landen Clay Member

The Liessel Mb also known as the Landen Clay is usually a dark-green hard and flaky clay and may contain silt. It is a shallow marine deposit which become sandy to silty to the east. and often has traces of bioturbation.

To the south the Liessel Mb can be overlain by the sandy Reussel Mb, the Oosteind Mb or other younger deposits. The lower part can be marly and light of colour towards the Gelinden, the Orp or the older Mesozoic deposits. The distribution can be quite patchy. Mean Thickness is 37 m with thickest parts approximately 100 m (true vertical thickness) in the western offshore area (Figure 2.2).

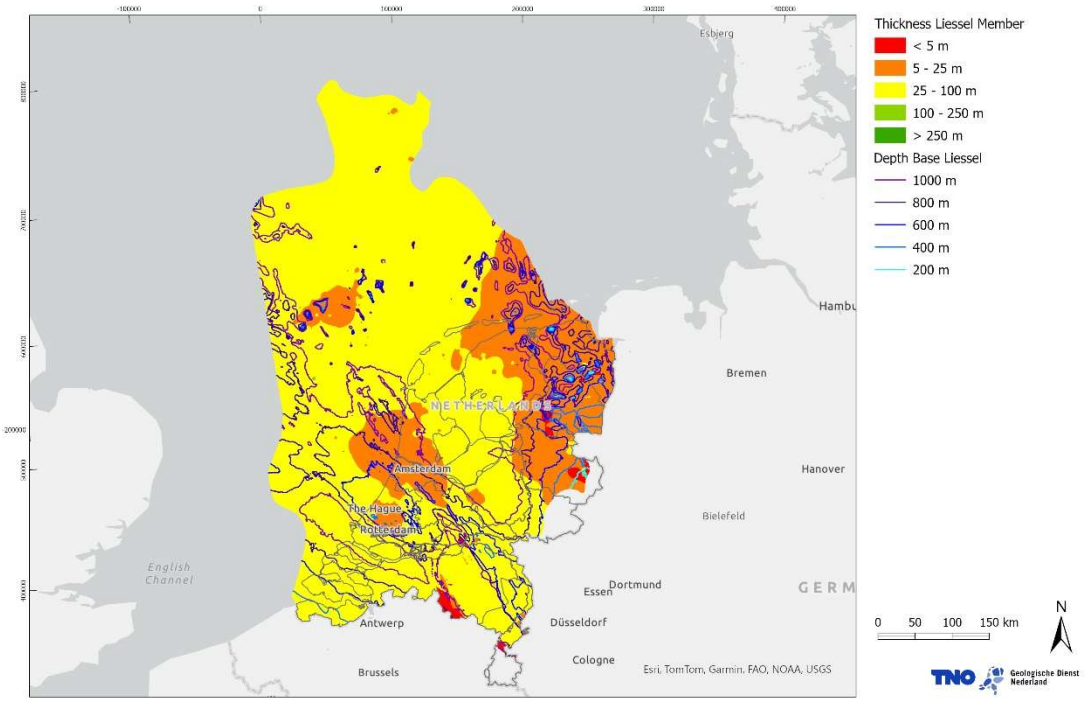

Figure 2.2 Thickness of the Liessel Member with contour lines of depth intervals of 200 m; maps for the depth of base and top of this Member in Appendix B

2.2.2 The Dongen Formation (De Wijk Member, Ieper Clay, Asse Member, Engelschhoek Member)

The Dongen Fm consists of the Asse Member, the Brussels Sands and Marls, the Ieper Member, the Engelschhoek, the Oosteind Member and the De Wijk Member. The Dongen Formation is globally a marine deposit with estuarine conditions and possible continental conditions in the southwest. Such an estuarine deposit is the Brussels Sands Member. Differentiation of the clays is based on the presence of the Brussels Sand and Brussels Marl Members. The differentiation of the clays is hard to recognize in wells, especially in the areas where the Brussels sands and marls are absent. Therefore the Dongen Formation is presented as a stacked formation also including the De Wijk Member at the base of the formation.

In this thickness map (Figure 2.3) the Brussels Sand Member is included for the total thickness. In the onshore area, where the Brussel Sands are well defined, the separate thickness maps made for the Ieper and the Asse Members (Figure 2.4 and Figure 2.5) can be used reliably. In the offshore where this distinction cannot be readily made the clays of the two members are combined in the Engelschhoek Member. In the onshore where the Brussels sands are absent (not deposited or eroded, Figure 2.3), the Dongen Formation thickness is thinning out. This in mainly around the West Netherlands Basin, the Roer Valley Graben and the Central Netherlands Basin. The thickness of the Dongen Formation is up to 890 m in the northernmost offshore (true vertical thickness). The mean thickness is around 355 m. The Dongen formation gently dips to the offshore and it's the shallowest towards the southwest in the Zeeland area and the east.

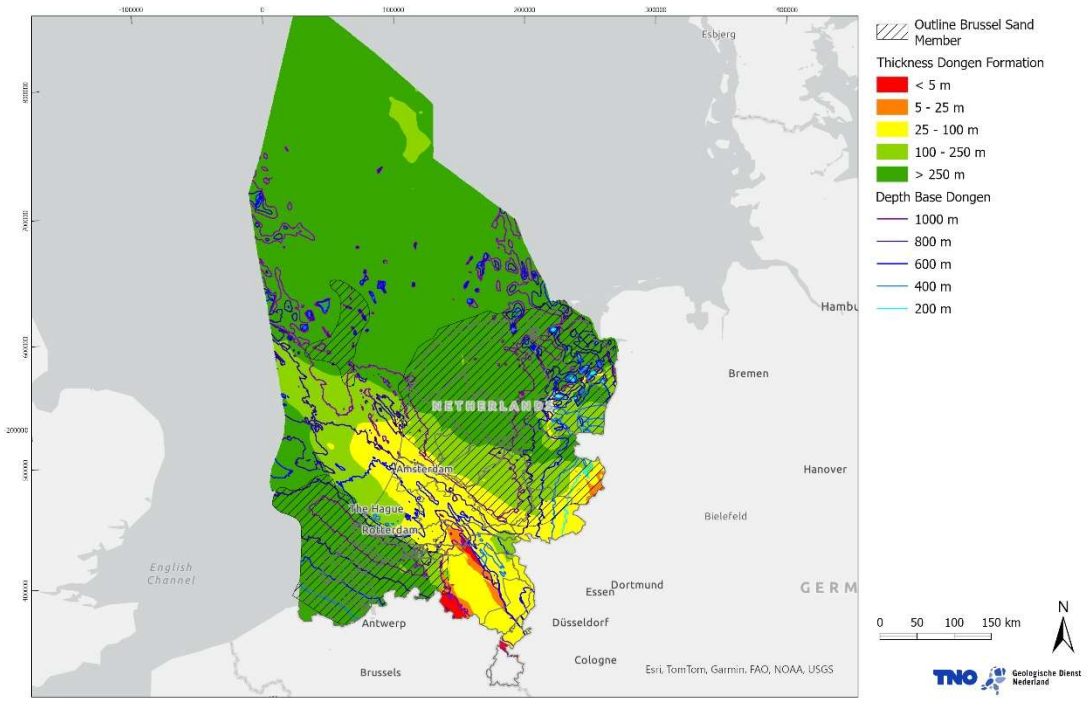

Figure 2.3 Thickness Dongen Formation with the outline of the Brussel Sand Member and with contour lines of depth intervals of 200 m; maps for the depth of base and top of this Member in Appendix B

2.2.2.1 The Ieper Member

The Ieper Member is a shallow marine deposit. It thickens towards the offshore area and thins towards the inland (Figure 2.4). The Ieper Member consists of a soft, tough clay and the base is usually brown-grey and locally red-brown-beige while the upper part can be green-grey. The overlying sands are variable based on the erosion history and can vary from the sandy Brussels Sand Member to younger units. Due to the various phases of inversion and erosion the definition of the upper boundary can become difficult. The lower boundary is usually marked by a sharp transition toward the Oosteind or the De Wijk Members. Mean thickness is around 220 m TV and is gradually grows thicker towards the northeastern offshore area.

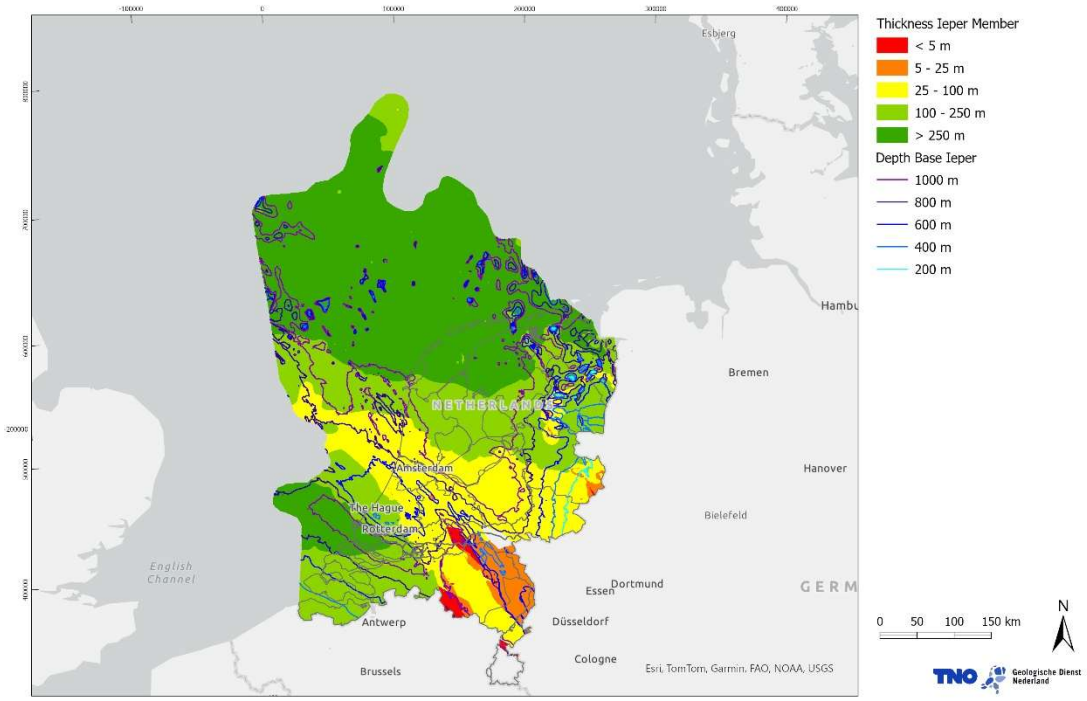

Figure 2.4 Thickness of the Ieper Member with contour lines of depth intervals of 200 m; maps for the depth of base and top of this Member in Appendix B

2.2.2.2 The Asse Member

The Asse member, is the upper most clay of the Dongen Formation and thickens towards the offshore area (Figure 2.5). It is a greenish-grey to blue-grey plastic clay deposited in open marine conditions at shallow depth. The upperpart of this clay can be sandy. Where the Asse Member is not eroded it is overlain by the Rupel formation in particular the sandy Berg Member and the distinction therefore can be clear. However if the Berg Member is not present, this clay is overlain by the Boom Member which makes the distinction of the clays quite complex. Right underneath the Asse Member the Brussels Sand Member is deposited. The boundary is usually very clear and can be locally transitional. The mean thickness is around 65 m (true vertical thickness).

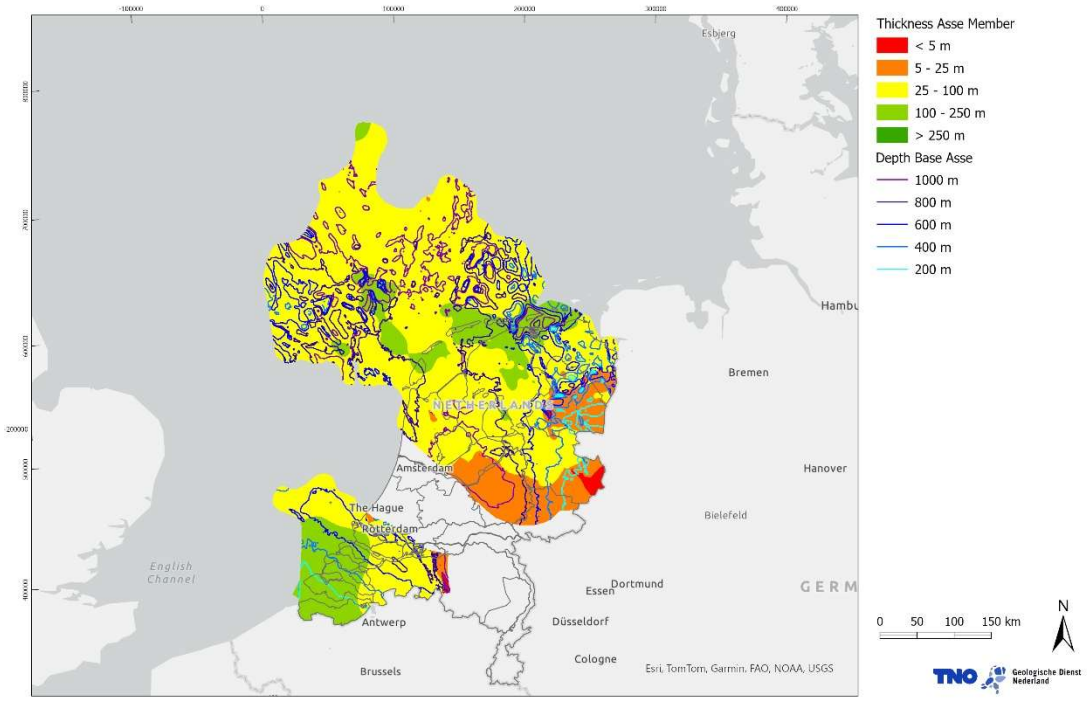

Figure 2.5 Thickness of the Asse Member with contour lines of depth intervals of 200 m; maps for the depth of base and top of this Member in Appendix B

2.2.3 The Boom Member

The Boom Member is a shallow marine deposit with possible anaerobic conditions, also known as the Rupel Clay. It is part of the Rupel Formation and belongs to the Middle North Sea Group. This clay is widespread, but the thickness varies a lot. The thickest sections are seen in the northernmost offshore blocks and in the Zuiderzee low area (Central Netherlands Basin) and the Roer Valley Graben area (Figure 2.6). Overall the thickness distribution is patchy in the onshore area. This clay is described as a pyrite rich, glauconite-poor with calcium carbonate concretions, and can become silty towards the top and base of the layer. The organic content varies a lot as well. Towards the basin margins this clay becomes sandy. This clay unit lays on top of the Berg Member (sand) or, where this Member is absent, on the Asse or Engelschhoek clays underneath. In these situations, it is difficult to mark the lower boundary of the Boom clay.

The thickest parts are around 200 m (true vertical thickness). The Rupel Formation outcrops towards Belgium in the south and Germany to the east The upper part might be overlain by the Steensel Member in the southeast and in other areas like in the northeastern offshore it could be covered by the deposits of the Veldhoven Formation. In parts where the Miocene erosion occurred, the Boom clay is overlain by the Breda Formation[15]. The mean thickness is around 65 m (true vertical depth). The top of the Boom clay gently dips towards the offshore area.

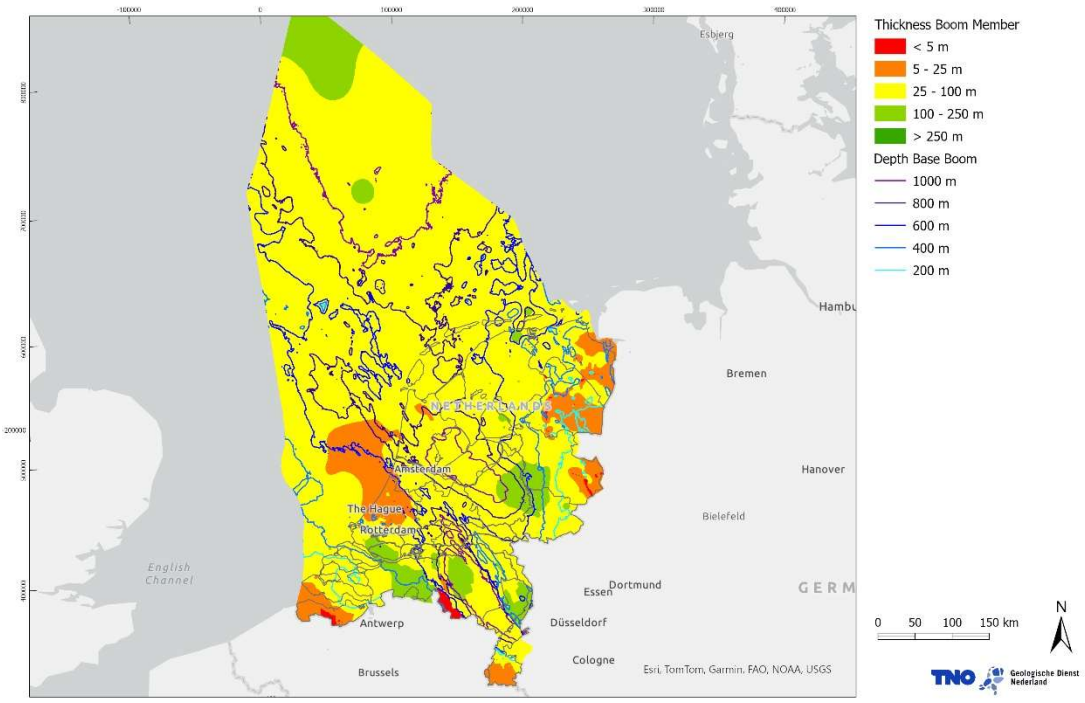

Figure 2.6 Thickness of the Boom Member with contour lines of depth intervals of 200 m; maps for the depth of base and top of this Member in Appendix B

15 Breda Formation | DINOloket

2.2.4 The Wintelre Member

The Wintelre Member is a shallow marine deposit and is part of the Veldhoven Formation[16] of the Middle North Sea Group. As seen in the thickness map (Figure 2.7), the Wintelre clays are mainly present in the Roer Valley Graben in a NW-SE trend. On the edges only a thin layer of clay persists between the Voort Member (lower boundary) and the Someren Member (Upper Member). In places where the Voort Member is absent, the underlying Boom Member can be distinguished by its higher silt content in the uppermost part.

In the recent drilled SCAN well SVG-01[17] this clay member appears to be very thick up to 266 m (true vertical thickness) at a depth of approximately 1500 m (NAP). This well is located in the Roer Valley graben where the Wintelre clay is the thickest. In this well the claystone is described as a firm brownish grey clay with some sandy, silty and calcareous intercalations (Formation Information Log on NLOG). At the edges this clay can be found at a depth of approximately 200 m (NAP). The mean thickness is around 80 m. Towards the northeast and southeast the clay package is thinning out and to the south the clay layer is bordered by faults.

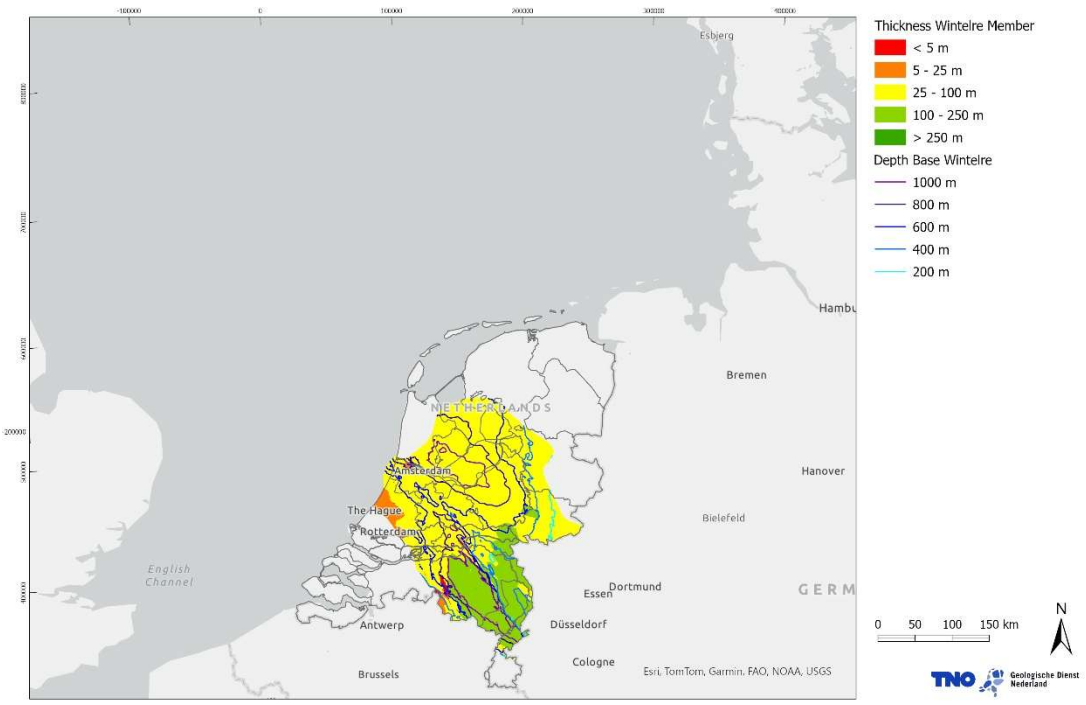

Figure 2.7 Thickness of the Wintelre Member with contour lines of depth intervals of 200 m; maps for the depth of base and top of this Member in Appendix B

2.2.5 Regional development

The Wintelre and the Boom Members are thickest in the Roer Valley Graben and surrounding areas, whereas the deeper Dongen and Liessel clays are more widely spread and, in contrast

[16] Veldhoven Formation | DINOloket
[17] https://www.nlog.nl/nlog-mapviewer/brh/3969940209?lang=nl

to the younger clays, thicker in the Zeeland area and in the northern on- and offshore regions. This phenomenon can be explained by the Laramide tectonic inversion pulse during the Palaeocene which coincides with the end of the Chalk deposition and the beginning of deposition of the North Sea group. This pulse caused locally reactivation of faults in the pre-existing basins such as in the Broad Fourteen Basin (onshore) and the Dutch Central Graben (offshore). Towards the Eocene another inversion pulse (Pyrenean) caused the erosion of parts of the Dongen Formation in the basins. Also, a clear shift is visible from the Lower North Sea clays (NL) towards the Middle North Sea clays (NM) clay deposits, where the concentration of deposition shifts from the regional offshore and nearshore towards the onshore Roer Valley Graben. After the uplift and erosion at the end of the Eocene, deposition shifts towards the onshore as seen by thicker depositions of the younger clays in the onshore area (Munsterman et al., 2025).

3 Log analysis

3.1 Methodology

The suitability of clay rich formations for disposal of radioactive waste is related to two important clay properties: low permeability and high sorption capacity. These properties are a function of the mineralogical composition of the clays, and of the volume % of clay minerals present in a formation and can vary significantly among and within the different clay formations.

Earlier studies about Paleogene clays include several sample-based studies largely focused on the Boom Member. These provided detailed geochemical and mineralogical characterisations and granulometric analyses of the samples to understand their spatial variability (Koenen, & Griffioen 2014; Koenen, & Griffioen 2016; Vis & Verweij 2014; Verweij et al. 2016a).

The log analysis in this work package aims to integrate existing sample-based information with well log data and to characterize the different Paleogene Clays also in non-cored wells, using core data for parameter definition and calibration. The log analyses performed include: mineralogical characterisation from spectral gamma ray logs; quantification of the volumes of clay minerals and clay particles (commonly referred to as volume of shale or Vshale in petrophysics) from the gamma ray log; calculation of the Total and Effective Porosity from density and/or sonic logs; and the estimation of permeability based on core data and NMR log (Nuclear Magnetic Resonance Log) results.

Different definitions are used for clays and shales in different disciplines therefore it is important to address these ambiguities at the beginning of this chapter:

- The term clay in geology refers to both a group of hydrous aluminium-silicate minerals, and to a particle with grain size < 1/256 mm, while the term shale refers to laminated and compacted clays. Shales are indurated clay sediments with a high clay mineralogical content on average about 40 wt% for Opalinus Clay and Callovo-Oxfordian Clay. Shales also includes other, non-clay, minerals (Mäder 2009, Gaucher 2006 and 2009).
- The term clay in petrophysics refers to clay minerals only, while shale refer to the combination of clay minerals plus fine-sized (clay) particles without implying any consolidation or stratification of the formations. These definitions are used to differentiate between the clay minerals that are responsible for the ”clay effect” on logs (high natural gamma ray, high sonic slowness, high neutron and low resistivity for hydrate clays), and the log response that is always lower than a 100% clay mineral response that is associated with variable amounts of clay size particles. The 100% clay mineral response can be derived from the shale response if the clay to shale ratio is known.
- The term clay in stratigraphic nomenclature is used to describe the dominant lithology at regional scale but does not exclude presence of variable volume of non-clay particles.

In this chapter the petrophysical terminology will be adopted, with the term shale used to indicate the combination of clay minerals and clay size particles, the term clay alone will be used only as stratigraphic attribute, while clay minerals and clay particles will be used when referring to the specific component.

All the data used for this log evaluation are publicly available, with well log data from NLOG.nl, Dinoloket.nl, and the DAPGEO-02 research well[18], core data from NLOG.nl, and several existing publications and reports on Paleogene clays (Verweij et al., 2016a, Verweij et al., 2016b, Koenen & Griffioen, 2014 as well as the TKI report Hoving et al., 2019). The full list of collected data can be found in Appendix C.

The workflow applied for the log evaluation includes:

1) Core data gathering and homogenisation
2) Well selection and data loading
3) Clay mineralogy interpretation with K/Th cross-plots
4) Volume of Shale computation and analysis
5) Porosity computation and analysis
6) Permeability characterisation and analysis

Core data gathering and homogenisation

The core data available are from three main sources:

- Routine Core Analysis (RCA) data, analysed and sampled according to the Oil and Gas standard technique, and XRD (Whole rock only). These data are available in the deeper wells including the newly drilled SCAN wells (from NLOG). Porosity was expressed in decimal and horizontal permeability in Millidarcy and depth in Measured Depth. This dataset is referred to in the text as NLOG Dataset.
- Porosity and Permeability (vertical) derived from grain size analysis using the methods from (Yang and Aplin 2004, as referred in Verweij et al., 2016a), XRD (both Whole Rock and clay fraction), XRF, ICP-MS, and ICP-ES. Porosity expressed in % and permeability in m^2 (Verweij et al., 2016a) and Hydraulic conductivity in m/s (Verweij, 2016a); and depths in TVDss. This dataset is referred to as the Verweij dataset.
- Porosity and Permeability data from core samples acquired and analysed according to Hydrogeologic standard techniques (Vis & Verweij, 2014) with porosity in decimal, hydraulic conductivity in m/d at 10degC (likely this is horizontal hydraulic conductivity, based on the values) and in m/s and depth in Measured Depth. This dataset is referred to as Opera TNO-411.

The homogenisation of the data included:

- Conversion of permeability from m^2 while in RCA in mD by multiplying the permeability in square meter by 1.01325e+15 and conversion of the Hydraulic conductivity in m/s to Permeability in mD, by multiplying the hydraulic conductivity per 1.01E+08, assuming the fluid to be fresh water. The conversion factor used, for consistency reasons, is the same used in (Verweij et al 2016a), this is slightly different from the conversion factor of 1.34E8 that is typically used for shallow groundwater with freshwater conditions at 10°C (density is 1000 kg/m3 and viscosity is 1.3 cP). These conversions were necessary to compare the data from different sources.
- Conversion of Potassium oxide (K_2O) in Wt% (weight Percent) measured by XRF (X-ray fluorescence), in elemental potassium in Wt% by multiplying K_2O values by 0.83. This was done to compare the mineralogical data from core and from logs.

[18] www.tudelft.nl

- Normalisation of the weight percent of the Whole rock XRD (WR-XRD) for clay content only. This was done to calculate the dry clay density for the petrophysical analysis.

Well log selection and editing

Many wells drilled for hydrocarbon-, geothermal- or water explorations in the Netherlands penetrate the Paleogene clays. Several of them logged the Paleogene clays with different logging tool combinations. To select the wells to be analysed in this project the following criteria were defined:

1) Wells that have Spectral GR logs in the Paleogene Clay, as the spectral GR allows for a mineralogical characterisation of the formations. Wells with limited log coverage were excluded.
2) Newly drilled wells as part of the SCAN project or other research wells that were not analysed in previous studies, due to time constrains only AMS-01, ORO-01, BLT-01 and DAPGEO-02 were analysed. DAPGEO-02 and ORO-01 were cored in the Paleogene clays. SVG-01, also cored in the Boom and Winterle member, was not included in this study as data were not available in time for this study.
3) Wells with core data, used to derive the main parameters for the petrophysical evaluation and for calibration of the petrophysical interpretation where possible. All core data available were included in the study but well log analysis was performed only on selected cored wells.

The well log data from the selected wells and within the interval of interest were loaded in the petrophysical interpretation software IP 2025 from Geoactive[19] and quality controlled. If the data quality was not adequate for the interpretation the logs were discarded.
The logs available in the selected wells included: Spectral GR used for clay typing, total Gamma Ray used for shale volume calculation, sonic compressional (DT) and or density and sometime neutron used for porosity calculation. NMR data was available for well DAPGEO-02. A detailed overview is presented in Figure 3.1, Table 3.1. Well selection and data availability, see text for details, (this table is also provided as digital deliverable, Appendix C).

Wells for the Borssele location were not selected for log analysis as only geotechnical and geomechanical logs were available. From these wells only measured hydraulic conductivities were used for calibration of the derived permeabilities.

[19] https://www.geoactive.com/interactive-petrophysics

Table 3.1 Well selection and data availability

		Spectral GR						Other Logs							Core Data		Remarks
	Interpreted	Rupel/Boom clay	Ieper clay	Landen/ Lissel clay	Asse clay	Veldhoven clay	Dongen clay	GR	DT (Sonic)	Density-Neutron	PEF (Photoelectric Effect)	Resistivity	Caliper	Special log	Poro-perm	XRD	Data quality/ availblility
A08-01	Y	Y	Y	Y			Y	Y	Y	Y	Y	Y					
F02-06	Y	Y	Y	Y			Y	Y	Y	Y	Y	Y	Y				
G10-03	Y	Y	Y	Y	Y		Y	Y									
GVK-01	Y	Y						Y	Y	Y	Y	Y	Y				large hole irregularities
HVB-01	Y	Y	Y	Y		Y		Y	Y	Y	Y	Y	Y				
K05-11	Y		Y	Y	Y		Y	Y	Y								data in Landen clays only
L01-03	Y			Y				Y	Y	Y	Y						limited data coverage
L06-02	Y			Y			Y	Y	Y	Y	Y	Y	Y				Spectral GR only has lmited coverage
MDZ-01	Y	Y	Y	Y			Y	Y	Y			Y					
AMS-01	Y	Y	Y					Y	Y	Y*		Y					* Neutron only
ORO-01	Y	Y	Y		Y			Y	Y	Y	Y	Y	Y		Y		core in Boom and Asse
BLT-01	Y	Y	Y					Y	Y	Y*		Y					* Neutron only
DAPGEO-02	Y	Y Paleogene clays						Y	Y			Y		NMR			DT coverage is limited
B02C0032 (BUR-01)	Y							Y	Y	Y*					Y		* Neutron only
B02G0352 (LWO-02)	Y							Y							Y	Y	
B11D0073 (GRD-01)	Y							Y	Y						Y		
B15F0214 (ESG-01)	Y							Y	Y	Y*	Y	Y			Y		core in Rupel/ logs in Landen *Neutron only
B16C0020 (EMO-01)	Y							Y	Y						Y		
B16G0058 (NNE-07)	N							No logs digitized							Y	Y	
WAV-10	N							Y	Y*			Y*			Y		core in Ieper, Landen and Dongen *Partial log coverage
WYK-12	N							Y				Y	Y		Y		
DON-01	N							SP				Y			Y		core in Veldhoven clays
VEH-01	N							SP				Y			Y		
AST-GT-02	N							Y		Y		Y			Y		
NKK-01	N							SP				Y			Y		
K05-F-02	N	No logs available														Y	
F15-A-05	N	No logs available														Y	

Clay Mineralogy:

The spectral Gamma Ray log measures the individual contribution of the three major producers of natural Gamma radiation in the formation: ^{40}K, ^{238}U, and ^{232}Th. The relative proportions of these isotopes are diagnostic for minerals and are used in several different interpretation charts. In this study the chart Lith-2 (Former CP-19) from the Schlumberger interpretation Chart 2009 was used. In this chart Potassium, expressed in percentage, is plotted on the X axis and Thorium in ppm on the Y axis; The Th/K ratio serves to distinguish the end members within an area delineated by varying mineralogical compositions between these two reference minerals. Within this region, the proximity to each end member indicates the relative abundance of the respective minerals. The identified end members include kaolinite, chlorite, Illite, montmorillonite, and mixed-layer clays.

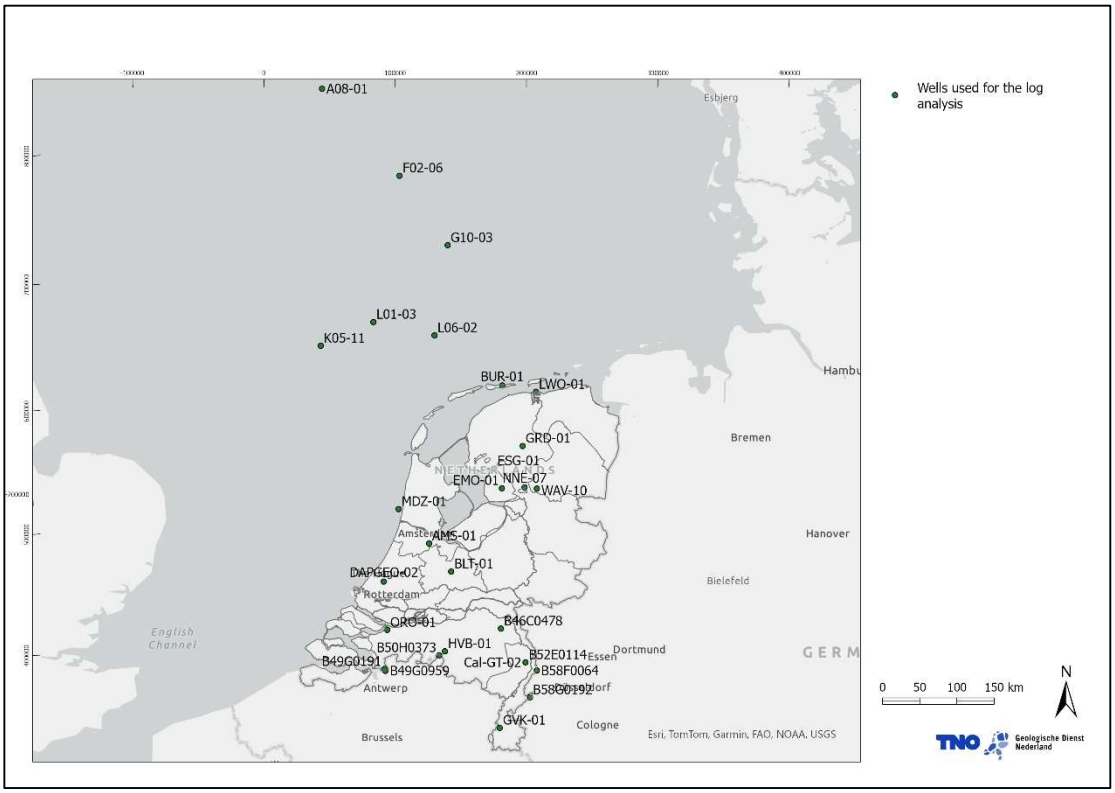

Figure 3.1. Overview of the wells used in this chapter.

The spectral GR data were plotted in one multiwell cross plot for each individual clay formation, and the average Th and K per formation per each well was used to define the average mineralogy per formation in each well. The log data were compared to core data.

The Volume of Shale:

The Volume of Shale, hereafter referred to as Vsh, is one of the main outputs for this study as it allows to understand the distribution of sandy material in the formation, it is used to calculate porosity and it highly affects the permeability.

In this study Vsh was calculated using the Gamma Ray method, this method was chosen for the wide availability of GR logs in the selected wells, other methods such as the Neutron-Density method were utilised, if data were available for cross calibration.
The GR method for Vsh calculation is based on a simple equation, that calculate the volume of the shale once the end member response 0% Vsh and 100% Vsh are defined on the log and cross checked on the mud logs. The total GR signal was used for this analysis.

Vsh=(GRlog-GRclean)/(GrShale-GRclean)

For wells with granulometric data (from Verweij et al, 2016a), the Vsh from logs were compared to the complement of percentage of sand from the grain size analysis.

Averages of Vsh for each interval of interest were computed for each analysed well. These averages were used to understand the areal variability of Vsh per interval but also to identify the wells with thicker formations and high Vsh, that are intervals with the best seal potential. For this analysis cross plots of Vsh vs thickness were used.

Porosity

Porosity is defined as the ratio of the pore volume over the bulk volume, depending on the different type of pores accounted for, Total or Effective porosity can be calculated.
When accounting for all the pores, including small pores filled with irreducible water and for large, interconnected pores the Total Porosity (PHIT) is calculated, when accounting only large, interconnected pore as Effective porosity (PHIE) is calculated. Core porosity is often Total Porosity.

Porosity is directly measured in the well only by the nuclear magnetic resonance tool (NMR), available only in DAPGEO-02, while in general it is derived from properties such bulk density, sonic slowness, hydrogen index etc or a combination of such. In this interpretation due to data availability, porosity was calculated using density and sonic log, with the density method being the preferred porosity method. The interpretation was performed using the interactive porosity module in IP, that calculates Total and Effective porosity using the selected porosity method (density or sonic) and applying to it a ''shale correction''. The shale correction uses the Vsh as input but also a series of properties of the shales derived from the log, such shale density or shale slowness, and a series of core derived properties such clay/shale ratio, the density of clay minerals and the porosity of clay minerals. The calculated total porosity will be for the large part determined by these inputs while the Effective porosity will be determined by the properties defined for the sandy part of the formation. Standard values were used for the sand properties.

Table 3.2 Summary table of the main clay (mineral) parameters derived from core data. Source of each parameter is indicated in the table

Formation	Average Dry Clay (mineral) density	Source of Clay (mineral) density	Clay/shale ratio	Source of Clay/shale ratio	Clay Mineral porosity	Source of Clay porosity
Rupel/ Boom	2.1	XRD CF averages calibrated in ORO-01	0.6	Calibration with ORO-01	0.45	calibrated average from BUR-01, ESG-01, GRD-01, EMO-01,
Asse	2.2	Calibration with ORO-01	0.7	XRD WR	0.45	From Rupel
Ieper	2.4	XRD WR (normalised) from 4 samples	0.67	XRD WR	0.45	From Rupel
Landen/ Liessel	2.4	XRD WR (normalised) from 1 sample	0.6	XRD WR	0.30	Calibration in WAV-10
Dongen/De Wijk	2.4	XRD WR (normalised) from 3 samples	0.6	XRD WR	0.35	Calibration in WAV-10

The clay properties were derived from core data, and specifically (summary in Table 3.2):

- Density of clay minerals dry: mineralogy dependent and was derived from the XRD volumes, clay fraction preferably, multiplied for the average literature density of

each clay type. When clay fraction was not available the whole rock was normalised to clay content and used for the calculation.
- **Density of clay minerals wet:** directly related to the clay mineral porosity this was derived by calibration with porosity in ORO-01.
- **Ratio of clay mineral over total shale:** this is derived from XRD-WR, for the Rupel Formation and Asse Member these derived XRD values were calibrated to the core porosity in well ORO-01.
- **Porosity of clay minerals:** from core analysis or calculated from dry and wet clay, if sonic method is used. If density method is used the wet and dry clay porosity are used, if sonic method is used the clay porosity must be indicated.

The parameters were either directly derived from the core data or determined through calibration of log data.

Permeability

Permeability is the measure of the rock's ability to allow fluids to flow; this can be measured either perpendicular (vertical permeability or Kv) or parallel to the bedding (horizontal permeability Kh). The ratio Kh /Kv (vertical permeability describes the permeability anisotropy, high ratios indicate that the fluid moves easily horizontally, in the Boom clays the ratio is reported to be between 5 to 60 in Wemaere et al 2008 and 2 in Aertens et al 2023 at the Mol site.

The permeability is one of the most critical properties that is used for many different purposes, but it is also characterised by the highest uncertainty. Direct measurements of permeability are limited to measurements on core samples or well tests, while more commonly it is calculated from porosity by defining a porosity-permeability transform using the core data. Generally, core porosity and core permeability are plotted in a semi logarithmic plot, with porosity on the X axis and permeability on Y axis. If a correlation between porosity and permeability can be established a regression equation is defined and used to calculate the permeability. If the data do not present any correlation, facies variability needs to be investigated, as different trends can be defined for different facies.

Advanced logging tools, such as the Nuclear Magnetic Resonance tool, also contribute to (horizontal) permeability evaluation by using empirical models that relate permeability to the measured porosity and the grain size distribution. Both NMR permeability models, the Timur Coates and the SDR, contain coefficients that need to be calibrated to core measurements. Standard coefficients, defined for deep and permeable formations, are available in literature and are commonly used in absence of core calibration, increasing significantly the permeability.

NMR data are available in well DAPGEO-02, where permeability was computed using standard coefficients as core data suitable for calibration were not available in the well. Other permeability measurements, performed with a permeability probe of the CORE DNA technology, are available in ORO-01, but they are permeability indicators and also require calibrations with core data.

In this study all the porosity and permeability data available (including horizontal and vertical permeabilities) were plotted in a series of conventional porosity-permeability cross plots.

3.2 Results

3.2.1 Clay Mineralogy

Plotting spectral GR data in the chart Lith-2 provides a larger datasets than using core samples alone for the mineralogical characterisation of the different Paleogene clays, as several wells have spectral GR and where available the GR has an average sampling rate of 15 cm, this allows to better understand the mineralogical variations both geographically and stratigraphically. Compositional variation from Montmorillonite to Mixed layer clays to Illite are likely due to diagenetic processes, while variations of Kaolinite content are likely related to the deposition itself.

The Chart Lith-2 uses the following ratios to define areas characterized by similar mineralogical composition:

- Th/K> 25 Heavy minerals
- 25< Th/K<12 Clay mineralogy dominated by Kaolinite
- 12< Th/K<3.5Clay mineralogy dominated by Montmorillonite and mixed clay mixed layer clay Illite-Montmorillonite, with this area Th/K ratio approaching 12 are Montmorillonite dominated while Th/K approaching 2.5 are mixed layer dominated
- 3.5< Th/K<2 Clay mineralogy dominated by Illite
- 2< Th/K<0.6 Glauconite
- 0.6< Th/K<0.3 Feldspar

Landen/Liessel Member

The mineralogy interpretation of the Landen clays from XRD, is based on a single XRD-WR analysis from well F15-A05 (Hoving et al. 2019) and indicate an average composition, after normalisation for clay content only, of 49% of 2:1(Swelling clays); 37% Illite and 14% Kaolinite. This interpretation is characterised by high uncertainty, derived not only from the limited number of samples available but also for the type of analysis itself, the Whole Rock XRD is in fact not the most suitable method for clay characterisation.

The mineralogy interpretation of the Landen clay from log data is based on the Spectral GR data from 14 wells (this number include some wells without a full petrophysical evaluation). The data distribution on the Lith-2 chart indicate a mineralogical variability of the clays from Montmorillonite rich to Illite rich, with a high mineralogy variability between and among wells. By analysing Figure 3.2, can be observed how most of the data points plot above the 3.5 Th/K ratio boundary indicating a dominance of Mixed Layer clay type mineralogy with variable amount of Montmorillonite type of clays, while that G10-3 and K5-11 are richer in Illite plot closer to the Th/K ratio of 2 in an area dominated by Illite.

The average Th/K ratio is displayed on the map in Figure 3.3, to show the spatial variation of the average clay mineralogy. Glauconite presence is also reported at well location as presence of this mineral impacts the Th/K ratio, details are discussed in paragraph 6.1.2.

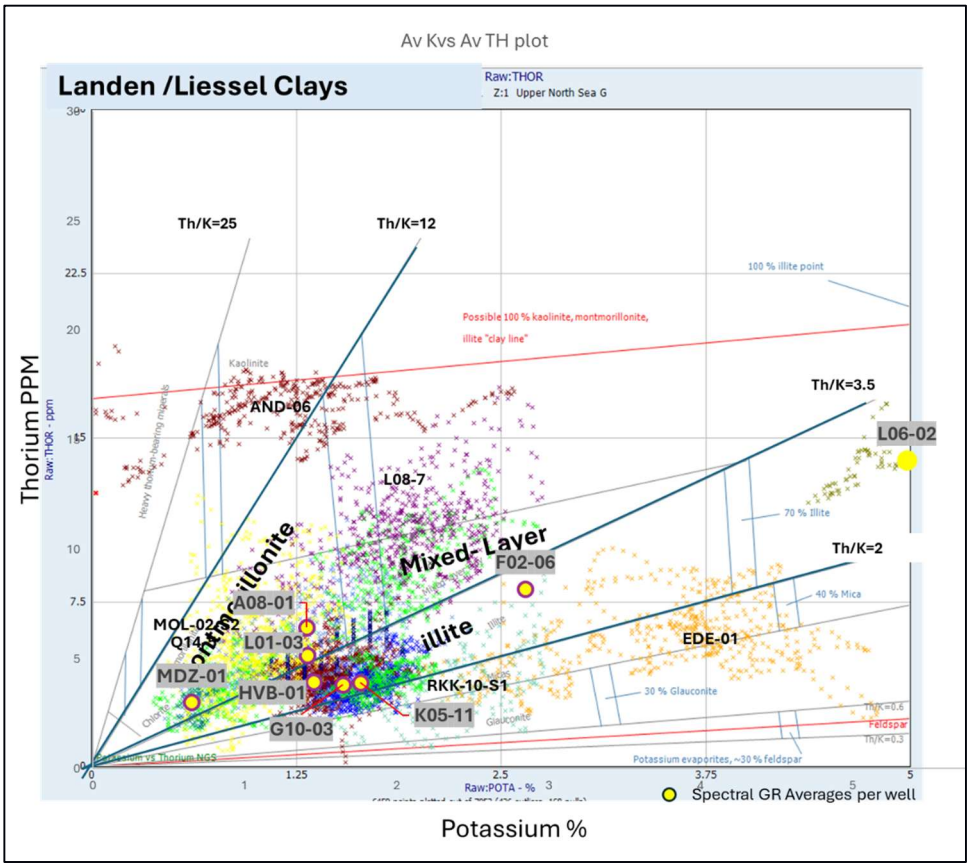

Figure 3.2: Plot Litho-02 for Clay mineral classification. The variability of Landen/Liessel clay can be observed. Average Th and K only for the wells with full petrophysical evaluation are plotted (yellow dots) see text for more details.

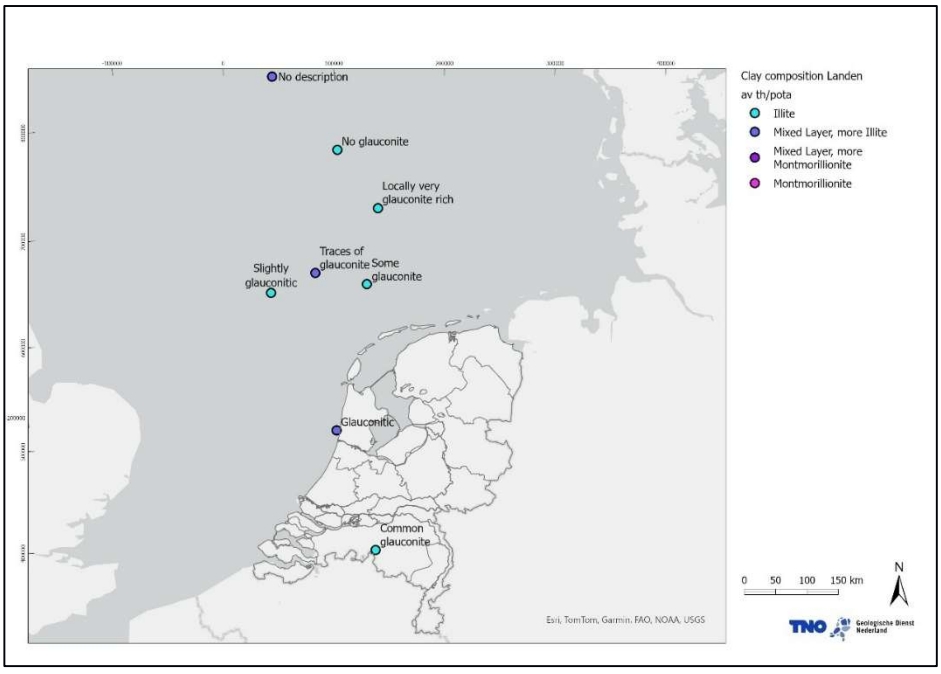

Figure 3.3: Map showing the average Th/K ratio in the Landen/Lissen clays per well, the colours indicate the dominant clay in that location, the presence of glauconite in the interval is indicated as this affects the Th/K ratio.

De Wijk Member/Basal Dongen Tuffite Member

The mineralogy interpretation of the Dongen clays of the De Wijk Member from XRD is based on 3 WR XRD measurements from F15-A05 and K05-F-02 (Hoving et al. 2019). The averaged normalised for clay content mineralogy is 57% of 2:1 clays (Swelling clays); 30% of Illite; and 12% Kaolinite. This interpretation is characterised by high uncertainty, derived not only from the limited number of samples available but also for the type of analysis itself, the Whole Rock XRD is in fact not the most suitable method for clay characterisation.

The mineralogy interpretation of the Dongen clays of the De Wijk Member from log data is based on the Spectral GR data from 6 wells. The data distribution on the Lith-2 chart indicate a mineralogical variability of the clays from Illite rich clays in K05-11 to Montmorillonite rich clay in MDZ-01 and A08-01 (Figure 3.4).

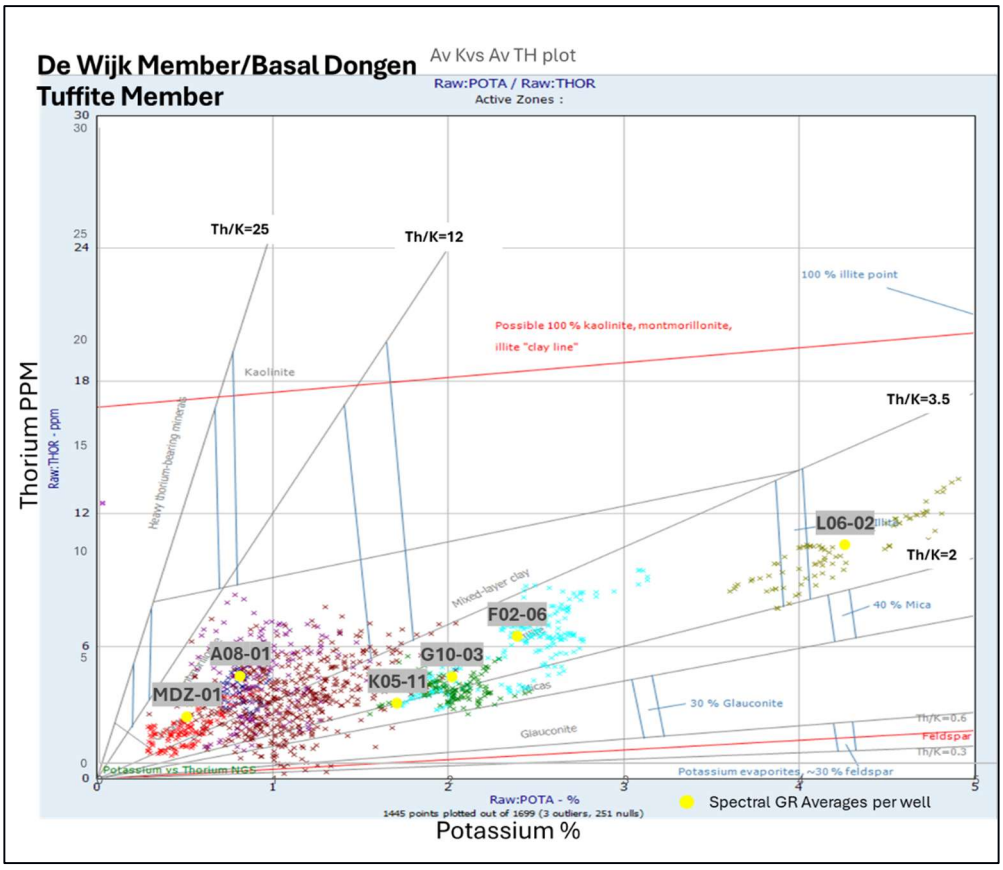

Figure 3.4: Litho-02 for Clay mineral classification. The variability of mineralogy of the De Wijk clay can be observed, Average TH and K are plotted (yellow dots) see text for more details see text for details.

The average Th/K ratio is displayed on the map in Figure 3.5, to show the spatial variation of the average clay mineralogy. Glauconite presence is also reported at well location as presence of this mineral impacts the Th/K ratio, details are discussed in paragraph 6.1.2

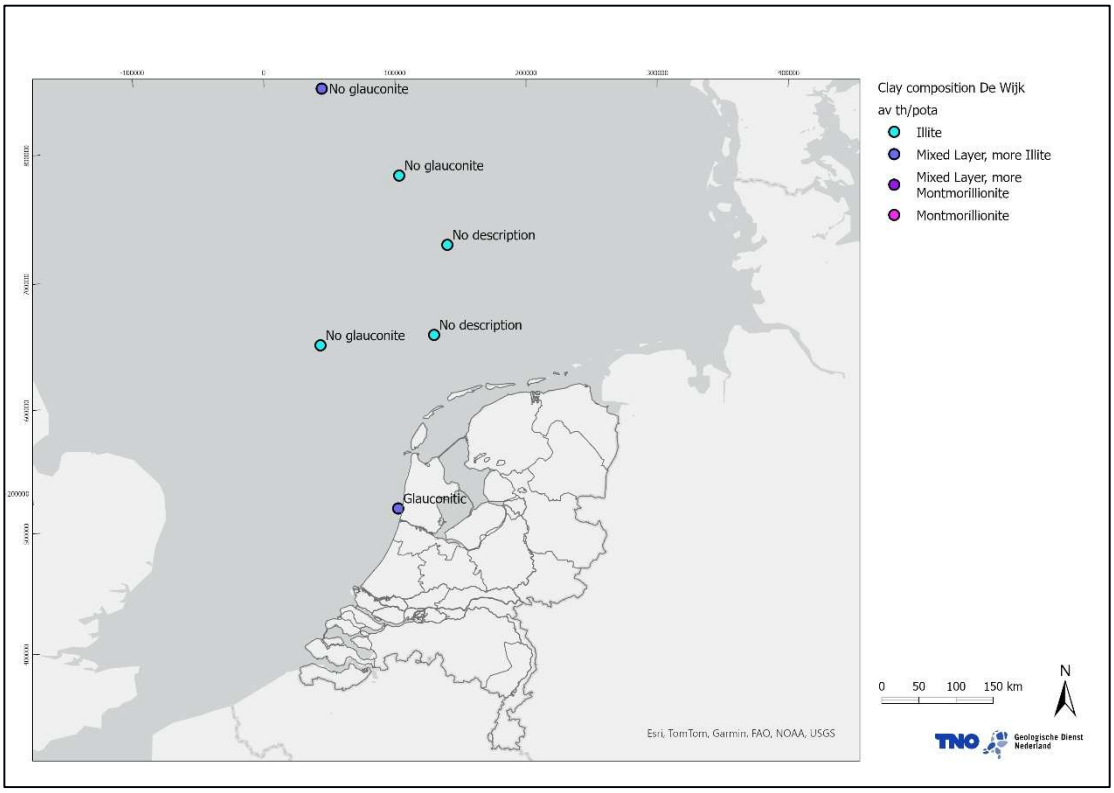

Figure 3.5 Map showing the average Th/K ratio of the De Wijk member per well, the colours indicate the dominant clay in that location, the presence of glauconite in the interval is indicated as this affects the Th/K ratio.

Ieper Member:

The mineralogy of the Ieper clay in the Netherlands is reported in Hoving et al., (2019), where XRD whole rock only were acquired in two wells: F15-A-05, K05-F-02. Note that the uncertainty in clay mineralogy from the whole rock (WR) XRDs are much higher than the one from the clay fraction (CF) XRD, the Whole Rock XRD is in fact not the most suitable method for clay characterisation.

To define the average Ieper clay mineralogy the XRD-WR data from the TNO2019R109 report were normalised for clay content only, resulting in an average of 48% of 2:01 clays (Swelling clays); 34% of Illite; and 18% of Kaolinite. This mineralogy is consistent with what can be observed in the chart Lith-2 (Figure 3.6), where mineralogical variability within the Ieper Member can also be observed. Illite richer wells such K05-11, G10-03 -01 can be identified together with Montmorillonite and Kaolinite rich wells such ORO-01 and A08-01. The majority of wells shows an average mineralogy dominated by Mixed layer clay. As general observation the Ieper clay seem to have a higher Illite content compared to Rupel.

The average Th/K ratio is displayed on the map in Figure 3.7, to show the spatial variation of the average clay mineralogy. Glauconite presence is also reported at well location as presence of this mineral impacts the Th/K ratio, details are discussed in paragraph 6.1.2

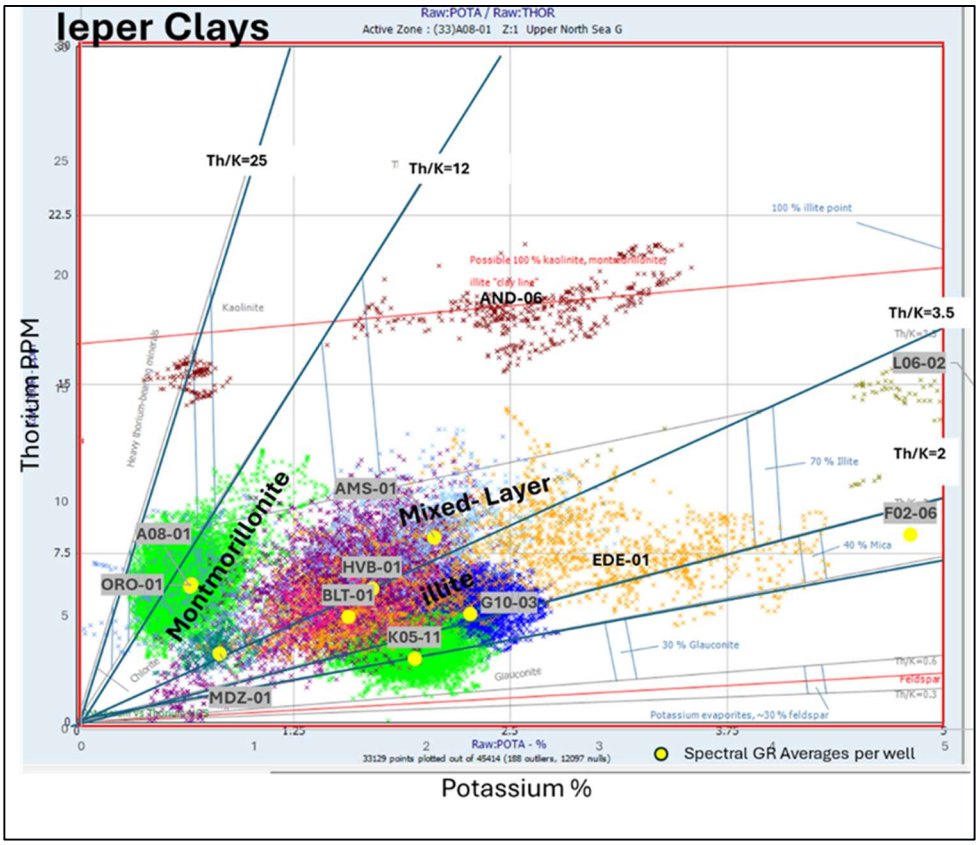

Figure 3.6: Plot Litho-02 for Clay mineral classification. The variability of mineralogy of the Ieper clay can be observed, Average TH and K only for the wells with full petrophysical evaluation are plotted (yellow dots) see text for more details.

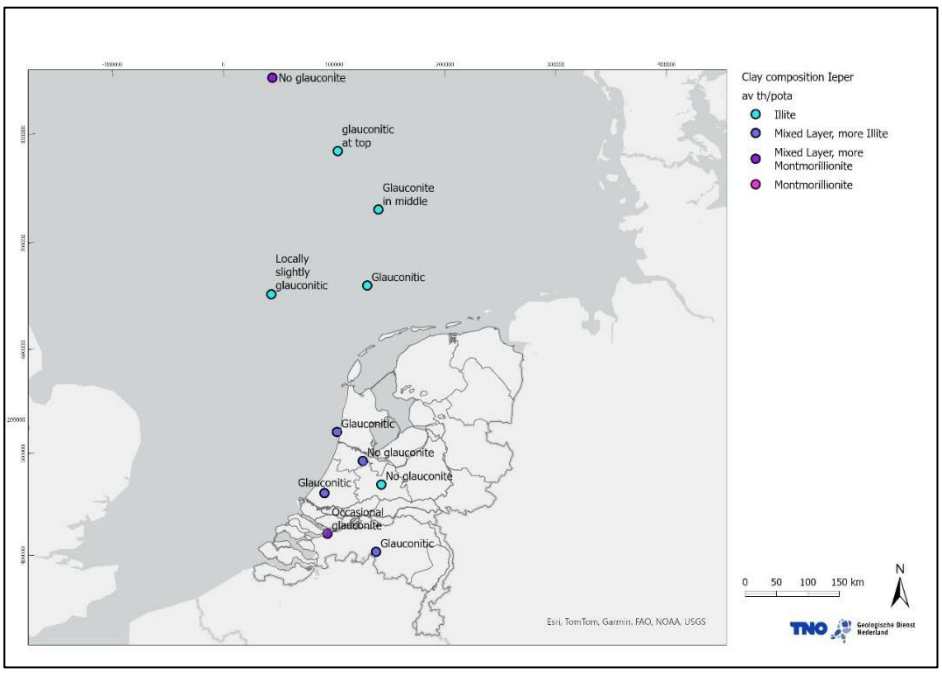

Figure 3.7: Map showing the average Th/K ratio in the Ieper clays per well, the colours indicate the dominant clay in that location, the presence of glauconite in the interval is indicated as this affects the Th/K ratio.

Asse Member

The mineralogy information for the Asse clays is limited to one XRD-WR from well F15-A05 (Hoving et al. 2019) The average from such analysis, after normalisation for clay content only is 73% of 2:1 clays (Swelling clays); 20% Illite; and 7% Kaolinite.

The spectral GR logs plotted in the Lith-2 shows also the Asse clays some mineralogical variability from Illite dominated mineralogy in K05-11 to Kaolinite rich on ORO-01 (Figure 3.8). The average Th/K ratio is displayed on the map in Figure 3.9, to show the spatial variation of the average clay mineralogy. Glauconite presence is also reported at well location as presence of this mineral impacts the Th/K ratio, details are discussed in paragraph 6.1.2

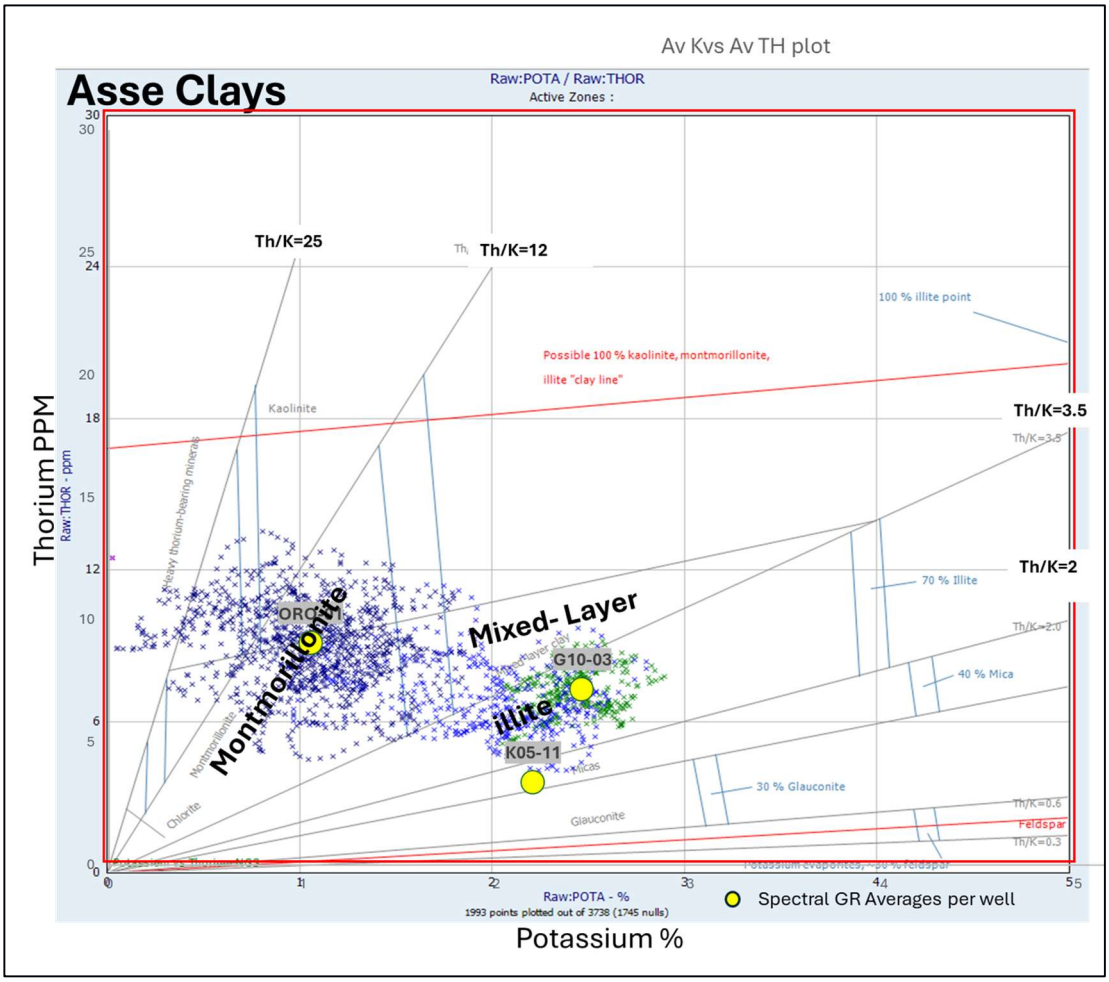

Figure 3.8 Plot Litho-02 for Clay mineral classification. The variability of mineralogy of Asse clay can be observed, see text for details.

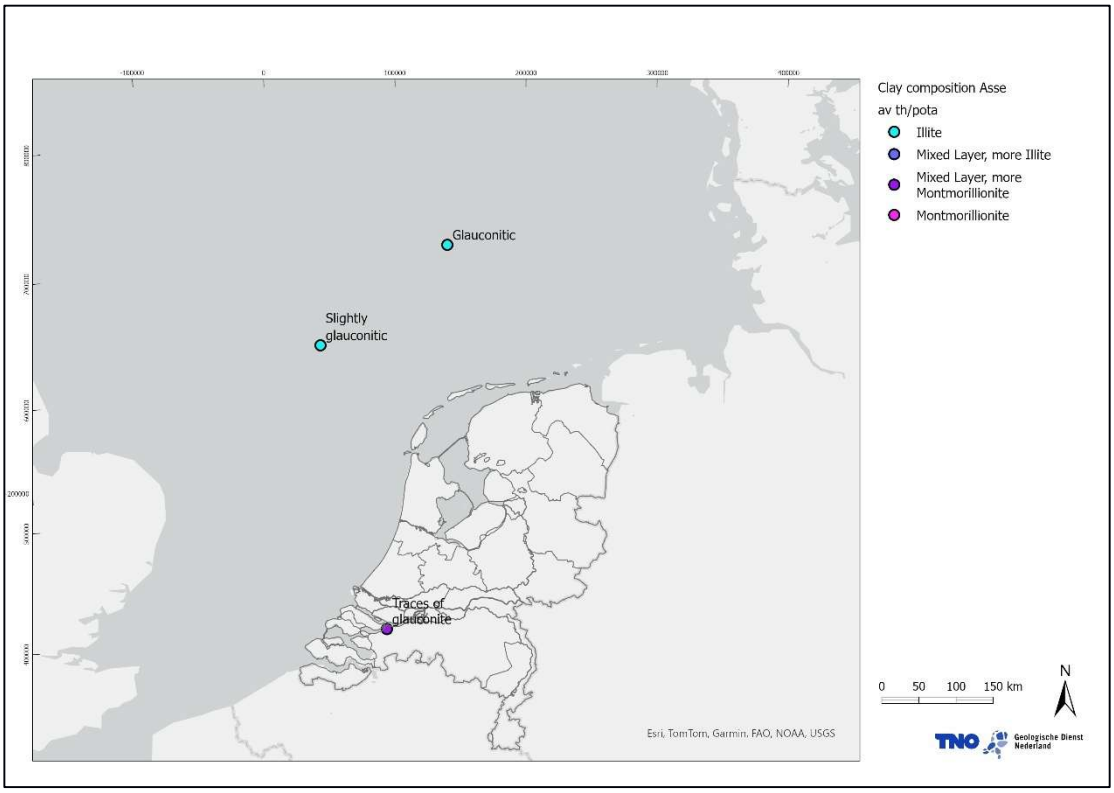

Figure 3.9: Map showing the average Th/K ratio of the Asse Clays per well, the colours indicate the dominant clay in that location, the presence of glauconite in the interval is indicated as this affects the Th/K ratio.

Rupel Formation/Boom Member:

The mineralogy of the Rupel clays in Netherlands is documented in the Opera-521 report (Koenen & Griffioen, 2014), where the results of the clay fraction X-ray diffractometry (XRD) performed on 30 samples from 8 wells, show an average mineralogy of: 35% of Smectite; 22% of Illite-smectite mixed layer, 18% of glauconite-smectite; 12% Illite; 5% Kaolinite; 7% Mixed layer Kaolinite-smectite; and 1 % Chlorite. These XRD results, despite the fact that they cannot be plotted directly in the chart Lith-2, seem consistent with the distribution of Potassium and Thorium from the spectral GR in the chart, where the dominant clay types are clearly Montmorillonite and Mixed layered clays in variable proportions in different wells. The clay mineralogy variability within the Rupel clays ranges from wells dominated by Montmorillonite and Kaolinite, such A08-01 and in part ORO-01, to wells characterised by dominant mixed layer clay with relatively higher Illite content such G10-03 and GVK-01 (Figure 3.10).

For a more direct comparison, XRF and ICP-MS data from Opera-521 report were plotted in the Lith-2 chart, as the ICP-MS provides quantification of Th content in ppm, while the potassium oxide (K_20) in Wt.% measured by the XRF can be easily converted to elemental potassium. The XRF data show higher potassium content than the one shown by the spectral GR, but this is due to the fact that the XRF data accounts for all the isotopes of potassium in the formation while the Spectral GR accounts only for its radioactive isotope ^{40}K.

Despite this difference related to data acquisition, the data show consistent results and confirms that the average mineralogy of Rupel clay includes Montmorillonite and Mixed layer clays overall with areas richer in Kaolinite (A08-01 and ORO-01) and areas richer in

Illite G10-03 and GVK-01 (Figure 3.10). The average Th/K ratio is displayed on the map in Figure 3.11, to show the spatial variation of the average clay mineralogy. Glauconite presence is also reported at well location as presence of this mineral impacts the Th/K ratio, details are discussed in paragraph 6.1.2

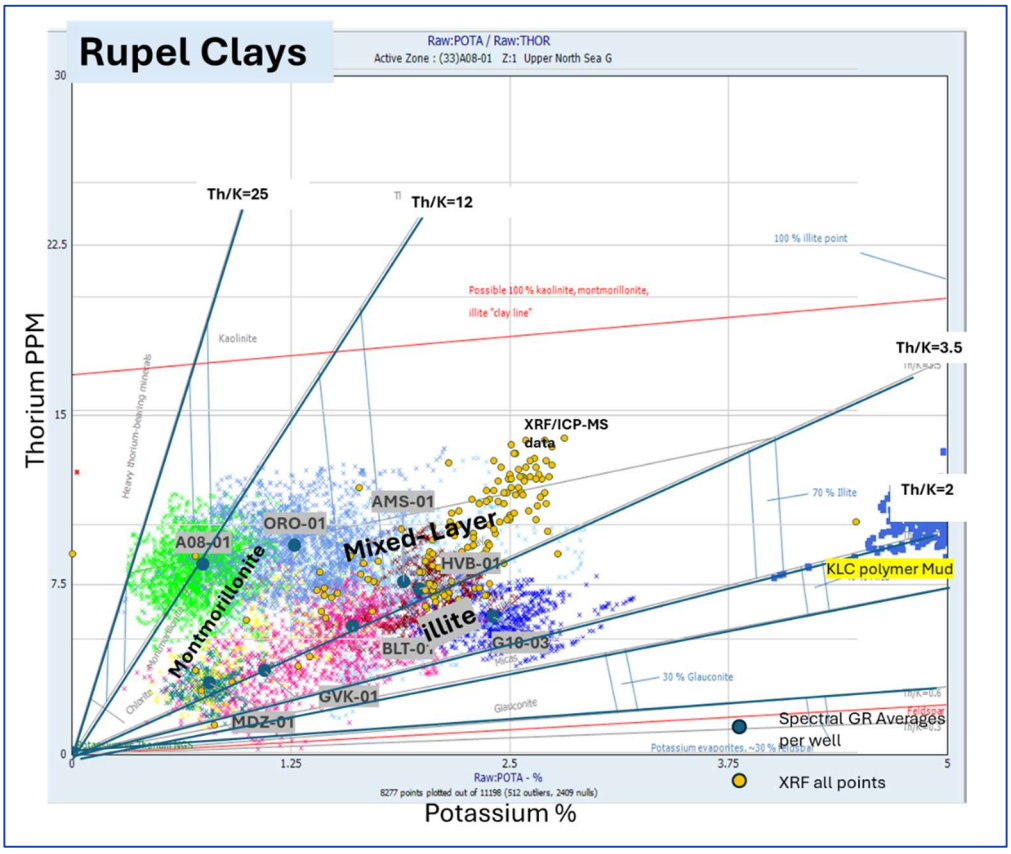

Figure 3.10: Plot Litho-02 for Clay mineral classification. K and Th from the spectral GR are displayed together with XRF and ICP-MS data. Note that K in the XRF data is overestimated (see text for explanation). Variability of clay mineralogy can be observed within the Rupel clays.

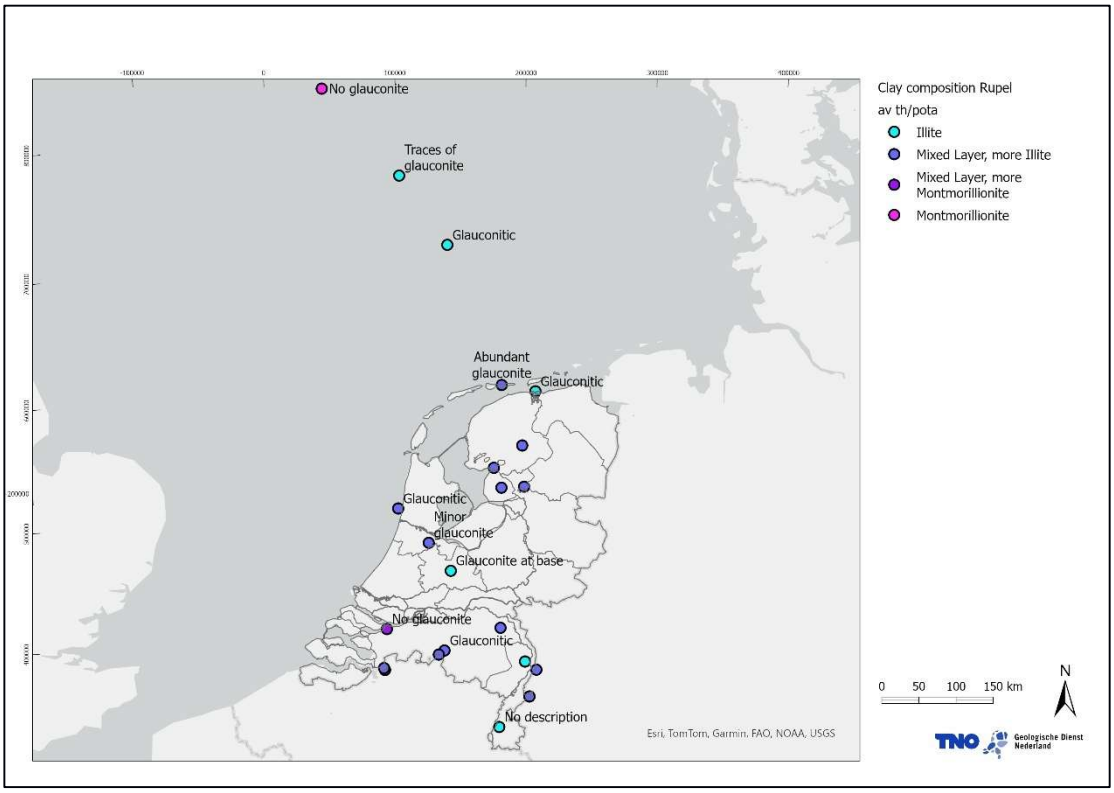

Figure 3.11: Map showing the average Th/K ratio of the Rupel Clays per well, the colours indicate the dominant clay in that location, the presence of glauconite in the interval is indicated as this affects the Th/K ratio.

3.2.2 Volume of Shale

The volume of shale was computed for all interpreted wells, using the GR method, the results were validated with mud logs and grainsize data from cores. An adequate match can be observed between the complement of volume of sand (1-Volsand) from the granulometric analysis presented in (Verweij et al. 2016a) and the computed Vsh in Figure 3.14.

Since one of the most general conditions for an effective seal is a large amount of clay minerals, arithmetic averages of Vsh per well and for each formation were computed and plotted against the thickness of each interval of interest (Figure 3.12).

The thickness for each formation in all the wells except DAPGEO-02 are based on NLOG stratigraphic interpretations, while in DAPGEO-02 the well tops are based on the biostratigraphic interpretation from Houben (2025).

In the analysed intervals a generally high (>0.6) average Vsh can be observed, indicating that most of the intervals contain limited amounts of sand. However, while some variability can be observed, there are no clean spatial trends (Figure 3.13). Generally lower Vsh are observed in the De Wijk Member, which is characterized by some very sandy parts and also in the Paleogene clays as defined in DAPGEO-02, where the Paleogene clay unit includes a high permeability sandy interval at the top and the low permeability, proved sealing silty and clay rich interval in the lower part.

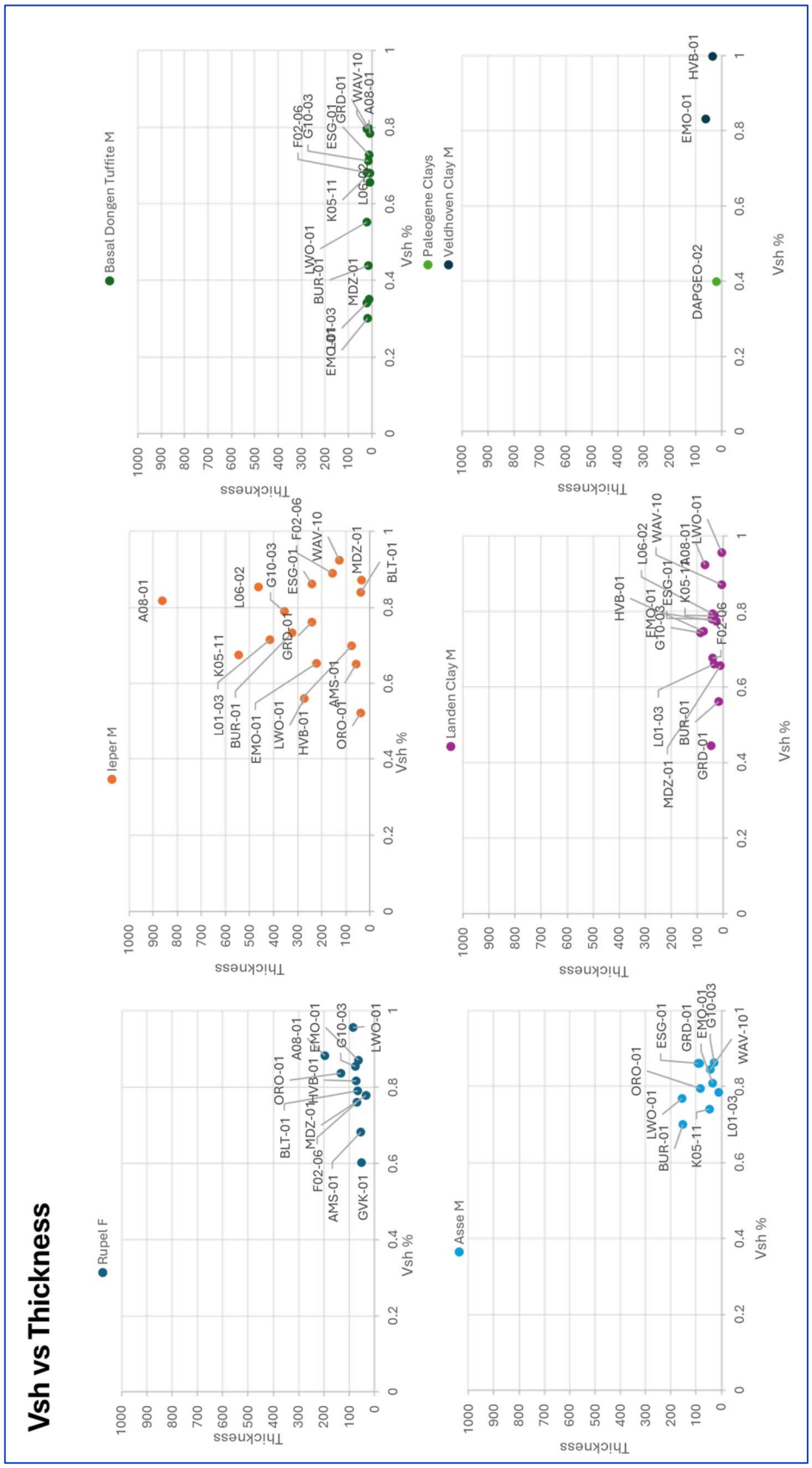

Figure 3.12: Vsh vs thickness cross plot, the combination of High Vsh and high thickness are preliminary indicators of good seal capacity.

The permeability data in these intervals are Horizontal Permeability from the MMR log are and are characterized by high uncertainty as they are not calibrated to core data as can be observed in the log plot from the DAPGEO-02 well presented in Figure 3.20.

More analyses are necessary to define what the minimum combination of Vsh and Thickness are to guarantee a good seal. These are function of a large number of factors such shale porosity and excess of pore pressure. As general indicator for similar clays and similar pore pressures, thick intervals with high Vsh are potentially better seals.

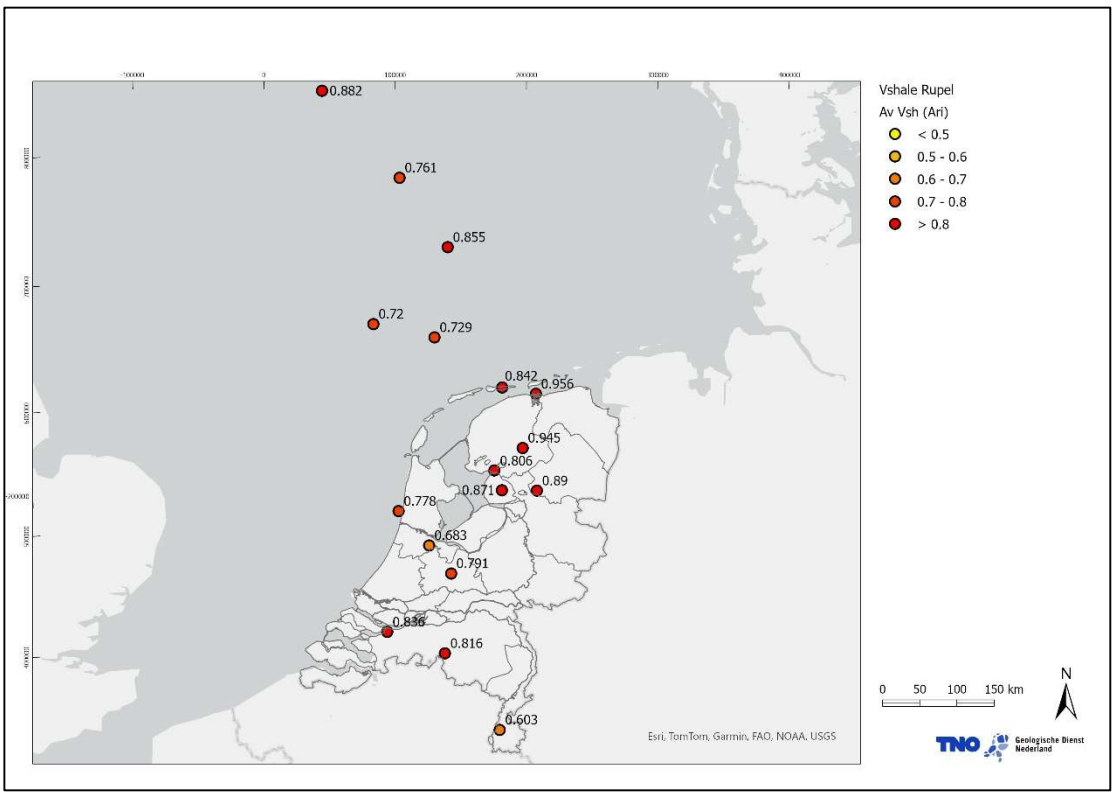

Figure 3.13: Spatial distribution of Vshale for the Rupel clays.

3.2.3 Porosity

The Effective and Total Porosities PHIE and PHIT, were calculated as described in the methodology section of this chapter.

Wells with core data available in combination with log data were used for calibration, specifically: BUR-01, ESG-01, GRD-01, and EMO-01, were used to calibrate the Total Porosity from the core, obtained through granulometric analysis to the Total Porosity calculated with sonic log in the Rupel clays. The porosity of the clay minerals, required as input for the Total porosity calculation in IP (Interactive Petrophysics Software from Geoactive), was adjusted until a match was achieved between core and log porosity (Figure 3.14). A similar procedure was followed to calibrate the porosity in WAV-10 for the De Wijk Member. The clay porosity calibrated with this procedure was used as a direct input for the calculation of Total Porosity from sonic log. Logs from well ORO-01 and RCA data from the Boom and Asse Members were used to calibrate shale clay ratio and dry clay density that were used as inputs for the Porosity log calculated from density log.

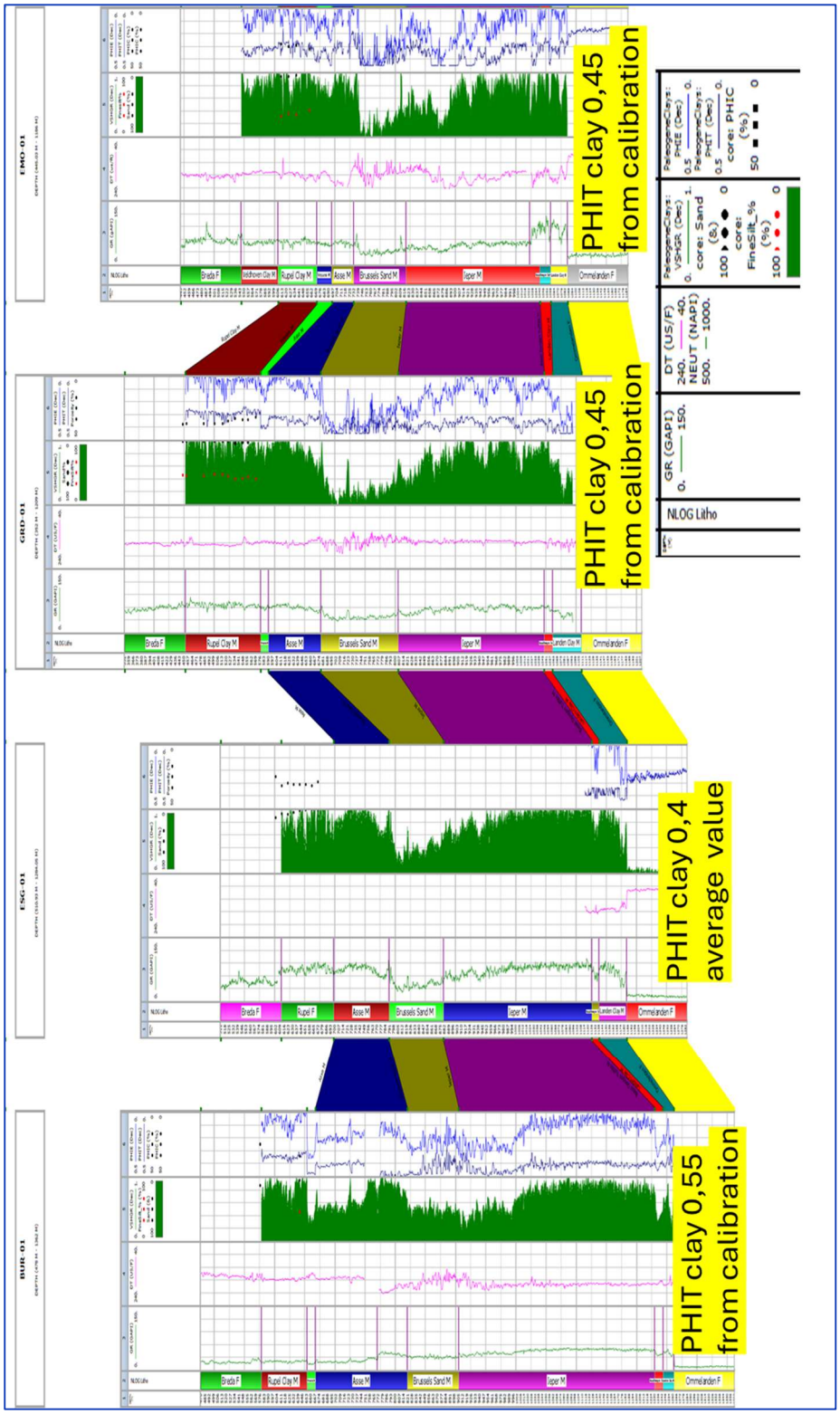

Figure 3.14 Cored wells with log data used for calibration the core data are from Verweij at al 2016. For each well are displayed from left to right, depth in MD, well stratigraphy, Gamma Ray log, Sonic in pink, density in red and neutron in green), computed Vsh with overlapped in black (black dots) sand % and in red the total of fine particles %, PHIT in dark blue and PHIE in lighter blue, black dots are Porosity from core. The volume of sands (1-Vsh) from both methods shows a very good match, while the porosity from log and core were matched by adjusting the clay porosity.

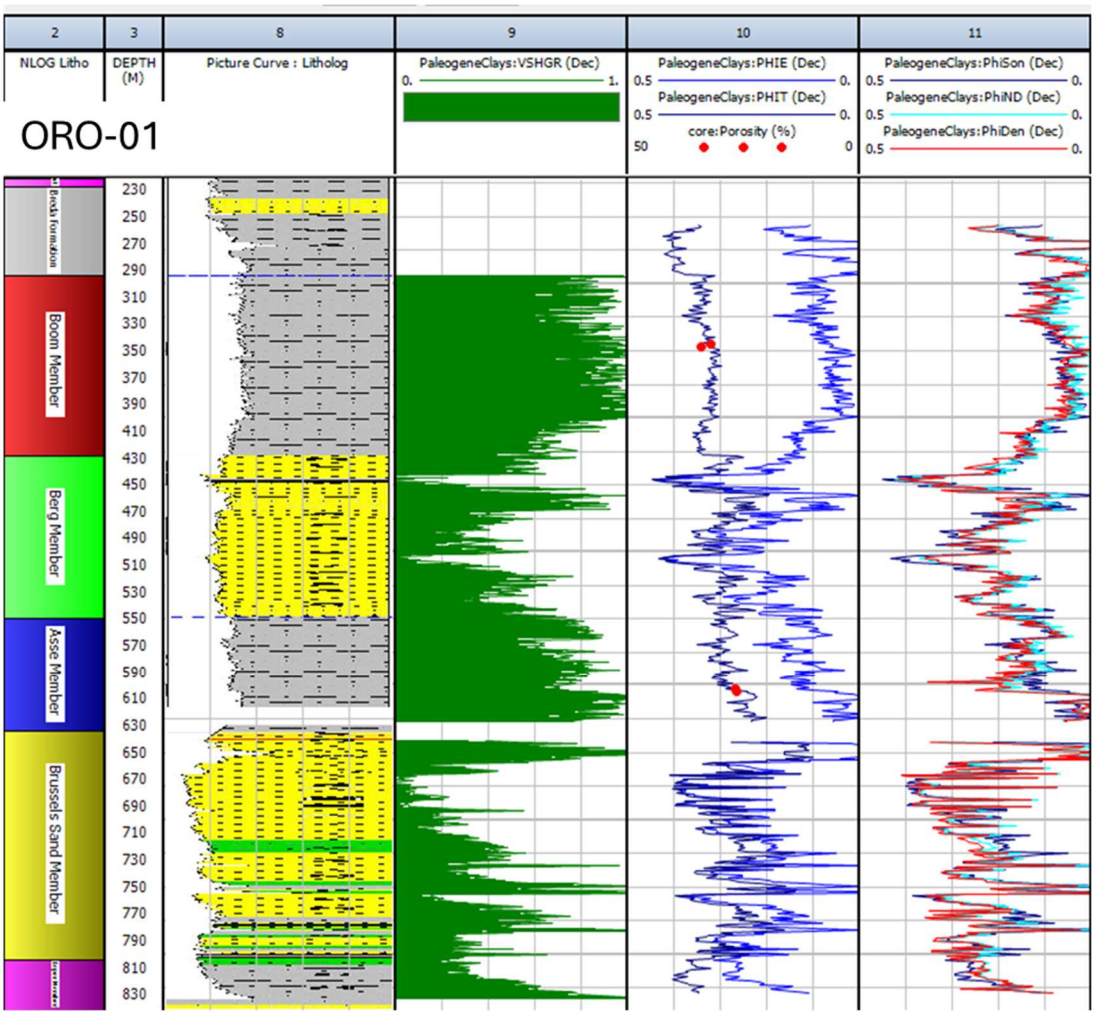

Figure 3.15: ORO-01 was used to calibrate the porosity using core data. The plot displays stratigraphy, depth in MD, lithology, calculated Vsh, calculated PHIE and PHIT and core porosity (red dots), and Porosity calculated with different methods.

As discussed in the methodology section the computed total porosity is highly affected by the parameters used to characterize the clay mineralogy and therefore core calibration is essential. To compare the porosity results and derive some regional observations arithmetic averages were calculated for each formation in each well and plotted against mid formation depth (Figure 3.17). This shows some porosity-depth trends related to porosity reduction with increasing burial depth. At least two compaction trends can be identified in the Rupel Formation, one from surface to 200m with fastest reductions of porosity, and one with gentler reduction of porosity with depth below 200m (Figure 3.16).

On a similar plot the core data from Verweij et al. (2016) and Opera TNO 411 (Vandenberghe et al., 2014) are presented, where the two trends can also be recognised. Shallower intervals, mostly analysed by core analysis show higher porosity ranges up to 60% porosity (at 30m depth), while deeper formation show porosities in the range 30-40%.

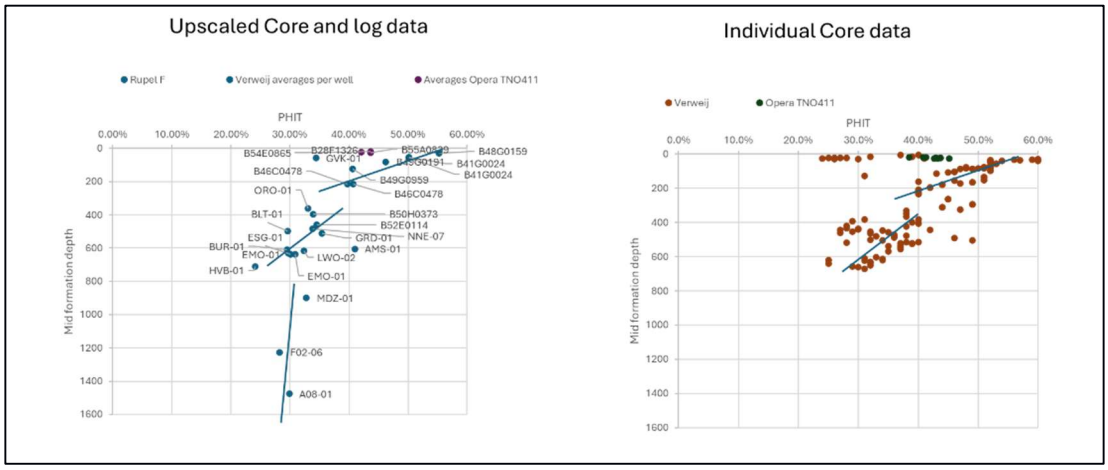

Figure 3.16: Total porosity (PHIT) vs mid formation depth for upscaled core and log data on the left and individual core data on the right. Both datasets are plotting data within the Boom Member clays Different porosity vs depth trends can be identified in the data.

The PHIT vs mid reservoir depth plot was made for each formation of interest. Some scatter can be observed which is likely related to facies variation.

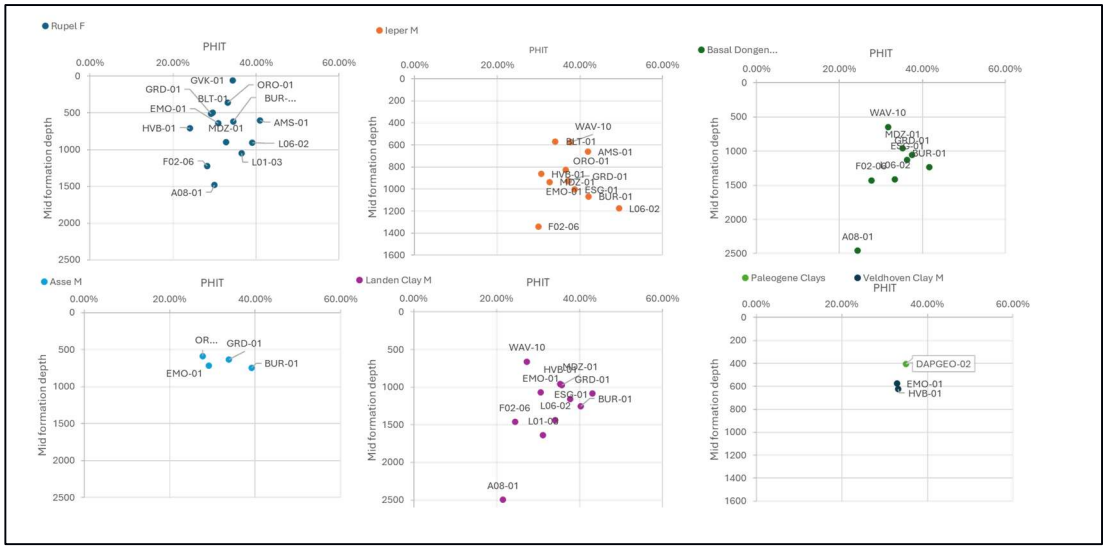

Figure 3.17: PHIT vs mid reservoir depth cross plot for each of the intervals of interest.

3.2.4 Permeability

All the available porosity (PHIT) and permeability (horizontal and vertical) data from cores and NMR logs for all formations of interest were plotted in a series of semilogarithmic cross-plots (Figure 3.18).

1) Plot a: Conventional core porosity and (horizontal) permeability from NLOG and Opera TNO411 datasets, cover a variety of Paleogene clay units and are coloured by unit according to NLOG stratigraphy. The samples from NLOG were acquired to characterise conventional Oil and Gas reservoirs (characterised by low Vsh and higher sand percentage) and were therefore focusing on more permeable parts of the unit. These samples are not indicative for the clay rich parts of the units but do highlight the heterogeneity that is present in the units. This plot shows the

limitations when using only legacy data and that it is not possible to perform unit specific analyses based on this alone.

2) Plot b: Log based, total porosity and uncalibrated permeabilities from NMR data from well DAPGEO-02, (Timur Coates plotted with pink dots and SDR model with grey dots). The stratigraphic interval is called undifferentiated Paleogene, as defined in Houben (2025), and no further subdivision into Formations or Members was possible. Since the NMR data are uncalibrated, they should be used only to derive qualitative observations and to observe the heterogeneity of the unit composed of high permeability sand and low permeability (probably sealing) silt and clays (see lithology description in well report as well as log plot in Figure 3.20). This plot also highlights the heterogeneity of the units and the influence of that heterogeneity on permeability.
3) Plot c: Porosity vs calculated horizontal permeability (Kv) derived from the Verweij et al. (2016) dataset (assuming kh/kv=5 or kh/kv=60 as indicated in Wemaere at al. (2008) and kh/kv =2 as indicated in Aertens et al. (2023)). This plot allows to directly compare the vertical permeabilities of the Verweij data with the horizontal permeability of the other datasets. Please note that the samples from the Verweij dataset, measured on clay samples, plot in the same range as the low permeable silt and clay intervals from the NMR dataset in Figure 3.18b.
4) Plot d: Vertical permeability (Kv) from the Verweij et al. (2016) dataset (orange dots); all samples of this dataset belong to the Boom Member and the hydraulic conductivity are calculated from grain size measurements. Measured permeabilities from the Borssele site in the Netherlands (Rizzo Associate Inc 2013) and measured hydraulic conductivity at Mol and Doel site (Wemaere et al. 2008) are plotted for comparison. For both dataset the hydraulic conductivity (in m/s) were converted to permeability (in mD) using, a conversion factor of 1.01E+08, this is the same conversion factor used in Verwej 2016a. Mol and Doel data consist of measurements of (vertical) hydraulic conductivity only, while Borssele data consist of porosity and hydraulic conductivity measured on different samples, with only two samples having both measurements. The sample with only hydraulic conductivity are plotted for comparison only using a fictitious 10% porosity. This plot shows that the estimated hydraulic conductivity of the Boom clay from grain size analyses fall in the same range as directly measured permeabilities.

The 4 plots presented in Figure 3.18 show the large variability of permeabilities within similar porosities and vice versa. This suggests the presence of different facies, each one characterised by different porosity-permeability trends as well as other processes influencing permeability (e.g., diagenesis). The influence of the facies can be observed in Figure 3.19 (left) where the porosity vs (vertical) permeability distribution of the Verweij dataset is coloured per sand content (1-sand content% = Vsh). The plot Vsh vs Permeability coloured per porosity Figure 3.19 (right) shows how porosity and permeability decreases with depth, which is related to compaction as well as diagenesis.

Similar observations about the impact of Vsh on the permeability were derived in an empirical study (Bourg, 2015). The study has demonstrated how in fine grained formations the volume of clay minerals in the formation affects the permeability more than the porosity; and that the porosity variations are largely controlled by burial depths. The author has also established that a 35% cut off on clay mineral class fraction (equivalent to the volume of clay minerals) corresponds to a major change in the shale microstructure from large grains framework supporting to clay matrix supporting. Below the cut off (<35% cut off), in the large grains framework support area, small increments of Vsh have larger impact on the (vertical) permeability that can quickly decrease by 6 orders of magnitude, because the fine

material partially fills the space between the grains, than above the cut off, where increments of Vsh produce reduction of vertical permeability only of to 1.5 orders of magnitude. Similar conclusions about the role of Vsh in permeability for the Opalinus clays were identified in the NAGRA 24-10 NTB report (NAGRA, 2024) where the transition between clay supported framework and grain supported framework was observed between 20-40 wt% clay.

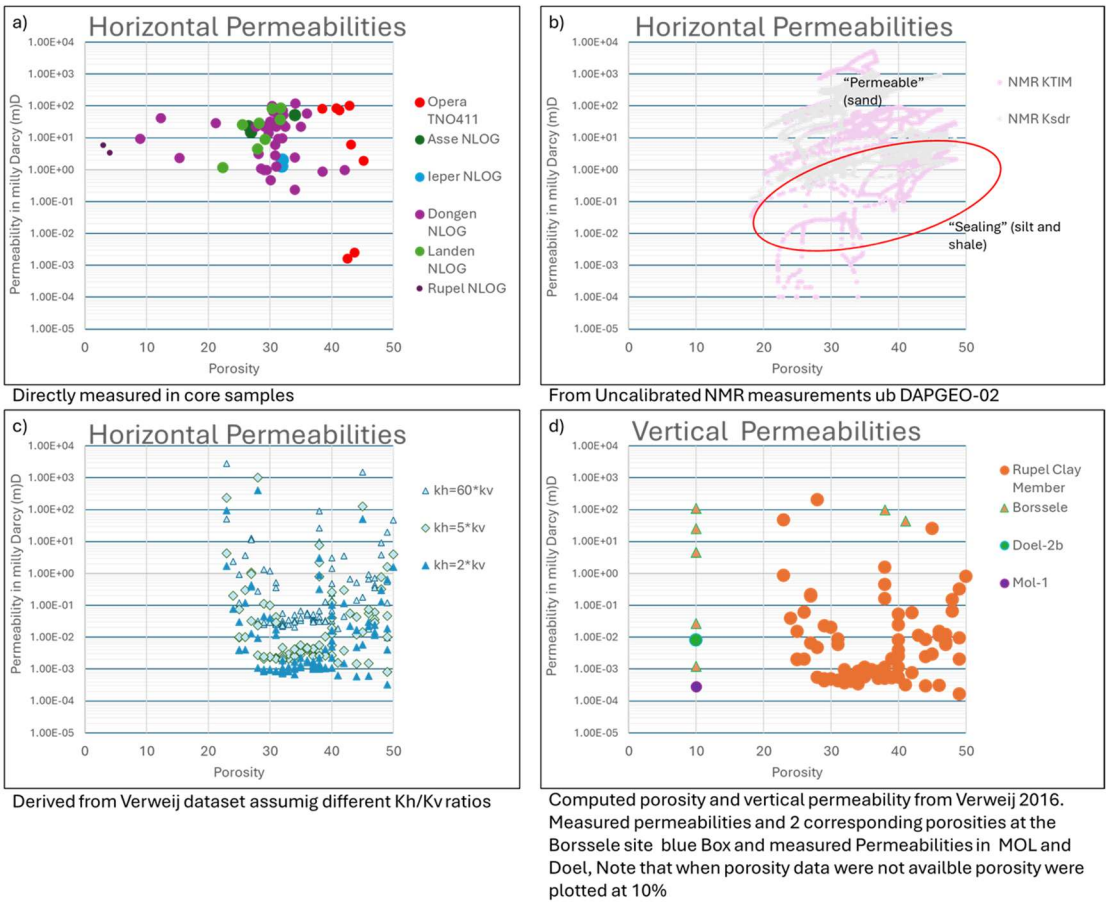

Figure 3.18: A series of Porosity and Permeability cross plots from different datasets plotted in a semi logarithmic graph. The plots show the large heterogeneity of data, the high uncertainty but also highlights in the Boom clay the existence of permeability compatible known seals. See text for more details.

Using a clay mineral class fraction cut off of 35% corresponds to a Vsh of 60-50%. This value is calculated using the clay to shale ratio of 0.6-0.7 as indicated by the XRD results.

The NMR data (in DAPGEO-02 well Figure 3.20) clearly shows that low permeabilities are also associated with fine grained dominated intervals poor in clay minerals that seem to be underrepresented in the core datasets. This observation confirms that a facies-based approach is the key to characterize such formations. To ensure that low-permeability, silty-rich intervals with low clay mineral content can be identified, a porosity permeability transform must be established for the facies with low Vsh. This is not possible with the data currently available as most of the information from the low permeability silty facies are from the uncalibrated NMR data set.

To predict the permeability in clay mineral rich facies characterised by high Vsh, qualitative predictions are possible when Vsh is known by using the graph in Figure 3.19 (left). Based on

this graph for example Vsh>80 %, vertical permeabilities can vary between $5X10^{-5}$ mD and 0.01 mD depending on their burial depth (i.e. $5X10^{-5}$ are expected below 700 m).

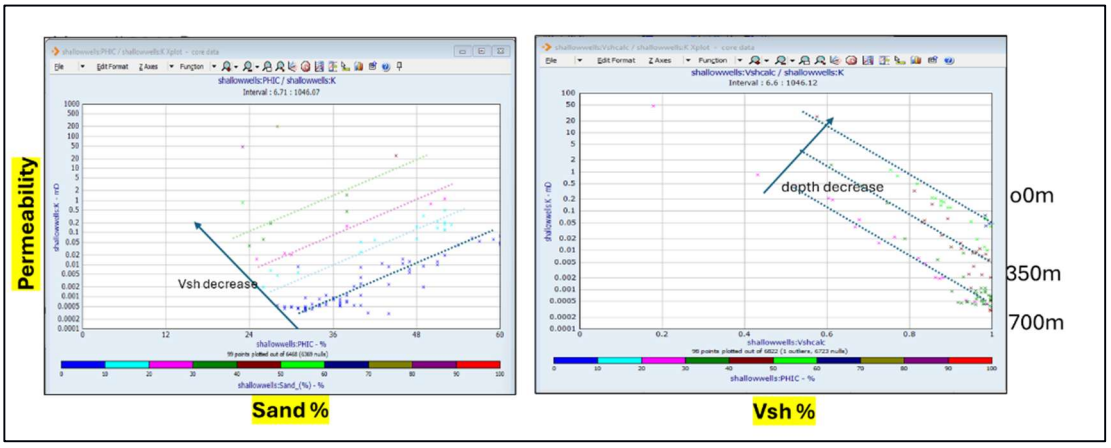

Figure 3.19: Plots of porosity vs vertical permeability coloured by sand content on the left and Vsh vs vertical permeability coloured by porosity on the right. In both graphs the Verweij dataset is plotted. The plot on the left shows how the porosity-permeability trends vary with Vsh, while the plot on the right shows how the burial depth (and therefore porosity) also affects the permeability.

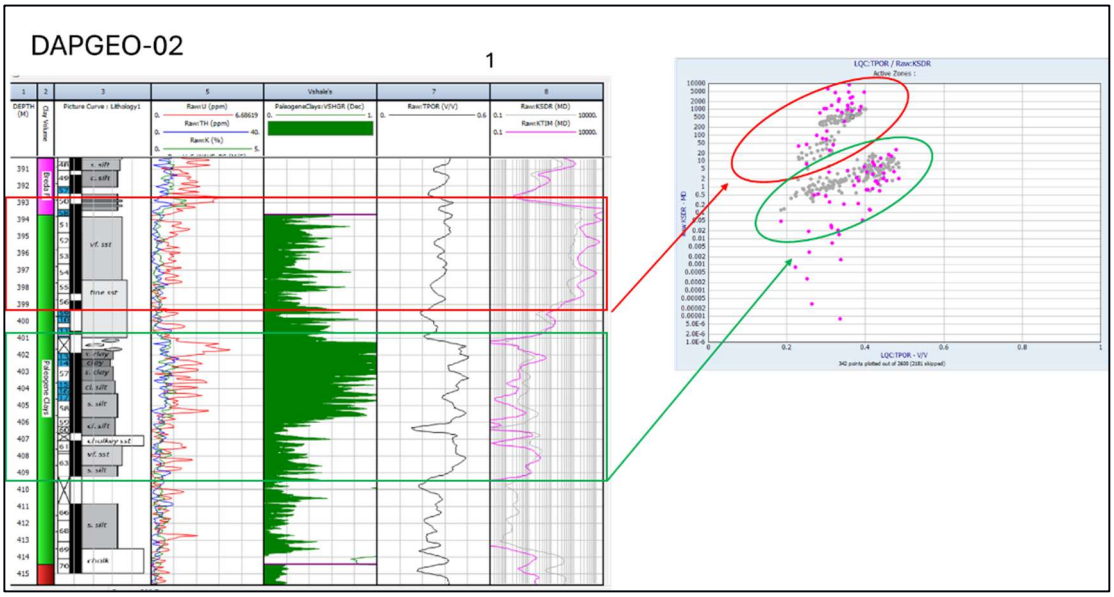

Figure 3.20: NMR data in DAPGEO-02 show the existence of low permeability in silty intervals characterised by low Vsh. In the log plot are displayed from left to right depth in MD, Stratigraphy based on Houben (2025), Core description, Spectral GR, calculated Vsh, total porosity from NMR, SDT and Timur permeabilities from NMR data. The porosity permeability cross plot on the left shows the high permeability sandy facies (in the red circle) and the two low permeability finer grained facies with high and one with low Vsh (in the green circle).

4 Seismic analysis

3D seismic data is available for the majority of the Dutch offshore as well as for large parts on the Dutch onshore area. Seismic data can be used not only for 3D mapping of subsurface units but also to identify faults, fractures, salt diapirs, (paleo) fluid flow structures such as pock marks or seismic chimneys, gas presence (e.g., bright spots), facies differences, sedimentological features such as submarine channels and fluvial fans, and general heterogeneity of the subsurface. Most of this information is recorded in the seismic signal and can be visualised using so called seismic attributes. Different types of seismic attributes enhance different properties of the seismic signal and can therefore be used to identify specific features. For the purpose of this study, the focus was on the identification of faults and fractures within the Paleogene Clay units.

A seismic analysis has been conducted using three 3D seismic volumes (Figure 4.1 and Table 4.1) covering an area of approximately 3820 km^2 in total in this study. The goal of this analysis is to *(i)* identify the fault and fracture zones and *(ii)* examine their seismic attributes within Paleogene clay intervals on- and offshore of the Netherlands. Fundamentally, the occurrence and geometry of faults and fractures can give key information about the mechanical behaviour and hence sealing properties of the Paleogene clay layers. Therefore, it is essential to identify the presence of these faults to assess their potential effect on the sealing capacity of clay sediments.

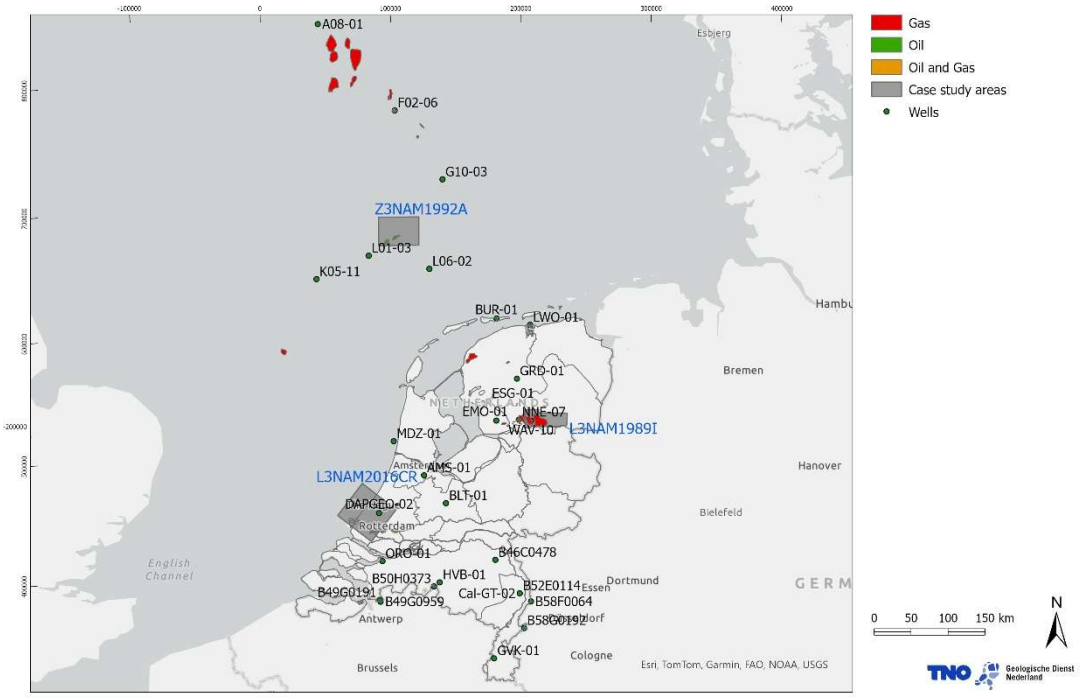

Figure 4.1. Location of 3D-seismic volumes used for in-depth fault and seismic attribute analysis.

Additionally, to be able to enhance fault identification on horizon surfaces in clay intervals, a seismic attribute analysis has been performed in areas of interests. Seismic attributes are derived geometric and statistical characteristics (obtained from seismic data) and can provide essential details for structural interpretations. This combined approach has been designed to determine small- and large-scale fault structures developed in various intervals of clay sediments in this study.

Table 4.1. Names of 3D seismic volumes used in our analysis and the area that they cover.

No	3-D Volume	Name	Area (km^2)
1	L3NAM1989I	De Wijk	521
2	Z3NAM1992A	F17/18	720
3	L3NAM2016CR	IJsselmonde	2,577

4.1 Methodology

The 3-D volumes used for seismic analysis have been acquired from NLOG website of TNO - Geological Survey of the Netherlands[20]. Amersfoort RD New and ED50-UTM32 coordinate systems have been used for on- and offshore volumes, respectively. Each seismic volume is processed with an acoustic impedance in the time domain. In order to validate the depth of top and base horizons of Paleogene Clay layers, numerous well data, acquired from NLOG[21], have been projected in each individual seismic volume.

For the seismic interpretation as well as the seismic attribute calculation the software Petrel® v. 2024 from Schlumberger was used. For two study areas an additional horizon cube interpretation was performed using the software PaleoScan® v. 2024 from Ellis. For each survey the top and base of the Paleogene Clay interval has been mapped using the respective seismic horizons. These horizon depths have been correlated with a general time-to-depth relationship using the Velmod velocity model v3.2[22]. Horizons were mapped using a combination of manual interpretation and machine learning guided tools (Schlumberger proprietary tool) to provide smooth and continuous surfaces for further seismic attribute analysis. Faults have been mapped in a very similar workflow, using a combination of machine learning guided interpretations combined with handpicked faults to gain in-depth insights for specific fault structures in different scales.

For the horizon cube interpretation in Paleoscan, the horizons interpreted in Petrel were used as guiding horizons for the generation of an semi-automated amplitude based model grid for the whole seismic cube in the stratigraphic interval of interest. The initial workflow generates horizon patches based on seismic signal similarity which need to be connected manually for several intervals to cover the whole study area and give geological guidance. Using the refined model grid as input, a 3D relative geological time model is created that can be used to export an unlimited number of chronostratigraphic horizons. A number of these horizons was selected and moved back to Petrel for the seismic attribute mapping.

Seismic surveys are generally used for the interpretation of stratigraphic units in the deeper subsurface by tracing seismic reflectors in 2D and 3D space. In addition to the visible geological information, the data within seismic surveys can also be used to derive information on amplitude, frequency, attenuation or other geophysical aspects recorded in

[20] https://www.nlog.nl/datacenter/smc-3d-surveys – 3D seismic data
[21] Datacenter | NLOG - wells
[22] Velmod-3.2 (March 2024) | NLOG

the seismic signal. These derived parameters can then again be used to identify geological properties in the subsurface.

For the context of this study the focus was on the identification of discontinuities in the seismic signal, signifying faults or fractures. For this purpose, the seismic attributes Chaos and Variance were selected. The seismic attribute Chaos enhances zones with a lack of consistency of the seismic signal in dip and azimuth, highlighting chaotic, faulted and fractured or geologically complex zones. The variance attribute primarily reveals discontinuities like fractures and faults by essentially measuring the variation or discontinuity within the seismic signal. A breakdown in seismic continuity (structural discontinuities) such as faults or fractures is indicated with high values when the variance attribute is calculated. In principle, Variance highlights changes in continuity, whereas Chaos identifies areas where the dip and azimuth are highly irregular. Both attributes are calculated for the whole seismic survey and are later mapped onto the interpreted horizons for visualisation.

Higher resolution figures can be found in Appendix E.

4.2 Results

4.2.1 F17/18 - Z3NAM1992A

The seismic survey is located in the southern part of the Dutch Central Graben at the transition to the Terschelling Basin to the east (Figure 2.1). Within the area of the seismic survey five not producing oil fields are located, the fields F17-FA Korvet, F17-FB Brigantijn and F18-FA Fregat are all located in the Upper Jurassic Friese Front Formation while the fields F17-NE Rembrandt and F17-SW Vermeer are located in the Upper Cretaceous Ommelanden Formation (Figure 4.2).

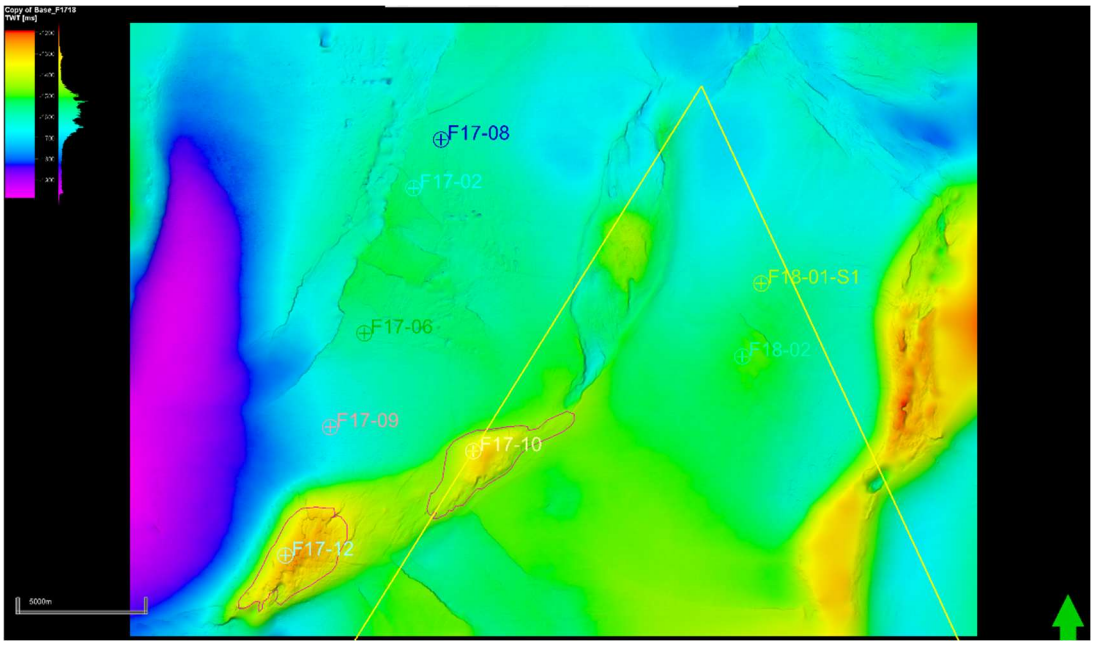

Figure 4.2 Time depth map (colour scale indicates depth from deep - purple to shallow - red) of the Base of the Lower North Sea Group with the location of the F17 Upper Cretaceous oil fields (red lines), selected wells and the transect shown in Figure 4.3 (yellow line).

This study area was selected because of the existence of the two oil fields in the Upper Cretaceous that are sealed by Paleogene clays, as well as the close vicinity to the well L01-03 which was analysed in detail in work package 3. The depth of the interval of interest is significantly deeper than in the other case studies, which is typical for the Dutch offshore area. The time depth of the Base Upper North Sea Group is between 700 and 1000 ms while the time depth of the Base Lower North Sea is between 1200 and 2000 ms. At this depth and in these sediments the velocity is can be approximated to 1 ms equals 1 m.

In the seismic survey 5 main horizons were interpreted using a mix of AI guided interpretation and manual interpretation (Figure 4.3 B). The horizons were selected based on their strong reflective signal and regional continuity. The stratigraphic position of these horizons was interpreted by linking to the stratigraphic interpretation of well F17-10 as well as regional understanding of the seismic signal. These horizons are the Base of the Upper North Sea Group, a bright reflector (peak) approximately at the Base of the Brussels Marl Member, a bright reflector (peak) within the Ieper Member, a reflector (peak) near the base of the Ieper Member as well as the Base of the Lower North Sea Group or Liessel Member (trough).

In addition a Multi-Horizon cube was generated for this case study area using Paleoscan. Based on the previously mentioned interpreted horizons a horizon model was created for the whole interval. This allows to extract additional horizons as well as attributes for these horizons even when the seismic reflector is less prominent or continuous. An additional 100 horizons were created using this method from which 5 were selected for the attribute analysis (Figure 4.3 C).

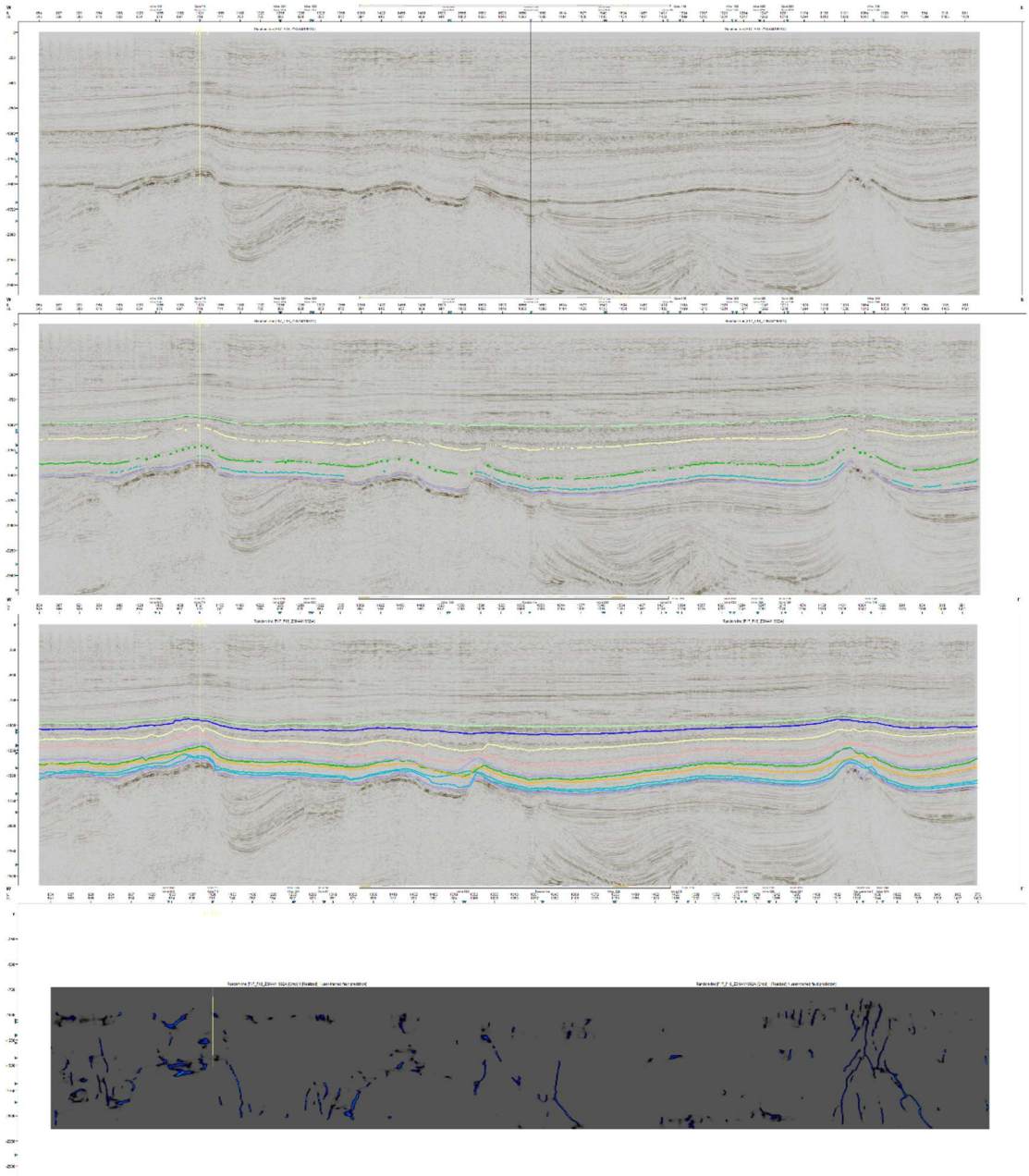

Figure 4.3 The transect show in Figure 4.2. A: Showing only the seismic signal as well as the location of well F17-10, located in the F17-Rembrandt field B: The seismic line with the location of the interpreted horizons (Light Green – Base Upper North Sea Group, Yellow – approximately Base Brussel Marl Member, Dark Green – Intra Ieper Member, Light Blue – near Base Ieper Member, Purple – Base Liessel Member) C: The seismic line with all horizons selected for the seismic attribute analysis D: The result of the AI guided fault interpretation along the same seismic line, dark blue colours indicate identified faults on the seismic

4.2.1.1 Seismic attributes

As the focus of this work package was on the identification and classification of faults and fractures in the Paleogene clays as well as their potential impact on the sealing capacity of the clays we chose two different seismic attributes (Chaos and Variance) whose main purpose is to visualize discontinuities in the seismic signal. In this report only the results of

the Chaos attribute are shown as the results of the Variance are very similar and do not provide additional information.

Base Liessel Member

The reflector at the base of Liessel Member marks the downward transition from the clastic North Sea Supergroup to the carbonates of the Chalk Group. It is a very strong reflector (trough) indicating the transition from softer sediments to the harder chalk of the Upper Cretaceous. The Chaos attribute highlights the fault zones in the north west and center of the cube as well as the salt walls in the east which have also been identified by the AI guided fault interpretation (Figure 4.4). Especially the fault zone in the center (also located above a salt wall) shows nicely the features related to faulting with a left-lateral movement component typical for the Dutch Central Graben.

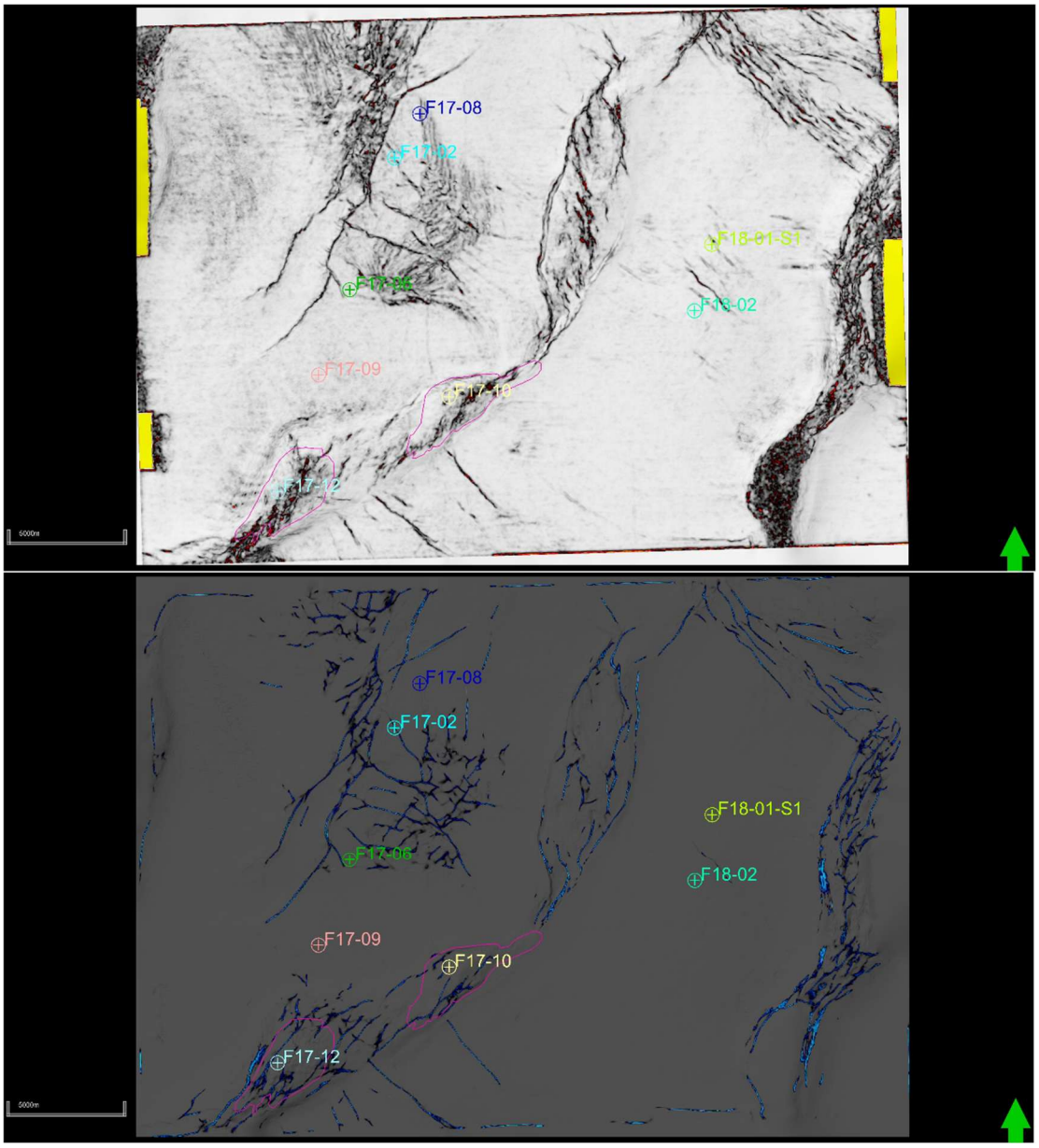

Figure 4.4 Map of the extracted seismic attributes at the Base Liessel Member A: Chaos attribute, B: the AI fault interpretation, dark blue colours indicate identified faults on the seismic

In between these clear faulted zones the horizon does not show any strong fracturing or faulting, suggesting a very homogenous distribution without obvious fracturing or other structures suggesting heterogeneity in the sediments.

The Liessel Member and the overlying De Wijk Member both are around 20 m thick each in the study area. The lower part of this interval shows the same characteristics as the Base Liessel Member while the first indication for more fractures especially between the big structures can be seen in the De Wijk Member.

Near Base Ieper Member

The Near Base Ieper Member is interpreted as a peak approximately 60 ms above the Base Liessel. The transition from the underlying member is not visible on seismic, the whole package being characterised by quite transparent, discontinuous, irregular reflectors.

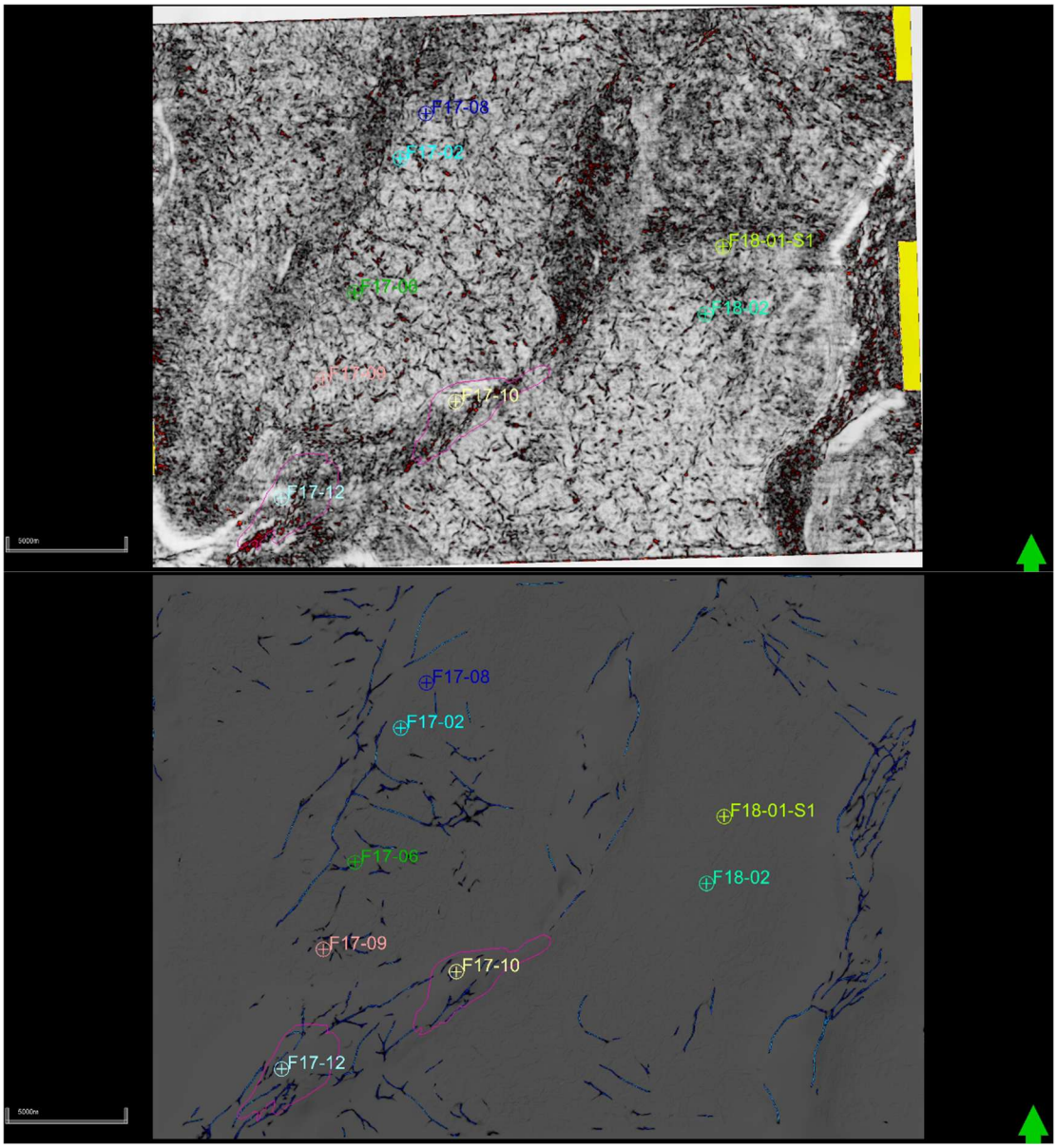

Figure 4.5 Map of the extracted seismic attributes at the near Base Ieper Member A: Chaos attribute, B: the AI fault interpretation, dark blue colours indicate identified faults on the seismic

On a map view showing the Chaos attribute (Figure 4.5) the reason for this irregular pattern becomes more evident. A fracture network can be seen that does not follow the classic structural trends but is more irregular and polygonal in shape – so called polygonal faults.

It was attempted to train the AI guided fault interpretation to also include these structures with very limited success. The best way to visualize these structures is using these seismic attributes.

The polygonal faults are visible throughout the whole Ieper succession from the Base Dongen Formation to the Base of the Brussels Marl Member. Towards the top the size of the polygons gets continuously smaller.

Near Base Brussels Marl Member

The Brussels Marl Member is the distal equivalent of the Brussels Sand Member and consists of brownish grey, silty, calcareous clay to marl. The seismic signal of this interval is more continuous and less irregular. The map view of the Chaos attribute (Figure 4.6) shows less of the classic polygonal fracture pattern and more of a pattern related to the general structural setting, orthogonal to the main structures. At the Top of the Brussels Marl Member even this pattern is less evident and a more homogeneous signal can be seen between the main fault zones.

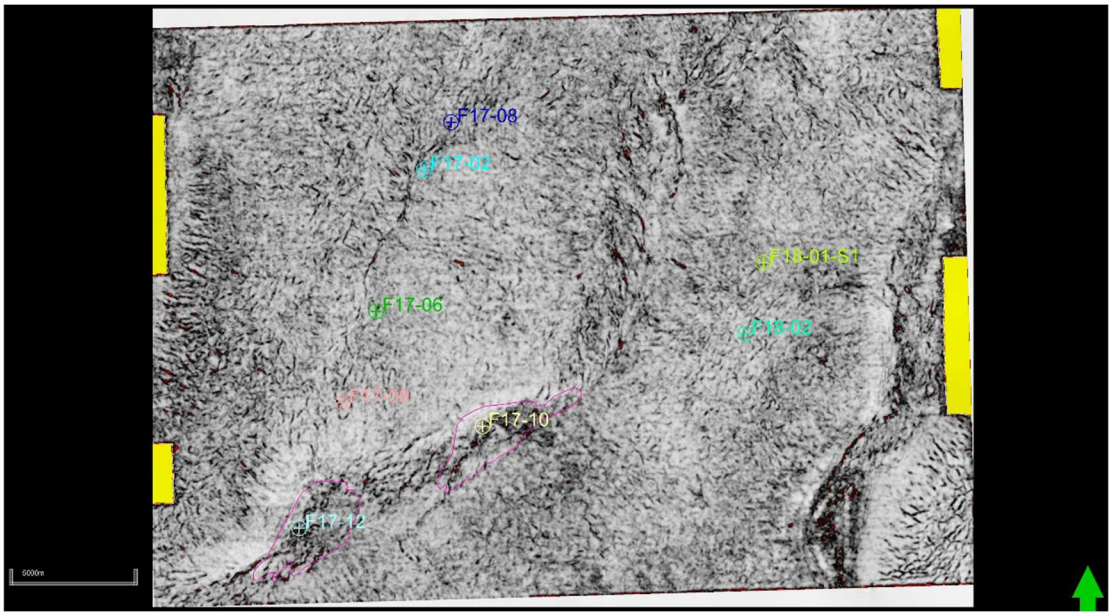

Figure 4.6 Map of the Chaos seismic attribute at the Base Brussels Marl Member

Above the Brussels Marl Member the seismic reflectors become more pronounced and the irregular pattern resumes. These reflectors represent the Asse Member of the Dongen Formation and the Boom Member of the Rupel Formation (Figure 4.3). The polygonal faulting is again apparent on the maps of the Chaos attribute, however with a much smaller size of the polygons.

Base of the Upper North Sea Group – Miocene Unconformity

The top of the Paleogene interval is formed by the Miocene Unconformity. A clear Unconformity and peak on the seismic which is overlain by the Late Neogene prograding sediments of the Eridanos Delta. This horizon represents an erosional surface and was

probably exposed for some time before rapid burial by the prograding delta system. The polygonal fault structures are again visible on the Chaos attribute (Figure 4.7).

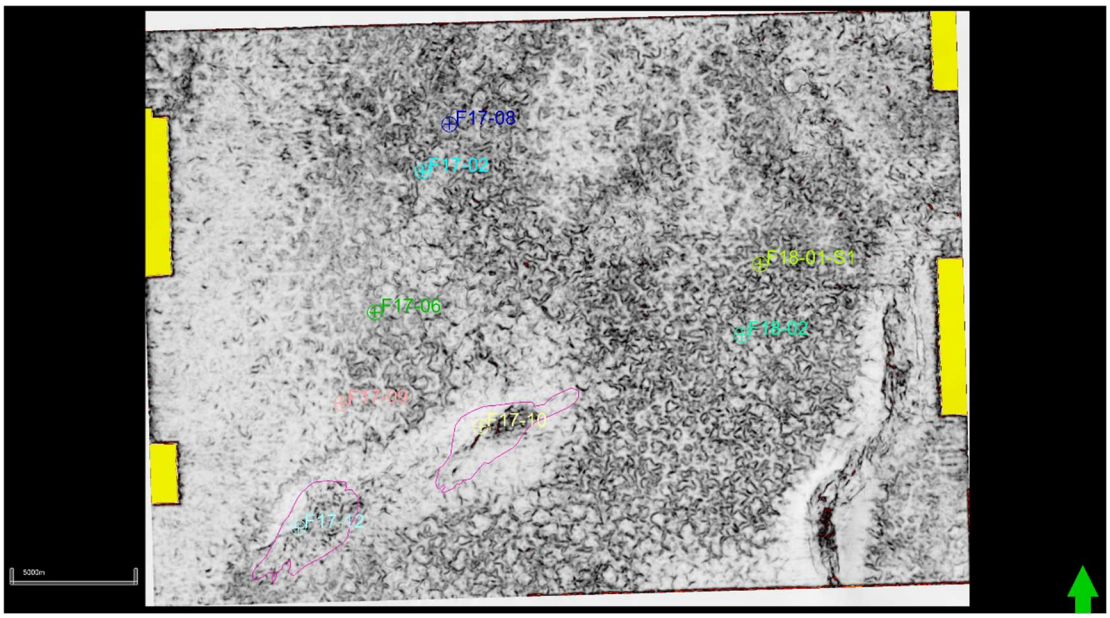

Figure 4.7 Map of the Chaos seismic attribute at the Top of the Middle North Sea Group below the Miocene unconformity

4.2.2 DeWijk – L3NAM1989I

The seismic survey is located in the southern part of the Friesland Platform at the transition to the Lower Saxony Basin to the east (Figure 2.1). Within the area of the seismic survey three gas fields are located, the fields De Wijk and Wanneperveen are stacked reservoirs, containing gas in the Triassic, Jurassic and Paleogene intervals (Figure 4.8). The Marknesse field is not producing and contains gas only in the Paleogene.

This study area was selected because of the existence of the three gas fields in the Lower Paleogene as well as the presence of wells WAV-10 and NNE-07 which were analysed in detail in work package 3. The depth of the interval of interest is between 200 and 1000 m. Due to the shallow burial and the location in the onshore, the upper boundary is not visible on the seismic. The time depth of the Base Lower North Sea is between 400 ms in the east and 900 ms dipping towards the west. At this depth and in these sediments the velocity is can be approximated to 1 ms equals 1 m.

The seismic data shows clear artifacts of the acquisition in the upper part of the survey, causing gaps in the seismic signal (white triangles in the upper part, Figure 4.9 A) and therefore to be difficult to trace and interpret. These artifacts are clearly visible on the attribute maps as a grid.

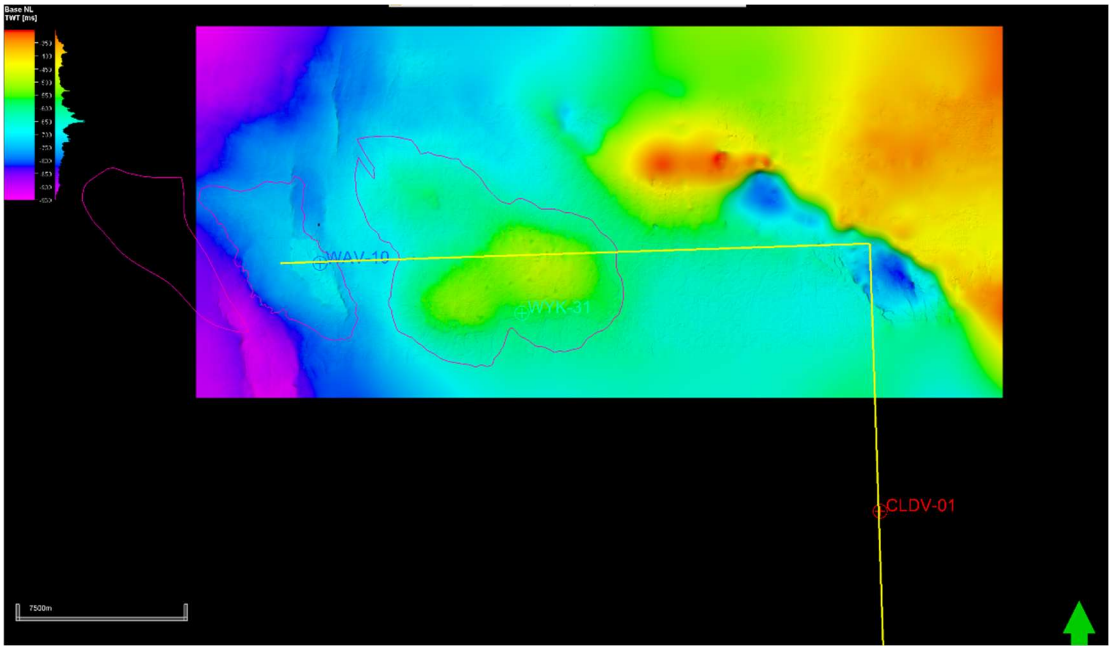

Figure 4.8 Time depth map of the Base of the Lower North Sea Group (colour scale indicates depth from deep - purple to shallow - red) with the location of the De Wijk, Wanneperveen and Marknesse gas fields (purple lines), selected wells and the transect shown in Figure 4.9 (yellow line).

In the seismic survey only the Base Lower North Sea Group was interpreted using a mix of AI guided interpretation and manual interpretation (Figure 4.9 B). Other horizon interpretations were not possible due to the low quality of the seismic. The stratigraphic position of these horizons was interpreted by linking to the stratigraphic interpretation of well CLDV-01 as well as regional understanding of the seismic signal. The quality of the seismic made the use of Paleoscan for a horizon cube impossible so additional horizons for the interpretation were created by horizontally shifting the Base Lower North Sea (Figure 4.9 C). This gives reasonable results as the depositional setting of the Paleogene in this area produced a layer cake arrangement. Based on the seismic interpretation maps were generated for the Intra Ieper Member (trough at the base of a set of stronger reflectors), the Top of the De Wijk Member (peak at the top of a set of stronger reflectors) and the Base of the Liessel Member/Lower North Sea Group (trough indicating the transition towards the harder sediments of the Chalk Group). The AI guided fault interpretation also only gave reliable results for the lower part of the survey up to the Base of the Lower North Sea Group (Figure 4.9 D).

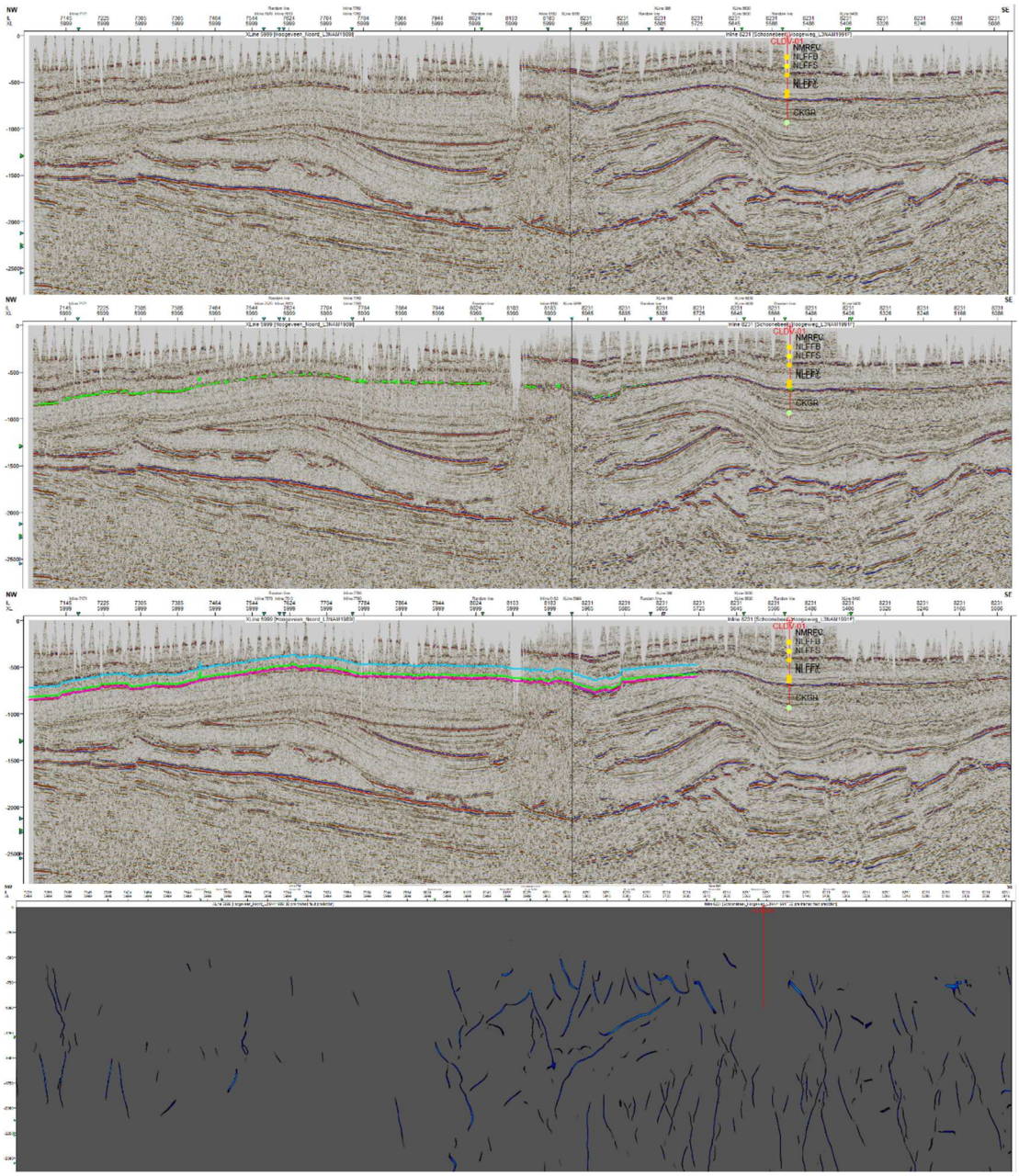

Figure 4.9 The transect show in Figure 4.8. A: Showing only the seismic signal as well as the location of well CLDV-01 B: The seismic line with the location of the interpreted horizons (Blue – Intra Ieper Member, Green – Top De Wijk Member, Purple – Base Liessel Member) C: The seismic line with all horizons selected for the seismic attribute analysis D: The result of the AI guided fault interpretation along the same seismic line, dark blue colours indicate identified faults on the seismic

4.2.2.1 Seismic attributes

In agreement with the previous case study the focus was on the seismic attributes Chaos and Variance, with the Chaos results presented and discussed here.

Base Liessel Member

Similarly to the offshore case study F17/18 the Base Liessel Chaos attribute mostly shows the location of the major fault zone in the east of the seismic survey. At the location of the De Wijk field as well as the Wanneperveen field the outline of the gas reservoir can be seen.

Gas in the pore space of sediments causes a density difference compared to water filled pore space. This density difference results in a so called “bright spot” on the seismic signal, a very strong reflector. The boundary between the gas filled pore space and the water filled pore space is picked up by the chaos attribute. Otherwise, the seismic character of the Base Liessel Member is again rather homogeneous and no other fracture patterns of depositional structures are visible (Figure 4.10).

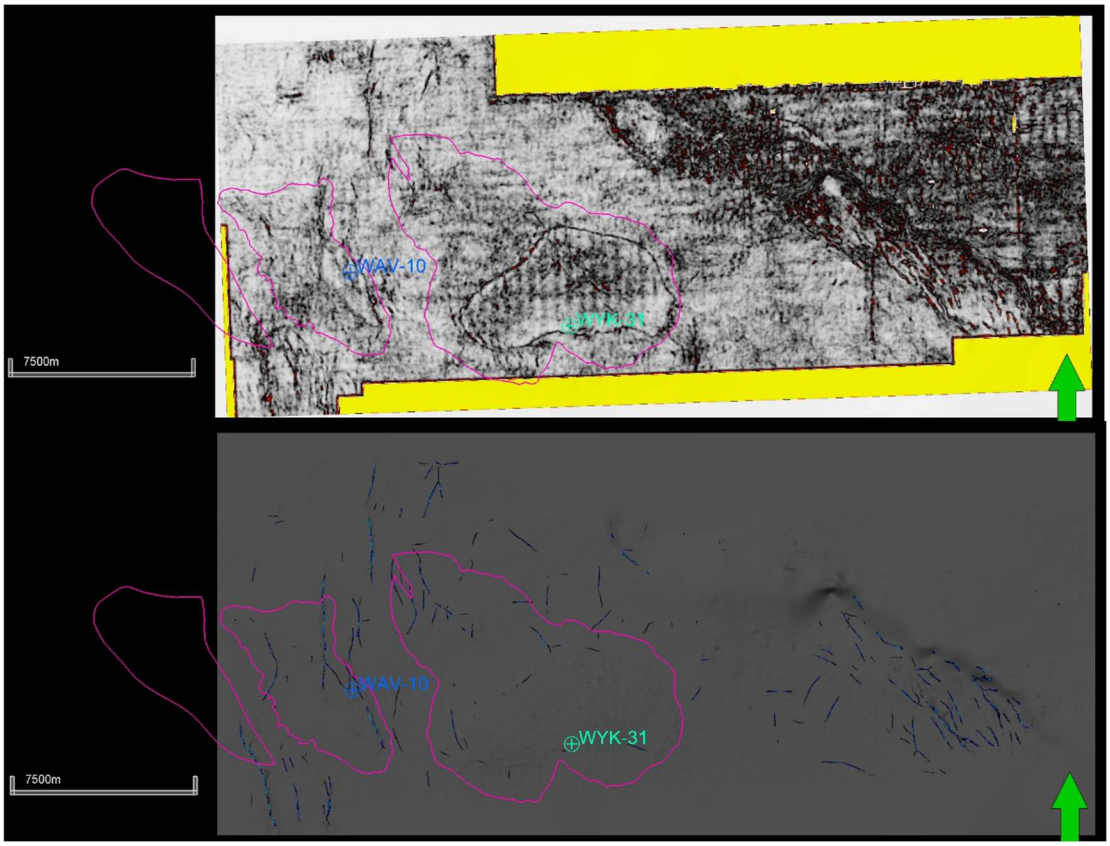

Figure 4.10 Map of the extracted seismic attributes at the Base Liessel Member A: Chaos B: The AI fault interpretation, dark blue colours indicate identified faults on the seismic

Top De Wijk Member

The Liessel and De Wijk Members are about 20 m thick each. Again, very comparable to the F17/18 case study, the polygonal fault structures start roughly at the base of the De Wijk Member, even though the De Wijk Member is considered a reservoir for the fields in this area. The polygonal pattern is less visible due to the checkerboard overprint from the seismic acquisition, but at the location of the De Wijk field in the centre of the survey polygonal features can be identified (Figure 4.11).

Intra Ieper Member

The lower part of the Ieper Member is again characterised by rather transparent, irregular seismic reflectors. The Intra Ieper Member layer was placed at the base of a set of more continuous strong reflectors that are traceable regionally in the Ieper Member (de Haan et al. 2020). The checkerboard signal from the seismic acquisition is more prominent but especially in the deeper parts of the layer the polygonal structures are clearly visible (Figure 4.12).

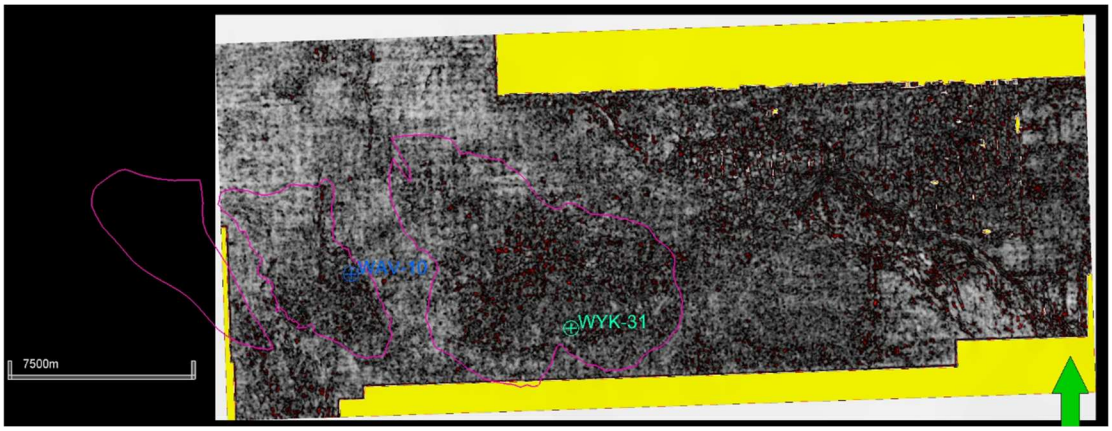

Figure 4.11 Map of the Chaos seismic attribute at the base of the De Wijk Member

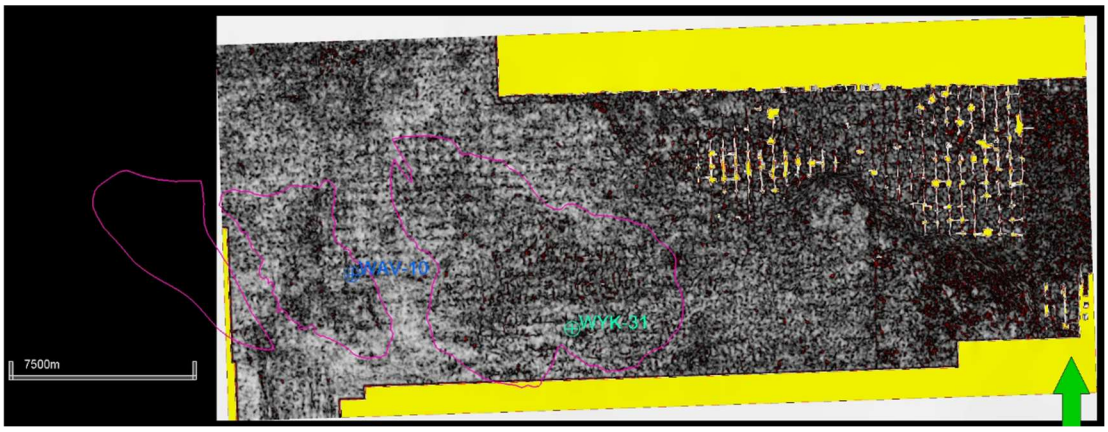

Figure 4.12 Map of the Chaos seismic attribute at the Intra Ieper Member

4.2.3 Monster/Donkersloot IJsselmonde – L3NAM2016CR and L3NAM2012AR

These merged seismic surveys are located in the West Netherlands Basin, bordering the Zeeland High in the southwest below the city of Rotterdam towards the coast (Figure 2.1). Within the area of the seismic surveys the field IJsselmonde is located as well as the well DAPGEO-1 which was analysed in detail in work package 3 (Figure 4.13).

The selection of these surveys was made with respect to the presence of the IJsselmonde gas field within the Oosteind Member (aka Basal Dongen Sand Mb) with Ieper Member serving as the seal. The reservoir is located above the 20 m thick Landen Fm and the top of the reservoir is at 510 m depth. The lower part of the IJsselmonde gas field is present at about 700 m depth in the Holland Greensand, which is below the level of interest of this study.

The depth of the interval of interest is between 300 and 1000 m. The base of the Upper North Sea Group can be inferred on the seismic. The stratigraphic subdivision for the Lower and Middle North Sea Groups is based on the stratigraphic interpretation of well PRW-01-S1[23]. The time depth of the Base Lower North Sea is between 400 ms in the east and 1000 ms dipping towards the southwest (Figure 4.13, Figure 4.14).

[23] https://www.nlog.nl/nlog-mapviewer/brh/106513602?lang=en

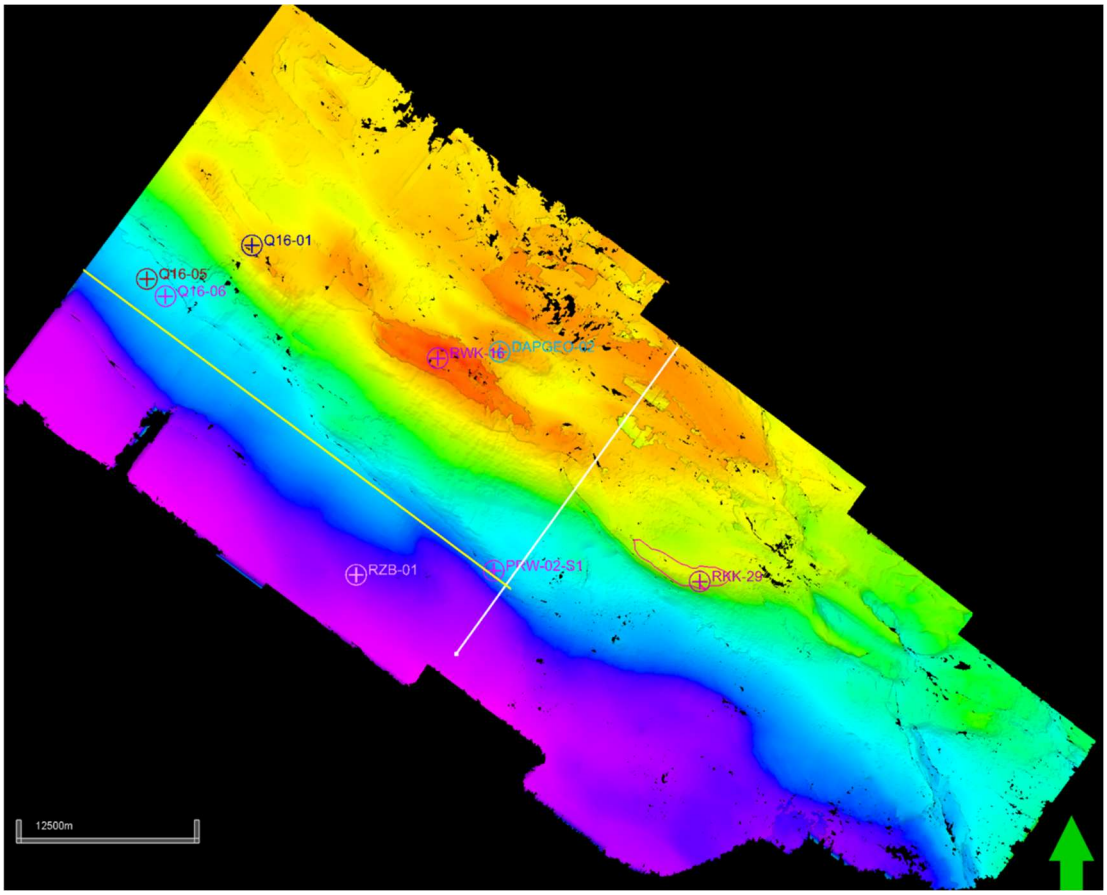

Figure 4.13: Time-depth map of the Base of the Lower North Sea Group (colour scale indicates depth from deep - purple to shallow - red) with well locations (circled cross), cross section line (white) and the gas field (red) are indicated. The locations of the cross-sections in Figures 4.14 and 4.15 are marked in white.

In the northeast of the case study area the Paleogene sediments are mostly eroded during the Pyrenean inversion pulse as well as again during the Miocene (Figure 1.1). Only the older units (basal parts of the Dongen Formation and Landen Formation) are preserved in smaller synclines, like at the location of well DAPGEO-02. At this depth and in these sediments the velocity is can be approximated to 1 ms equals 1 m.

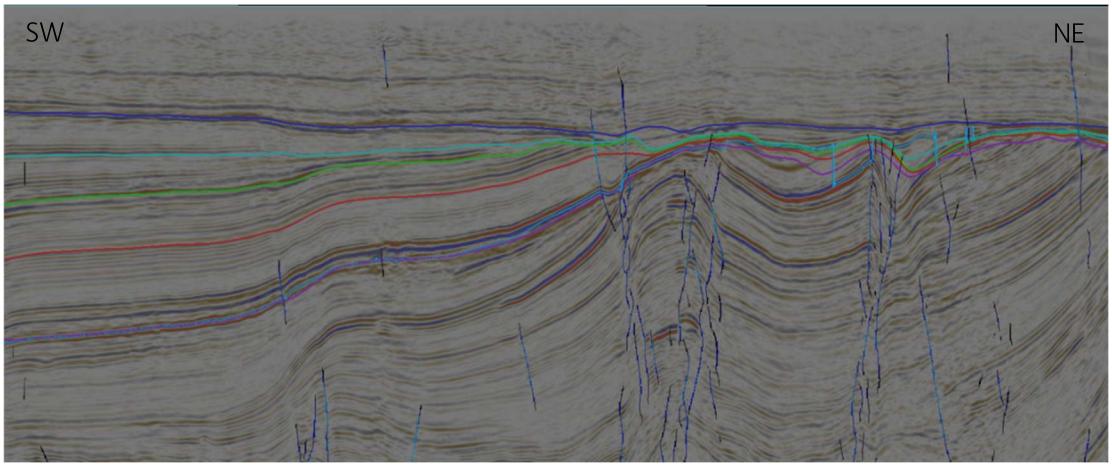

Figure 4.14: SW-NE orientated cross-section displaying the dipping geometry of clay intervals and cross-cutting faults. Cross-section line is shown in Figure 4-13.

For this case study area, a Multi-Horizon cube was available for the whole interval (produced using Paleoscan) from an earlier in-house test case study. In the northeastern part of the cube, in the area of the uplift and erosion, the interpretation of the Multi-Horizon cube is less exact due to the difficult structural setting making a detailed interpretations for the individual units challenging (Figure 4.14). From this horizon cube six horizons were selected for the seismic attribute analysis in addition to the interpreted Base Lower North Sea horizon that was also available for the whole merged survey (Figure 4.15 B). The horizons were linked to stratigraphic interpretation results from a nearby well when possible. Based on this selection, the following members were inferred (from bottom to top); Base Landen Formation (Liessel Member) (purple), near Base Oosteind Member (white), Intra Ieper Member (red), near Base Asse Member (green), near Base Rupel Formation (light blue) and Base Upper North Sea Group (blue) (Figure 4.15 C).

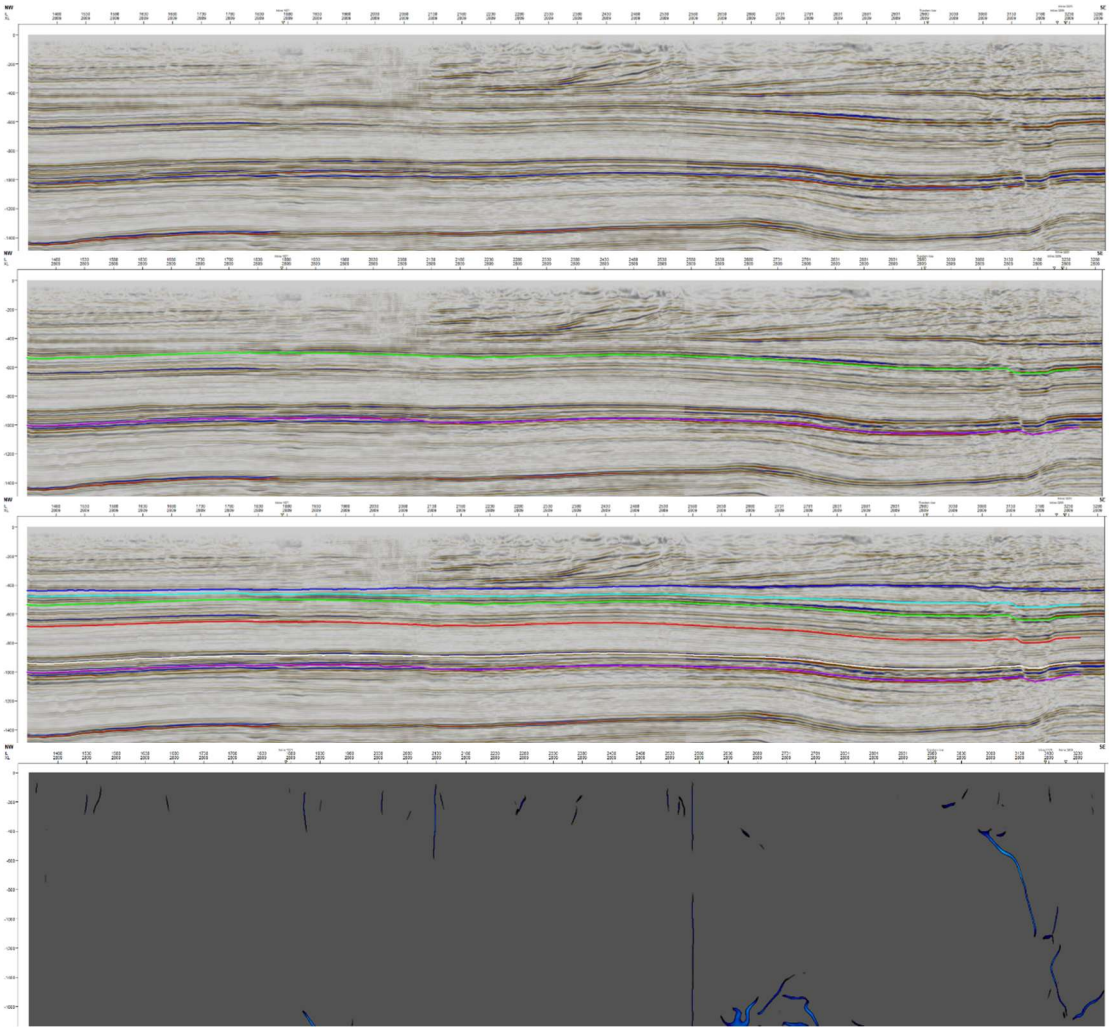

Figure 4.15: NW-SE orientated cross-section of the 3-D survey showing A: The original seismic image, B: Horizons with analysed seismic attributes (Base Landen Fm and near Base Asse), C: Interpreted horizons; Base Landen Fm (purple), Base Oosteind Mb (white), Intra Ieper Mb (red), near Base Asse Mb (green), near Base Rupel Fm (light blue) and Base Upper North Sea (blue) , D: The result of the machine learning guided fault interpretation along the same seismic line, dark blue colours indicate identified faults on the seismic. Cross section line is indicated in Figure 4.13.

4.2.3.1 Seismic attributes

In contrast to the two other study cases, the results of Variance Attribute analysis are presented for the IJsselmonde 3-D survey as this gives a better view of the faults and folds in this area.

Base Landen Formation (Liessel Member)

Most faults are observed toward the northeast margin of the volume as shown in Figure 4.16. The faults predominantly show a NW-SE-trending orientation. Specific fault structures such as polygonal faults are not present based on the conducted experiments. Along the northeastern margin more complex structures can be seen as a result of the uplift, folding and erosion of the strata. The IJsselmonde field (pink line on Figure 4.16) is also located on one of the anticlines related to this folding.

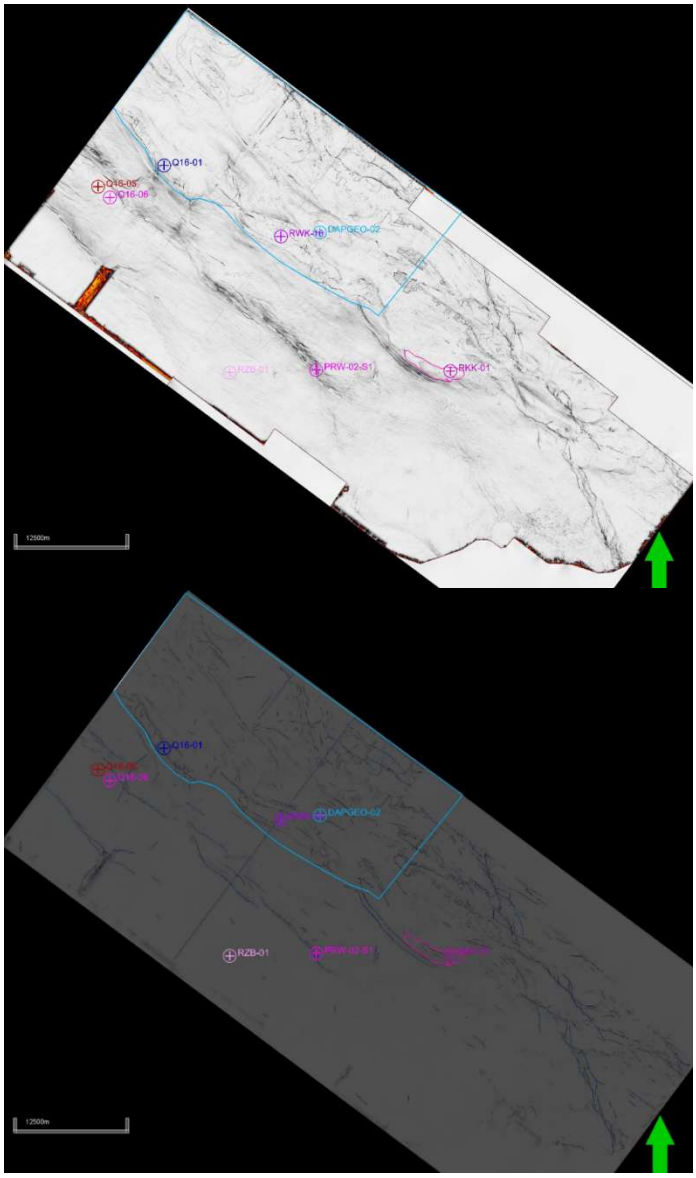

Figure 4.16: A: Result of Variance Attribute analysis is shown for base Landen Fm, B: result of the AI Fault interpretation for the same horizon, dark blue colours indicate identified faults on the seismic. The blue outline in the northern part shows the area of main erosion.

Near Base Oosteind Member

The crosscutting faults visible toward the northern margins in this volume are probably related to the erosion and difficult interpretation of the units. No apparent polygonal faults can be detected (Figure 4.17). In the southwestern part of the case study area, the main structures are NW-SE trending reactivated normal faults. The IJsselmonde gas field is located in the Oosteind Member with the Ieper Member as the seal. The total thickness of the Ieper is unknown in the area as none of the wells have been interpreted in detail for the North Sea Supergroup, however well RKK-32 shows a total thickness for the Dongen Formation of 80 m. The top of the reservoir is at 510 m.

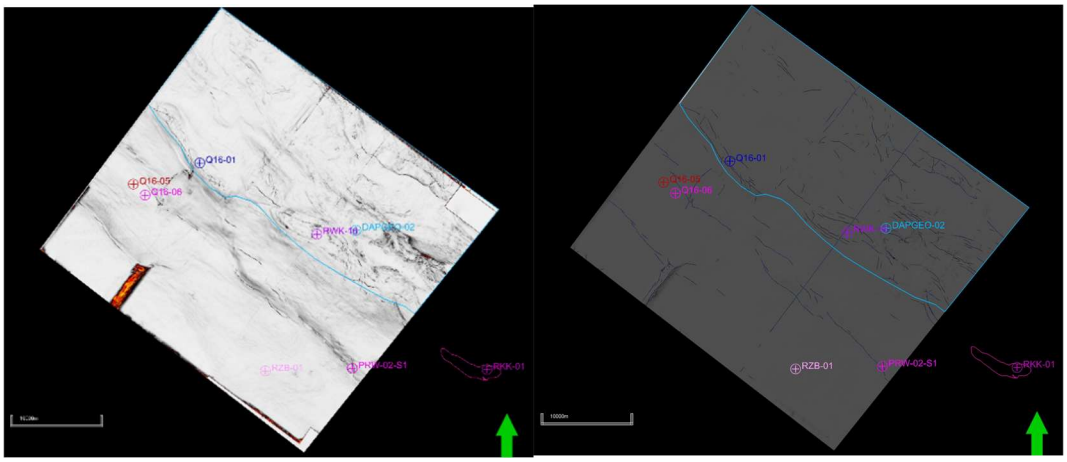

Figure 4.17 Variance attribute for the near Base Oosteind Member (left) and AI fault interpretation for the same unit (right), dark blue colours indicate identified faults on the seismic. The blue line indicates the area of uplift and erosion of the Paleogene units in the case study area, the purple line indicates the location of the IJsselmonde gas field.

Intra Ieper Member

The Ieper Member has a thickness of about 300 m at the location of well PRW-01 and RZB-01. The interpreted horizon is located within the Ieper Member and at about 2/3rd from the base. It marks the transition from a more transparent seismic facies at the base of the Ieper Member to a more clearly layered facies towards the top where the unit becomes more sandy (Figure 4.18).

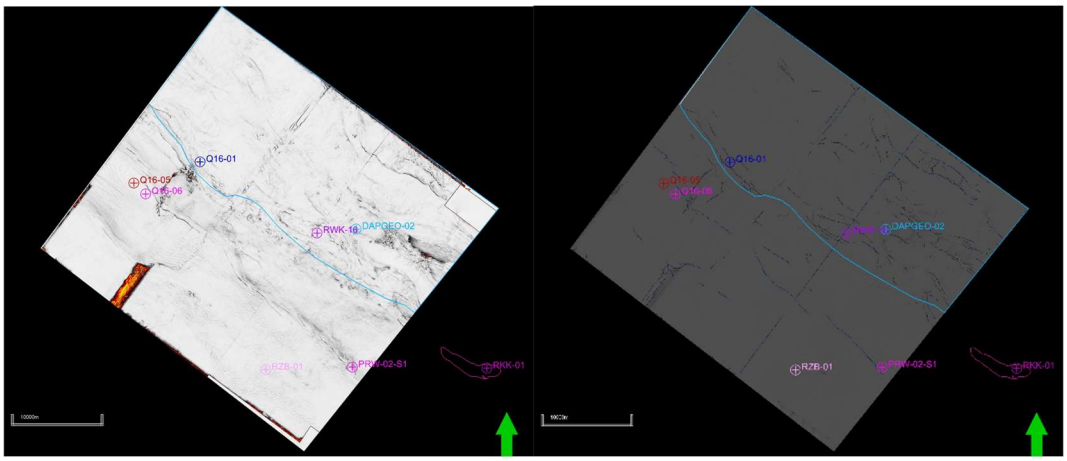

Figure 4.18 Variance attribute for the Intra Ieper Member (left) and AI fault interpretation for the same unit (right), dark blue colours indicate identified faults on the seismic. The blue line indicates the area of uplift and erosion of the Paleogene units in the case study area, the purple line indicates the location of the IJsselmonde gas field.

The same NW-SE trending faults can be seen in the southwestern part of the case study area while the northeastern part again is disturbed by the erosion and folding. In contrast to the other case study areas, the Ieper Member in here does not show any signs of polygonal faulting.

Near Base Asse Member

The Asse Member overlies the Brussels Sand Member in this area. At the location of well PRW-01 it is about 60 m thick. Apart from the previously mentioned NW-SE trending faults in the southwestern part of the area the Asse Member does not show any other notable features.

Near Base Rupel Formation

The Rupel Formation overlies the Asse Member and is marked by the sandy Berg Member at the base before grading into the Boom Member. The thickness of the Rupel Formation in well PRW-01 is approximately 100 m with 90 m of Boom Member identified. The distribution of the Rupel Formation in this area is reduced to the southwestern margin of the seismic survey due to uplift and erosion.

Base Upper North Sea Group

The Base Upper North Sea Group marks a major unconformity in the area. The NW-SE trending faults are still visible in the southwestern part of the case study, No fluid escape structures like pockmarks or mud volcanos are visible (Figure 4.19). The irregular features seen in the southwest and around wells Q16 are a result of poor seismic quality in these areas and do not reflect geological features.

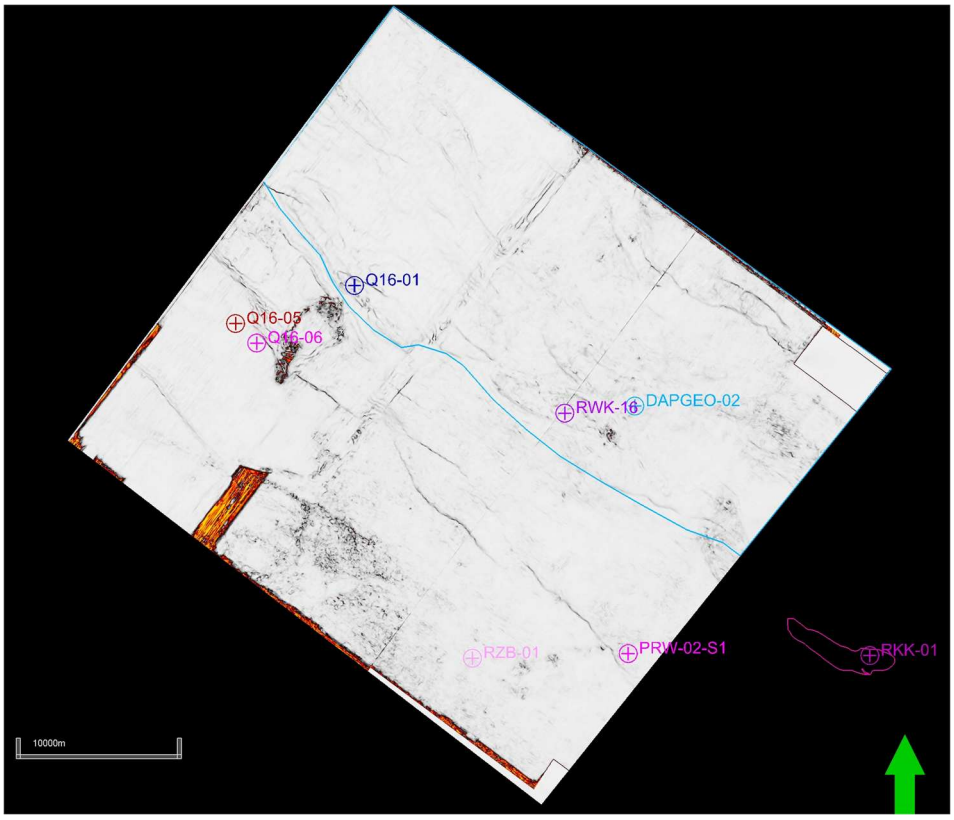

Figure 4.19 Variance attribute map for the Base Upper North Sea Group. The blue line indicates the area of uplift and erosion of the Paleogene units in the case study area, the purple line indicates the location of the IJsselmonde gas field.

5 Regional assessment of sealing capacity

Because direct measurements of the properties of Paleogene clays are sparse, in addition to more direct log and core data also indirect evidence of sealing capacity is analysed. The main indirect types of data are:

- Pressure higher than hydrostatic pressure (overpressure) in as well as below the Paleogene clay units;
- The presence of hydrocarbon fields and gas or oil shows;
- Events during drilling such as the drill string getting stuck due to sticky clays.

These topics will be discussed below and integrated with the results of this study.

5.1 Overpressure distribution in North Sea Group and Chalk

In case the fluids in the subsurface can move freely, the pressure of the fluids in the pores will be in hydrostatic equilibrium. This means that the pressure is determined by the weight of the column of fluids above. Because everything is in equilibrium in this situation, no fluid movement is expected. However, if fluids get trapped due to low permeability deposits, the pressure can become higher than hydrostatic, which is called overpressure. The existence of overpressure is a very good indication of low permeability, because the permeability must be low enough to severely restrict flow on geological time scales. A lack of overpressure is not necessarily an indication of higher permeability, because pressure diffusion can have happened in the past or laterally.

For overpressure to develop in the subsurface, an excess of fluids is required in addition to the low permeability. This can happen in several ways. During burial of sediments, they are compressed and compacted and the pore volume decreases. In particular during rapid burial, the fluids cannot escape fast enough and overpressure develops. This can also occur due to tectonic stresses which compress the rock. Another option is inflow of fluids or gas from deeper sources which is stopped by a sealing layer. This often causes more local overpressure. Finally, in situ formation of in particular gas has the same effect.

In the Pressure SNS database[24] pressure and overpressure for the Dutch on- and offshore have been collected (TNO, 2015). Figure 5.1 shows the data collected for the North Sea Supergroup and for the underlying Chalk group as a function of depth. Figure 5.2 and Figure 5.3 show the spatial distribution of the measured overpressure points in the North Sea Supergroup and the Chalk group respectively. In the North Sea Supergroup most data points are (near-) hydrostatic. Only 5 points have an overpressure in excess of 5 bar (0.5 MPa) and 4 points more than 1 MPa (points in green on Figure 5.1). These overpressures are observed in

[24] https://www.nlog.nl/pressure-southern-north-sea-psns-database, access date 25/8/2025.

the B and F blocks and are deeper than ~1 km. The single shallow (< 500 m) observation is highly uncertain.

The overpressure measurements in the underlying Chalk (Figure 5.1 right and Figure 5.3), which could have the North Sea Groups as seal, are more numerous and spread over a larger area. The general trend shows an increase in overpressure from south to north.

The presence of overpressure in the Lower North Sea Group in the Dutch Central Graben is already well known. Winthaegen and Verweij (2003) already estimated an overpressure of 35 to 55 bar based on seismic interval velocity data. 2D basin modelling studies in the southern part of the Dutch Central Graben showed that the present-day pressure conditions in the Chalk could be related to the rapidly increasing rates of sedimentary loading during Pliocene and Quaternary times (Nelskamp et al., 2012). These sedimentary loading rates increase northward. The Lower North Sea Group mudstones act as a transition zone between the overpressured Chalk Group and the normally pressured Upper North Sea Group sediments in the northern offshore (TNO, 2015).

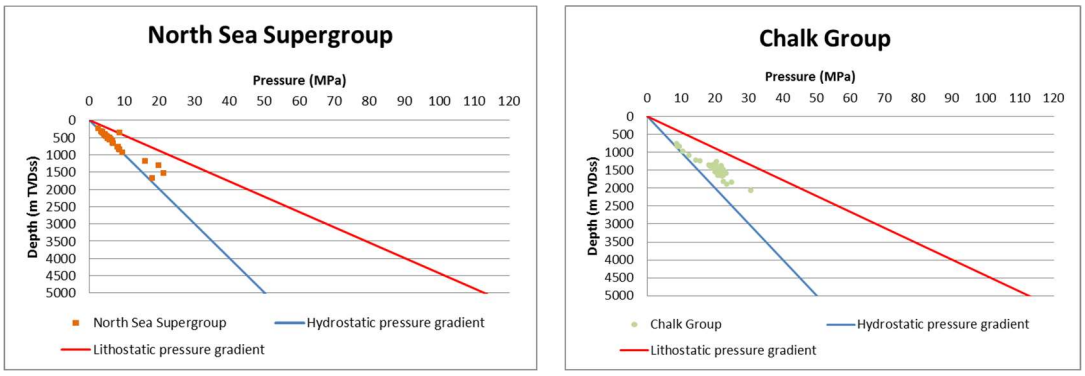

Figure 5.1 Pressure in the North Sea Supergroup (left) and underlying Chalk Group (right) from the Pressure SNS database. The blue line shows the hydrostatic pressure gradient and the red line the lithostatic pressure gradient.

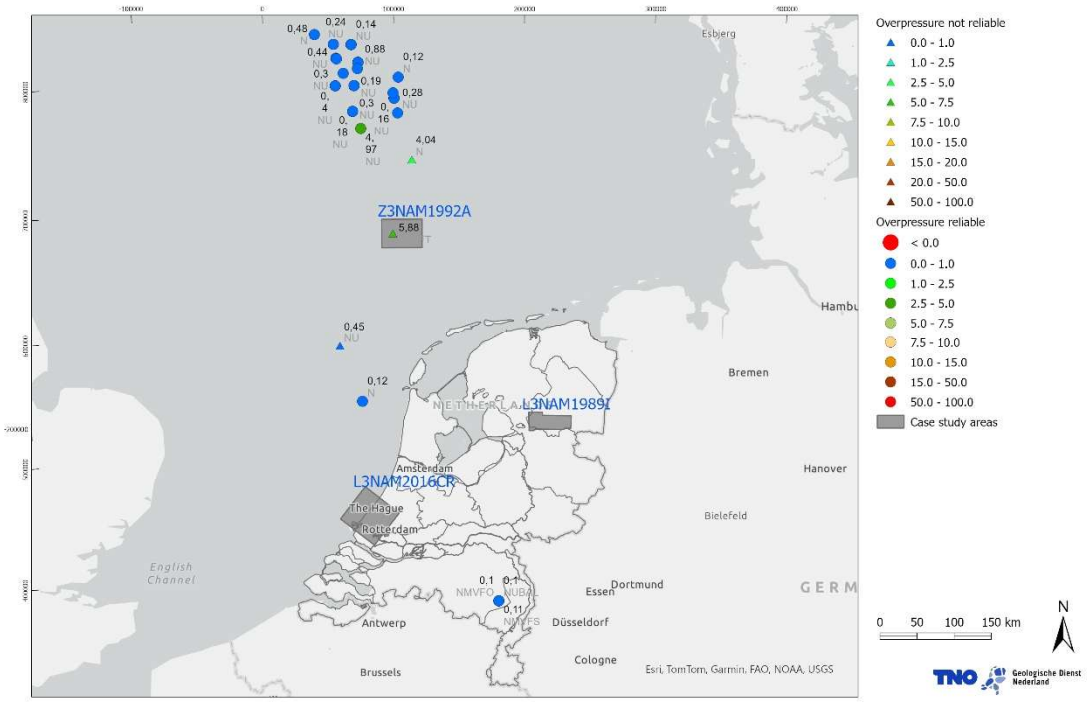

Figure 5.2 Measured overpressure (MPa) for the North Sea Supergroup according to the results of the Pressure SNS database (TNO, 2015). Grey rectangles indicate the 3D seismic data used for the case studies.

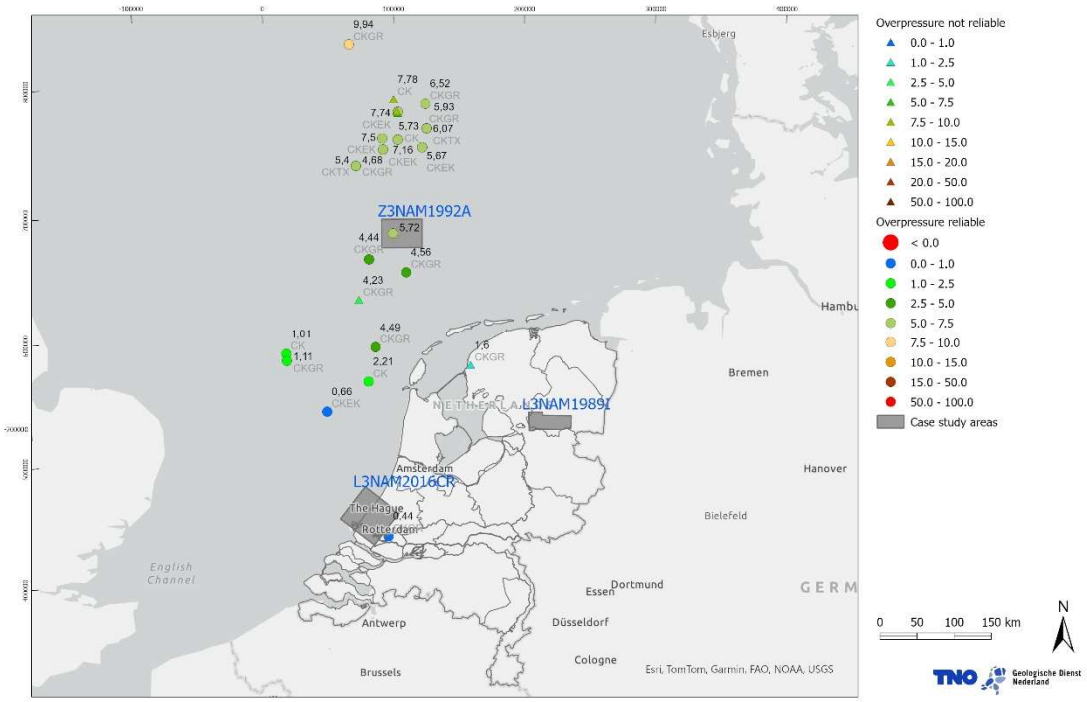

Figure 5.3 Measured overpressure for the Chalk Group according to the results of the Pressure SNS database (TNO, 2015). Grey rectangles indicate the 3D seismic data used for the case studies.

A very rough proxy for the pore pressure is the mud weight used in drilling. The drilling mud is used to keep the drilled hole stable and prevent upward flow of gas. By increasing the density of the mud, the pressure in the hole is increased. In the case of overpressure, the mud weight needs to be increased. Also the possible presence of gas requires increased mud weights. For production wells, the reservoir section is generally drilled with lower mud weight to prevent the mud from entering the formation and impairing the near-well permeability.

TNO (2015) also present data of mud weight and analyse the mud weight pressure in the North Sea Groups in different regions. Highest mud weights are used in the A and B blocks and the Dutch Central Graben. In the Broad Fourteens basin and in particular the West Netherlands basin, which are more to the south, mud weights used are much lower, even when the reduced depth interval is taken into account. This is consistent with the fact that towards the south, more sand is expected.

As an example Figure 5.4 shows the mud weight for well F17-10 which was drilled in the F17-NE Rembrandt oil field and is located in the Dutch Central Graben. Clearly visible is the increase in mud weight in the Lower North Sea sediments and the jump to higher mud weight in the Chalk where the oil is located.

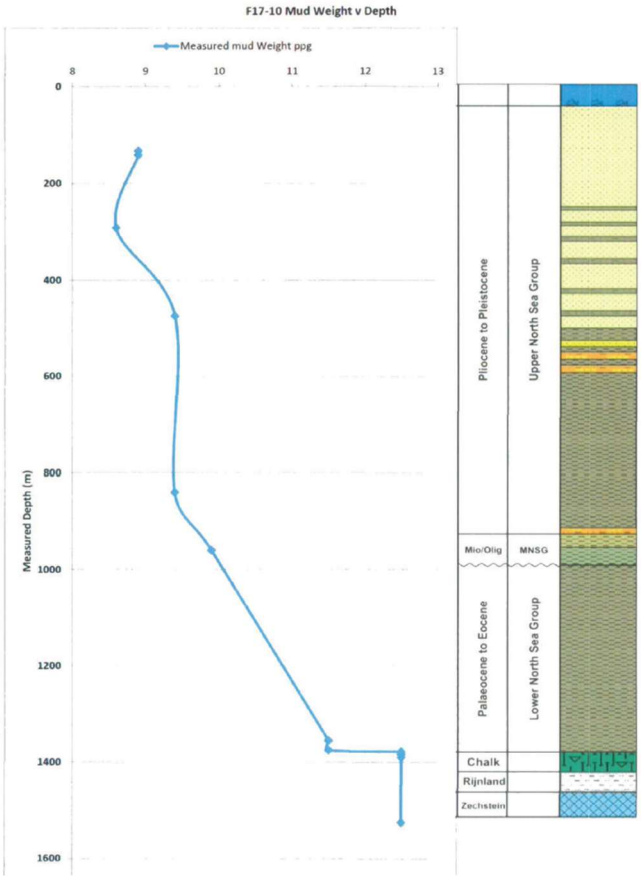

Figure 5.4. Mud weight (in ppg) as a function of measured depth for F17-10 (from Final well report, Wintershall Noordzee BV from nlog.nl). Units used in the graph are pounds per gallon (ppg). The more commonly used unit in the Netherlands is specific gravity (sg). 10 ppg is equivalent to 1.2 sg and 12.5 ppg is equivalent to 1.5 sg.

5.2 Hydrocarbon fields and shows

5.2.1 Hydrocarbon fields

For hydrocarbons to be trapped, three conditions need to be fulfilled:

- A structural trap to avoid the hydrocarbons migrating laterally.
- Presence of a seal that prevents vertical migration.
- A reservoir to hold the hydrocarbons

A seal works in two ways: water-filled small pores prevent hydrocarbons from entering due to capillary forces (entry pressure) and low permeability suppresses movement of fluids. Thus, the presence of an oil or gas field is an indication of low (vertical) permeability in the layer above and depending on the geometry also to the side.

In Table 5.1, the list of Dutch oil and gas fields is presented that have a Paleogene seal. The locations are shown in Figure 5.5. The table shows the reservoir and the seal per field. In several fields, there are reservoirs at multiple depths (e.g. De Wijk and IJsselmonde). In that case only the reservoirs relevant to this discussion are listed. Two groups can be distinguished:

- Reservoirs in the Chalk Group (either Ekofisk Formation or Ommelanden Formation) for which the seal is the Landen Formation, most likely Liessel Member. These are offshore, except for Harlingen UC, which is the northern most onshore field in the list.
- Reservoirs in the Dongen Formation (De Wijk Member or Oosteind Member) above the Landen Formation for which the Ieper Member is the seal. These are all onshore: De Wijk and IJsselmonde.

Overall, this suggests that the Landen Fm is only a seal north of De Wijk gas field and mainly in the offshore. The thickness map (Figure 2.2) shows that the Liessel Mb is thin near De Wijk and IJsselmonde. In the De Wijk field, the Landen Fm is less than 10 m in most wells. In this field, the Landen Fm also contains gas and is listed as a reservoir, albeit with very poor porosity and permeability (Field Development plan 2016). In the two gas fields slightly to the west (Wanneperveen and Marknesse), the Landen Fm is not listed as a reservoir. The thickness is similar with 10 to 13 m and the formation is listed as “impermeable” in the production plan (Field Development plan 2016). In IJsselmonde which is in the south-west of the Netherlands, the Landen Fm is known to be sandier (Figure 1.1). In conclusion, in the areas where the Liessel Mb is thicker, it might be a seal, in particular further to the north.

The Ieper Mb, which is much thicker in most areas (Figure 2.4), appears to be an effective seal.

Presence of an oil or gas field is a less good indication of low permeability than overpressure (overpressure was discussed in the previous section). A formation can act as a seal to hydrocarbons, but have some permeability due the entry pressure for gas and oil. In general, a gas field is a better indicator of low permeability than an oil field, because the overpressure with respect to the water is larger for gas than for oil. This is illustrated in Figure 5.6, which shows the pressure with depth for gas and oil compared to water. Due to their lower density, the pressure changes with depth are smaller for hydrocarbons. This effect is larger for gas than for oil because the density of gas is much lower. The larger the thickness of the gas or oil column, the larger the difference with the hydrostatic pressure. The presence of heavy oil without a gas cap can indicate that gas has been able to escape in the past.

Table 5.1 Overview of gas and oil fields with Paleogene clay seals (for stacked reservoir only the relevant reservoir and seal are listed)

Field name	Type	Reservoir(s)	Seal
F02a Hanze	Oil	Ekofisk Fm	Landen Fm, Liessel Mb
F06b Snellius	Oil	Ekofisk Fm	Landen Fm, Liessel Mb
F06b Zulu North	Oil	Chalk Gp, probably Ekofisk Fm	Landen Fm
F17-NE (Rembrandt)	Oil	Ommelanden Fm	Lower North Sea Grp, probably Landen Fm
F17-SW (Vermeer)	Oil	Ommelanden Fm	Lower North Sea Grp, probably Landen Fm
Harlingen UC	Gas	Ommelanden Fm	Landen Fm, Liessel Mb
De Wijk	Gas	De Wijk Mb (aka Basal Dongen Tuffite Mb), Landen Fm, Ommelanden Fm	Ieper Mb
Wanneperveen	Gas	De Wijk Mb (aka Basal Dongen Tuffite Mb)	Ieper Mb
Marknesse	Gas	De Wijk Mb (aka Basal Dongen Tuffite Mb)	Ieper Mb
IJsselmonde	Gas	Oosteind Mb (aka Basal Dongen Sand Mb)	Ieper Mb (probably)

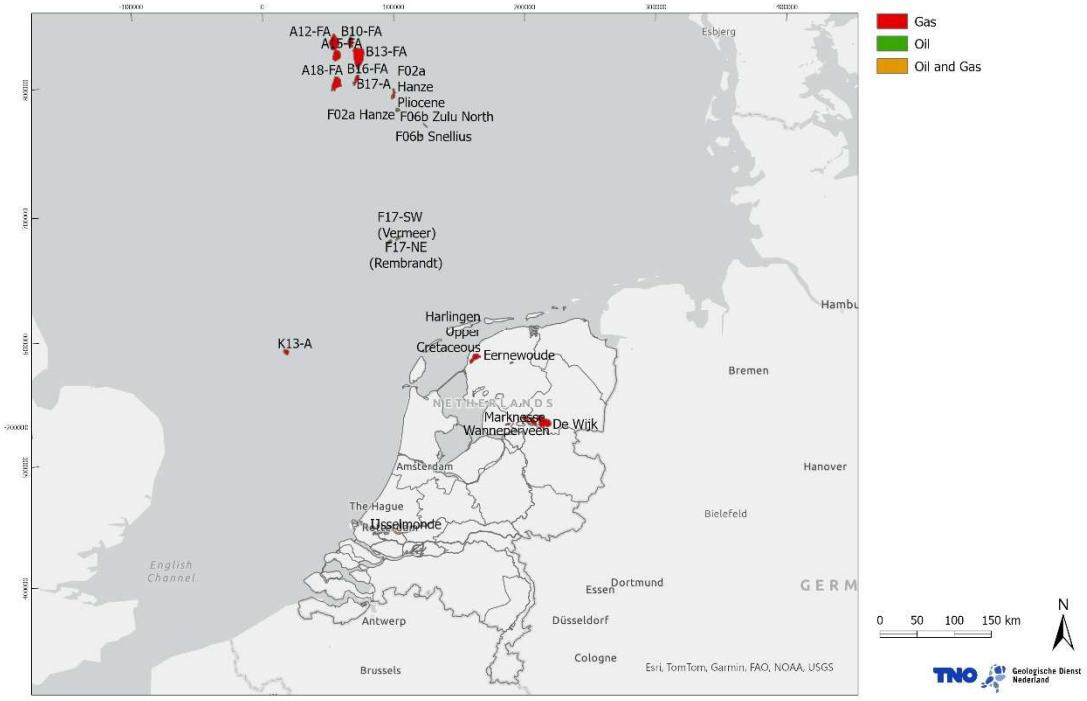

Figure 5.5 Map with the location of the oil and gas fields in the North Sea Supergroup and the Chalk group as mentioned in Table 5.1.

Please note that due to the complexity of oil and gas migration, the absence of oil and gas, even if all other prerequisites are present (source, migration path and reservoir) cannot be interpreted as evidence of a lack of sealing capacity of a clay.

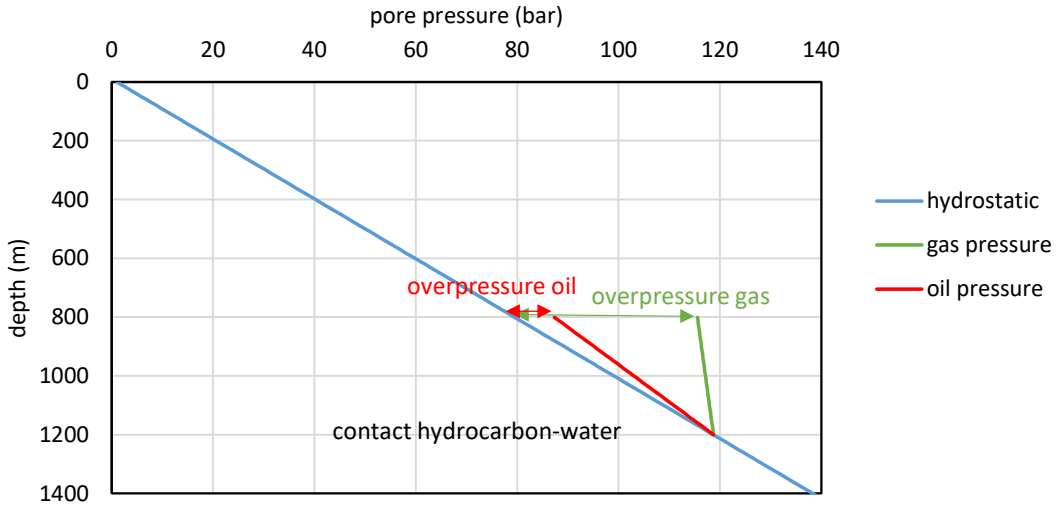

Figure 5.6. Pore pressure of water (hydrostatic assuming a density of 1000 kg/m^3), gas (assumed density of 80 kg/m^3) and oil (assumed density of 800 kg/m^3) as a function of depth for a hydrocarbon column from 800 m (depth of the seal) to 1200 m depth (depth at which the hydrocarbons start).

The three case study areas (Figure 4.1) which were analysed in Chapter 4 are discussed in more detail below:

De Wijk, Wanneperveen, Marknesse

The De Wijk and Wanneperveen gas fields are conventional (thermogenic gas from the Carboniferous and Zechstein Formations below) but shallow gas fields. The fields were discovered around 1950 (De Wijk in 1949, Wanneperveen in 1951). Production started in 1959. The more westerly, very small field Marknesse was discovered in 1983, but never produced. The De Wijk field includes the following subsurface reservoirs (Figure 5.7):

- De Wijk Member (NLDOWY; previously named Basal Dongen Tuffite Member), Liessel Member (NLLALI; previously named Landen Clay Member) and Ommelanden Formation (CKGR; also referred to as Ommelanden Chalk)
- Muschelkalk Formation (RNMU)
- Rogenstein Formation (RBSR)
- Z3 Carbonate Member (ZEZ3C) / Carboniferous

Wanneperveen and Marknesse have the following reservoirs:

- De Wijk Member (NLDOWY)
- Vlieland Sandstone Fm (KNNS)
- Lower Buntsandstein Sg (RBS)

The shallow reservoir of interest in this report is the De Wijk Mb, which is located at a depth of around 500 m in De Wijk, 650 m depth in Wanneperveen and around 1 km near Marknesse. The seal is formed by the Ieper Mb. The other reservoirs are much deeper (> 1000 m) and are not further discussed here. The De Wijk member is a layer of around 20 m thick and is described as an unconsolidated clay with siltstone intercalations (description based on the field development plan, update from 2016).

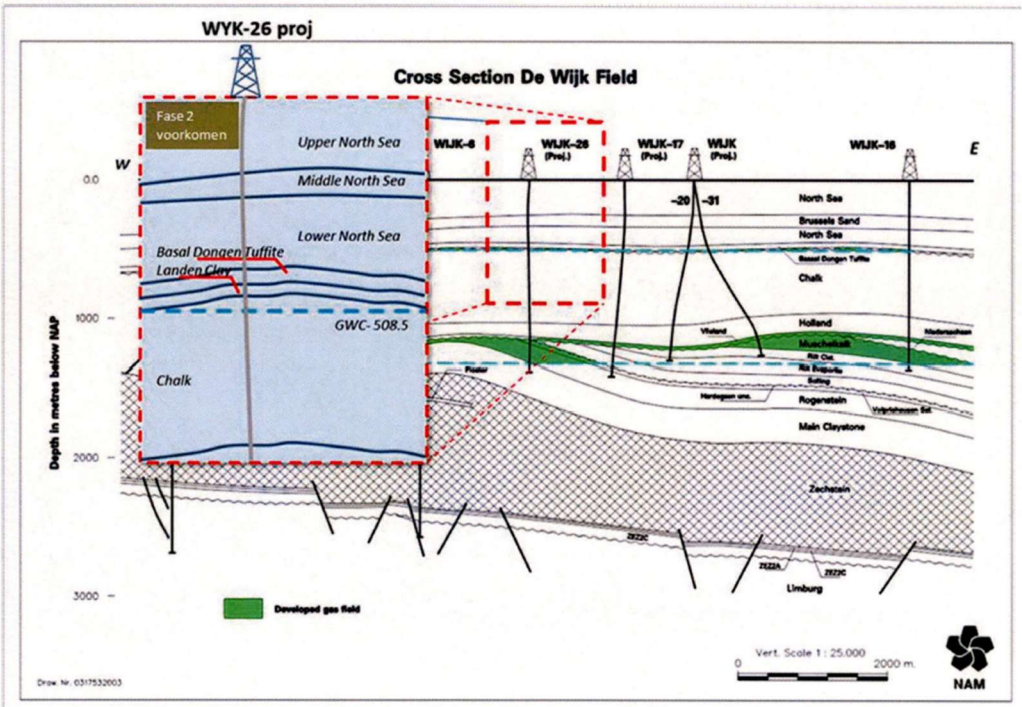

Figure 5.7 Structure of the De Wijk gas field from the Field development plan (2016).

Figure 5.8 shows core pictures of the seal (Ieper Mb) and the reservoir (De Wijk and Liessel Mb). The De Wijk Mb and Ommelanden Fm are separated by the lower permeable Liessel Member (NLLALI; previously named Landen Clay Member), which in De Wijk contains some gas. In the De Wijk field, it mainly consists of somewhat unconsolidated clay with a high marl content and some very fine sandy intercalations. In some wells, the presence of the Liessel Mb is not interpreted. In the Wanneperveen field, the Landen Fm/Liessel Mb is considered sealing.

Based on information from the field development plans, the De Wijk Mb is slightly overpressured. The pressure is 61 bar at 500 m depth in De Wijk and 79 bar at 650 m depth in Wanneperveen, which would be consistent with 10 to 15 bar overpressure.
The deeper formations are also slightly overpressured (Verweij and Hegen, 2015; overpressure is 19 bar in RBSH in WAV-08). This is a low overpressure for this reservoir compared to other areas, because water can move away laterally (westwards).

Figure 5.8 Core photos of the well De Wijk-31 in the De Wijk field. On the left is an example of the Ieper Member just above the reservoir, the central photo shows the very heterogeneous De Wijk Member and on the right is an example of the Liessel Member at the base of the interval.

F17 Rembrandt and Vermeer
The unproduced F17 Rembrandt and Vermeer oil fields are both in the Ommelanden Fm with the seal formed by the Lower North Sea group, probably the Landen Fm. They are located at a depth of 1300 to 1400 m and are considerably overpressured as would be excepted form their location in the Dutch Central Graben (section 5.1). The overall area is considerably overpressured below the North Sea Groups. In well F17-06 overpressure at the bottom of the Lower North Sea Group is estimated at 59 bar at a depth of 1530 m. The uncertainty on the observations is high due to probe plugging. However, the chalk (Ommelanden Fm) below shows high overpressures and mud weights used in drilling are consistently high: ~1.3 to 1.4 sg in the lower part of the North Sea Group and 1.5 sg or higher in the chalk below (see also Figure 5.4 showing the mud weight for F17-10).

Mud weights used in the nearby F18 block (~10 km distance) are generally lower than those in F17: 1.1-1.2 sg in the Lower North Sea Group to 1.25 sg in the chalk below. In the F18 block is only one oil field (Fregat), which is in the Friese Front Fm at a depth of more than 2 km. There are no oil or gas fields at shallower depths. Assuming that the mud weight indicates less overpressure in the F18 block, this can be interpreted in different ways:

- The permeability of the Lower North Sea Group is higher, prohibiting accumulation of oil and gas and building of overpressure.
- The permeability below the chalk is lower preventing upward migration of oil and gas and avoiding build-up of overpressure.
- Absence of closure which prevents the accumulation of hydrocarbons.

Based on the seismic attributes of the base Liessel Mb in Figure 4.4, the latter is a likely explanation. The F18 area (wells F18-01-S1 and F18-02) shows very little relief at the base of the North Sea Groups.

IJsselmonde
The IJsselmonde field in the south-west of the Netherlands is a stacked reservoir like the De Wijk field. The shallowest reservoir is gas-filled in the Oosteind Mb (previously Basal Dongen Sand) and the seal is the Ieper Mb. The top of the reservoir is at 510 m depth. Below the reservoir is the Landen Fm, which is around 20 m thick. Very little information is available about this field. No direct information could be found about the source of the gas or the existence of overpressure. However, the gas is likely to be thermogenic given the fact that there is another gas field below in the Holland Greensand at a depth of ~700 m and cores from a depth of 550 m are described as oil-impregnated in IJS-06. Nearby fields Rotterdam, Berkel, Lekkerkerk and Alblasserdam do not show gas at such shallow depth. In Barendrecht-Ziedewij gas shows have been recorded at the level of the Ieper and Asse Members. A much more thorough analysis of the subsurface situation is required to understand why the shallow gas field IJsselmonde occurs in this location and not anywhere else.

5.2.2 Gas shows

Gas shows are recorded during drilling as part of the mud logging but can also be interpreted from well testing as well as core analyses. They are also called direct hydrocarbon indicators and record in which formations in the wellbore hydrocarbons have been encountered. Gas shows are commonly interpreted on a qualitative basis, indicating zones where the amount of recorded gas exceeds a baseline. This baseline is dependent on the drilling parameters such as the rate of penetration, the mud weight, the type of drill bit, drilling events such as pauses during drilling or change of the bit but also the measuring equipment.

The information shown in this chapter has been taken from the EBN Hydrocarbon Show database (www.ebn.nl, accessed 07.25) and includes only the data for the North Sea Supergroup based on well log interpretation.

Gas shows in the shallow subsurface can be either thermogenic or biogenic. Usually the presence of longer chain hydrocarbons (C2 – C5) are indicative of a thermogenic origin. The reverse conclusion, however, is not possible. Biogenic gas is often formed in situ and can therefore be present in permeable as well as impermeable layers. Using the gas column height, e.g., in the shallow, biogenic gas fields in the A and B blocks can give an indication of the sealing capacity of the overlying interval (Ten Veen et al., 2013) but the presence of a gas show does not allow for further interpretations. Thermogenic gas and oil are usually formed in deeper source layers and migrates along higher permeable zones and faults into the reservoir. The presence of a thermogenic hydrocarbon reservoir is indicative of a lower permeable layer above (the seal) as well as a higher permeable migration pathway laterally or below. Gas shows within low permeable layers as well as above hydrocarbon reservoirs could therefore be an indication of such a higher permeable migration route e.g., though coarser, silty or sandy intervals within the layer, and therefore indicative of fluids migrating through the formation.

Stacked gas shows can be indicative of fluid transport and therefore of poor sealing properties. Figure 5.9 shows all gas shows recorded in the Middle and Lower North Sea Groups stacked in stratigraphic order, with the lowermost layers having the largest symbols. In several areas these stacked gas shows appear to be clustered.

Area 1 is in the northern part of the Dutch Central Graben and in this area the F02a Hanze and F06b Snellius and Zulu North oil fields (Figure 5.5) are located. The area is overpressured as seen in Figure 5.2 and Figure 5.3. The main seal for the oil fields is the Liessel Member (Table 5.1). Seeing stacked gas shows in the area together with the presence of oil fields without a gas cap can signify that the clay layers are not sealing for overpressured gas in the area.

Area 2 is located in the southern part of the Dutch Central Graben and the area of the F17-SW Vermeer and F17-NE Rembrandt oil fields. The Chalk in this area again shows significant overpressure (Figure 5.3) suggesting a similar process of seal failure for gas as in area 1. De Bruin et al. (2025) have also identified natural seepage in the area of well F17-14 with an unknown source for the gas.

Area 3 is located onshore, along the coast north of Groningen. No known oil or gas fields are located in the Chalk or Lower North Sea Group in this area, which might be related to the very effective Zechstein seal in this area. There are also no pressure measurements available for this region. The Liessel Member of the Landen Formation is relatively thin in the area (Figure 2.2) while the overlying clay formations have relatively low percentage of shale related to the more proximal depositional setting of the area.

Area 4 is located onshore in the area of Friesland Platform. The De Wijk, Wanneperveen and Marknesse gas fields are located in this area. In these fields the Liessel and De Wijk Members can act as reservoirs (see section 5.2.1, Figure 5.7) while the Ieper Member is the main seal.

Area 5 is located along the south-western margin of the West Netherlands Basin where also the IJsselmonde hydrocarbon field is located. This area is located in a more proximal depositional setting, close to the paleo-coastline for most of the Paleogene. In addition, the West Netherlands basin experienced uplift and erosion during the Paleogene, as well as

significant structuration. The gas shows line up along the margin of these eroded layers suggesting migration pathways along faults (Figure 5.10, Figure 4.14).

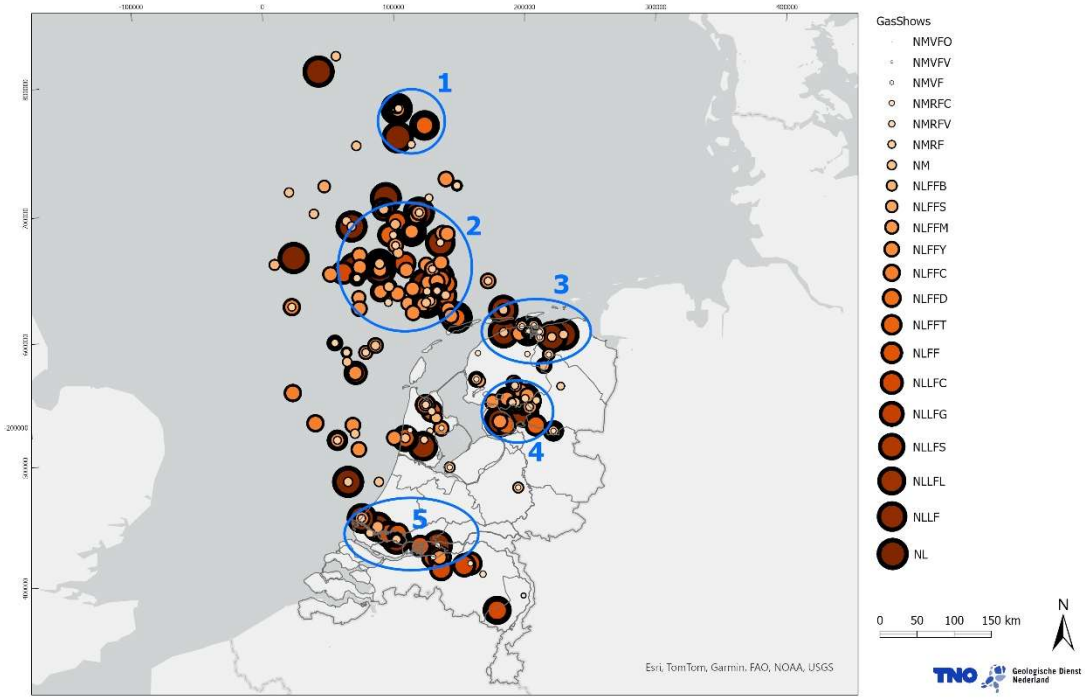

Figure 5.9 Map showing the location and stratigraphic position of all gas shows of poor, fair and good classification in the Middle and Lower North Sea Groups. Please note that the legend still uses the old short names for the individual members and formations (see Table 1.1).

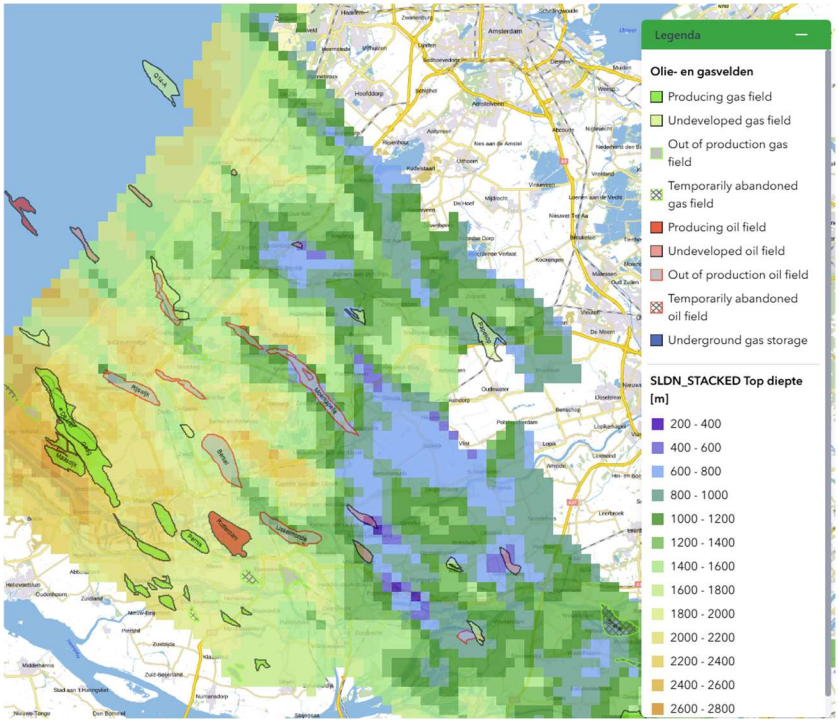

Figure 5.10 Illustration of the oil and gas fields in the West Netherlands Basin aligning with the top of the Nieuwerkerk Fm (source: ThermoGIS.nl).

In addition to these observations it should be noted that most stacked gas shows occur in the intervals of the Landen and lower part of the Dongen Formations (Appendix F). The shallowest unit appears to be the Ieper Member in most cases. The Ieper Member is the thickest layer of the Paleogene clays, suggesting that this member is in most cases enough to prevent further fluid migration upwards. In addition, most gas shows in the Middle and Lower North Sea Groups are classified poor to fair. Only very few gas shows have received the classification good. This is different for the Upper North Sea Group where more gas shows of the classification good have been recorded. It is, however, assumed that most of these gas shows are related to biogenic gas and not to migrated thermogenic gas (de Bruin et al., 2022).

5.3 Drilling events

The drilling events dataset of EBN contains information on special occurrences during drilling where the geological component contributed to the situation. Drilling events are situations such as mud loss, stuck tools or gains while the identified underlying geological cause has been linked to things like faults, swelling clays, shallow gas or anomalous pressures (Hoetz & Nijhuis, 2019, www.ebn.nl accessed 07/25).

In the context of this study, the focus was on the drilling events in the Middle and Lower North Sea Group and there especially on the events linked to either swelling clays (clay balling or stuck tubulars) that could be indicative of abundant smectite in the layer (Kariuki and Van der Meer, 2004) or to anomalous pressures or shallow gas.

The database shows 113 events linked to swelling clay in the Middle and Lower North Sea Groups (Figure 5.11).

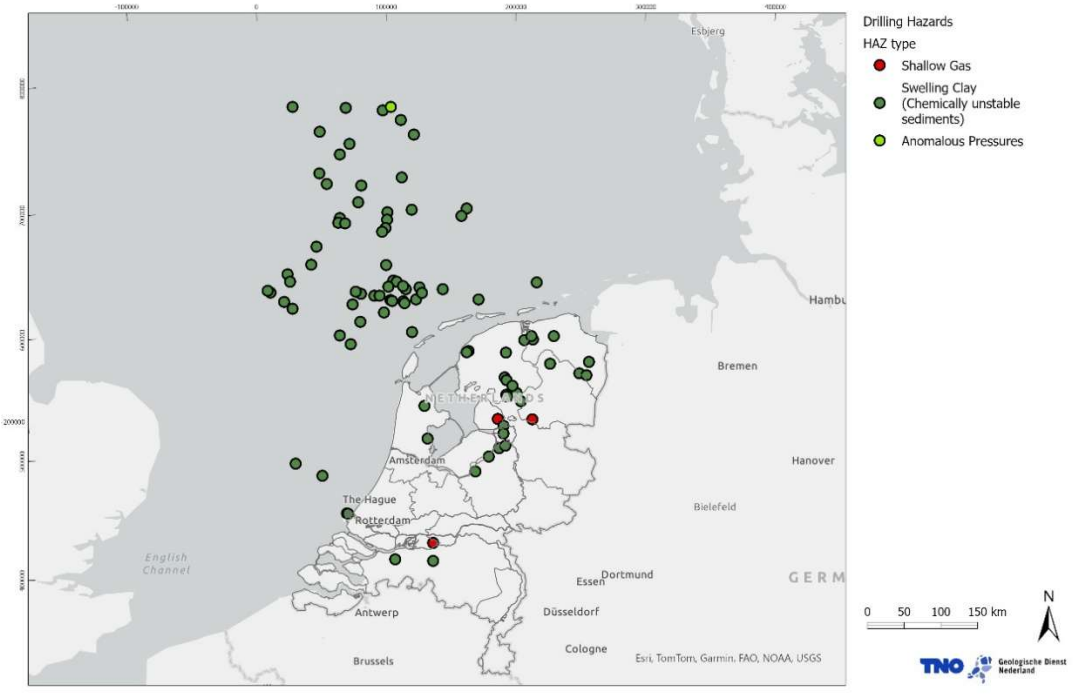

Figure 5.11 Drilling hazards according to the EBN drilling hazard database (EBN, accessed 07/25) showing all wells that encountered events in the Middle and Lower North Sea Group related to swelling clay, shallow gas or anomalous pressures.

Most of these events are linked to the Landen (Liessel Member) and Dongen (Asse, Ieper and De Wijk Members) Formations (Appendix G). In addition, Three events are linked to shallow gas, all onshore, two in the area of the De Wijk, Marknesse fields and one in the West Netherlands Basin. Anomalous pressure was recorded once in the database in a well in the area of the F02a-Hanze field which is also related to the presence of gas below the Miocene Unconformity. All four cases are in line with the observations mentioned in Chapter 5.2.2.

6 Discussion

6.1 Log and seismic analyses

6.1.1 Polygonal faults

Polygonal faults are a common sedimentological feature found in more than 100 sedimentary basins (Xia et al. 2022). They are most commonly found in fine-grained sediments such as Mudstones, Claystones, Shales or Chalk. Their formation is usually non-tectonic, presenting as layer-bound normal faults with varying strike directions, small fault throws (between 10-50m), and limited fault displacement (< 100 m). They occur at varying depths, between just below the surface down to 2000 m below sea bed and have also been described in outcrops. They are most commonly found in sediments of Cretaceous age and younger. The first description of polygonal faults was in the Ieper clay in Belgium (Henriet et al. 1991), the emergence of 3D seismic data has made the identification and interpretation of these faults more easy, leading to their identification worldwide. Xia et al (2022) give a detailed overview of the types of polygonal faults identified as well as their geological setting and potential generation mechanism.

Five different generation mechanisms have been proposed for polygonal faults, Density inversion, Gravity sliding, Low coefficients of friction, Syneresis and Shear failure. An overview of these mechanisms as well as their occurrence according to literature is summarised in Table 6.1.

For the North Sea Basin in the Netherlands the most likely mechanisms are density inversion as well as syneresis. Syneresis is linked to very early compaction and intraformational overpressure, when the clays are still in a gel like state with a framework supported porosity of 65-75%. Syneresis does not require rapid burial or extension to form and can occur in more heterogeneous sediments while density inversion is linked to deeper, more rapid burial and more homogeneous thick clay intervals. Veschuren (2019) looked at several Belgian outcrops and studied the exposed fault patterns on different scales and concluded that for the Ieper clay onshore Belgium syneresis is the most likely formation mechanism due to the prevalence of silty intercalations while a combination of both can have occurred in the offshore where the Ieper Member is thicker and more homogeneous clay rich. One of the main questions is the effect of polygonal faults on the sealing capacity of the Paleogene clay intervals. Several studies suggest that polygonal faults act as pathways for fluid migration (e.g., Ding et al., 2013; Seebeck et al., 2015; Han et al., 2016). However, there is no direct evidence for fluid migration through existing polygonal fault systems and the interpretation is mainly based on circumstantial evidence only. Pockmarks at sea floor or the top of the interval (Base Upper North Sea Group Figure 4.7) with polygonal faults suggests that there was at least fluid flow during genesis of the faults. Also the presence of stacked gas shows in areas with identified polygonal faults as well as overpressure hints at some potential for fluid migration through these intervals.

Table 6.1 An overview of formation mechanisms of polygonal faults identified in different study areas (from Xia et al. 2022)

Genesis mechanism	Description	Key study area	References
Density inversion	After drainage during compaction, the top and bottom of the mudstone becomes dense, forming low permeable sealed layers. The water in the middle of the mudstone cannot be expelled, generating overpressure. When it is critically overpressured, hydraulic fractures may occur with faults and collapses forming at the top, leading to the formation of PFs.	North Sea Basin Lake Hope region Farafra Oasis of Western Desert of Egypt	Henriet et al. (1988,1991) Cartwright (1994a), Cartwright (1994b) Cartwright and Lonergan (1996) Watterson et al. (2000) Tewksbury et al. (2014)
Gravity sliding	Downslope gravitational collapse produces a strong alignment of fault strikes perpendicular to the direction of sliding towards the depocenter.	Outer Moray Firth of northern North Sea	Higgs and McClay (1993) Clausen et al. (1999)
Low coefficients of friction	Low coefficients of friction can increase the displacement on localised fault surfaces and the concentrated stress around the dislocation loop may bound the slip zone. It may enable the outward propagation of the polygonal fault after initial slip which eventually coalesces with others into a polygonal fault system.	Eormanga Basin North Sea Basin	Goulty (2002) Goulty and Swarbrick (2005) Goulty (2008)
Syneresis	Syneresis occurs during the early stage of compaction and dewatering, and the three-dimensional contraction of smectite-rich gels favors the PF formation. This genesis mechanism is driven by the interparticle attractive forces between clay particles, and mainly occurs in layers composed of smectitic claystone and carbonate chalks.	Stable Subbasin North Sea Basin Qiongdongnan Basin	Cartwright (1996) Lonergan et al. (1998b) Hansen et al. (2004) Wu et al. (2009) Sun et al. (2010) Han et al. (2016)
Shear failure	The conversion of opal-A to opal-CT reduces the bulk rock volume and induces differential compaction and shear failure during regional diagenetic processes of siliceous sediments. It is accompanied by stress changes, and therefore can cause PFs initiation.	Vøring Basin, Møre Basin, Sanzhao Sag of Songliao Basin Great South Basin	Cartwright. (2011) Davies and Ireland (2011) Ding et al. (2013) Li et al. (2020)

Other studies have also linked polygonal faults to hydrocarbon migration and the presence of shallow gas or gas hydrates (Ding et al., 2013; Alrefaee et al., 2018; Velayatham et al., 2021). On the other hand the De Wijk, Marknesse and Wanneperveen gas fields in the onshore have the Ieper Member with interpreted polygonal faults as top seal (Figure 4.12). Also, studies in outcrops show cemented fault planes and clay smearing which might even hinder lateral flow (Lonergan et al., 1998a; Turrini et al., 2017). In general it can be concluded that polygonal faults increase the vertical permeability of clay layers compared with undisturbed formations but are probably still sealing to a certain degree with respect to fluid migration.

6.1.2 Impact of glauconite

Although most of the differences in clay mineralogy are expected to be caused by changes in provenance (Griffioen et al., 2025), diagenesis and formation of minerals also plays a role. Montmorillonite and smectite type clays can gradually transform into mixed layered clays and to Illite in a process called illitisation. Illitisation occurs mostly at elevated temperatures (> 70°C) (Pytte and Reynolds, 1989), although fluid salinity and pH and availability of K are also important factors. Illitisation could explain some of the mineralogical variations observed in the analysis of the spectral GR log discussed in chapter 3, while provenance could better explain mineralogical variation between Kaolinite and Montmorillonite.

Also very relevant for the depth range of interest in this report is the in-situ formation of glauconite, which is commonly observed in Paleogene sediments. Glauconite is mineralogically related to clay minerals and high in Potassium, which gives it a GR signature similar to clay. In terms of grainsize however, it is often silt or sand-sized (Keijzer, 2025) which could have implications for the permeability of glauconite-rich clays. Although the process of the formation of glauconite is still debated, the most widely accepted theory to date is described by Lopez-Quiros et al. (2020) and includes a two-stage formation model in which in the first stage Fe(III)-rich glauconitic smectite is formed which is gradually enriched in K^+ to from the K-rich glauconite. The glauconitisation process occurs at low temperature in confined sub-oxic, partially reduced micro-environments at or near the sediment-water interface (Lopez-Quiros et al., 2020). Residence time near the sediment-water interface and thus sedimentation rate is an important factor controlling the extent of the glauconitisation.

Due to the enrichment in K compared to Th, the presence of glauconite will move the apparent mineralogy on the Lith-2 charts from Chapter 3 in the Illite direction. To investigate the impact of glauconite on the charts, the lithological descriptions of the wells analysed in Chapter 3 were investigated for trends in glauconite. In most wells some glauconite is described, sometimes in all Paleogene clay formations, sometimes in some. Figure 6.1 shows the glauconite in the lithological description together with Litho-2 plot for the Boom Member and Figure 6.2 shows the spatial distribution.

The two wells with composition closest to montmorillonite (wells A08-01 and ORO-01) have no glauconite described in the Boom Member, which is consistent with this description. Well A08-01 is the only well with no description of glauconite presence in any of the relevant formations. In all the wells identified with Illite as average composition, glauconite is described but in varying amounts.

Figure 6.2 shows the spatial distribution of the glauconite description and the mineralogical composition for the Boom Mb/Rupel clays. No spatial trends could be identified for this member nor for any of the others (figures in Appendix D), which could be due to the low density of the data points compared to the variability in composition. This variability is for example seen in the wells HVB-01 and ORO-01 which are relatively close: HVB-01 has consistently more glauconite described than ORO-01, in particularly in the Boom Mb. The average mineralogical composition in HVB-01 is closer to Illite (Figure 6.1 and Figure 6.2), which is consistent with the lithological descriptions. Also wells A08-01 and F02-06 (two most northerly wells) are very different and relatively close, as are BUR-01 and LWO-01 (two most northerly onshore wells).

It should be noted that in several of the descriptions, it is mentioned that the glauconite is mainly present as silty or fine-sandy particles within the clay rather than as clay. For example in BUR-01, the Boom Mb is described as a dark-green to grey-green, plastic clay

with small amounts of fine grained sand and silt particles of which 20 to 40% are glauconite. Thus shale content based on GR only (instead of SGR) should be used with care when glauconite is described and/or predominantly Illite composition is observed in these Paleogene clays.

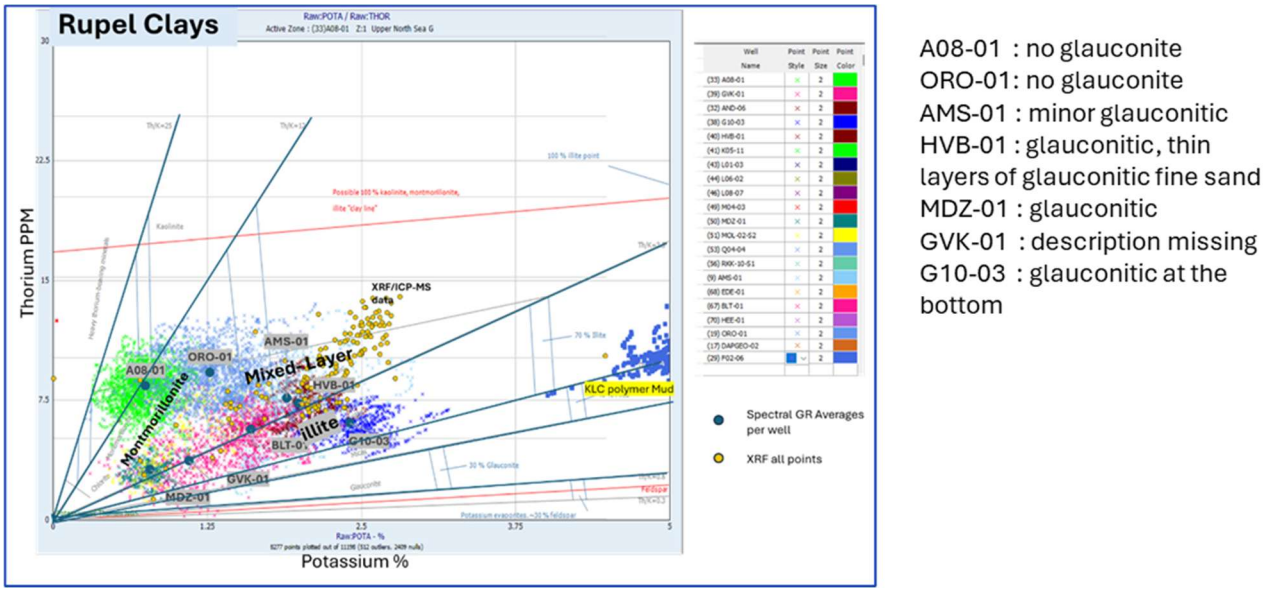

Figure 6.1. Description of the presence of glauconite from the lithological description for the Boom Mb (Rupel Clays) and the Th-K relation (Figure 3.10).

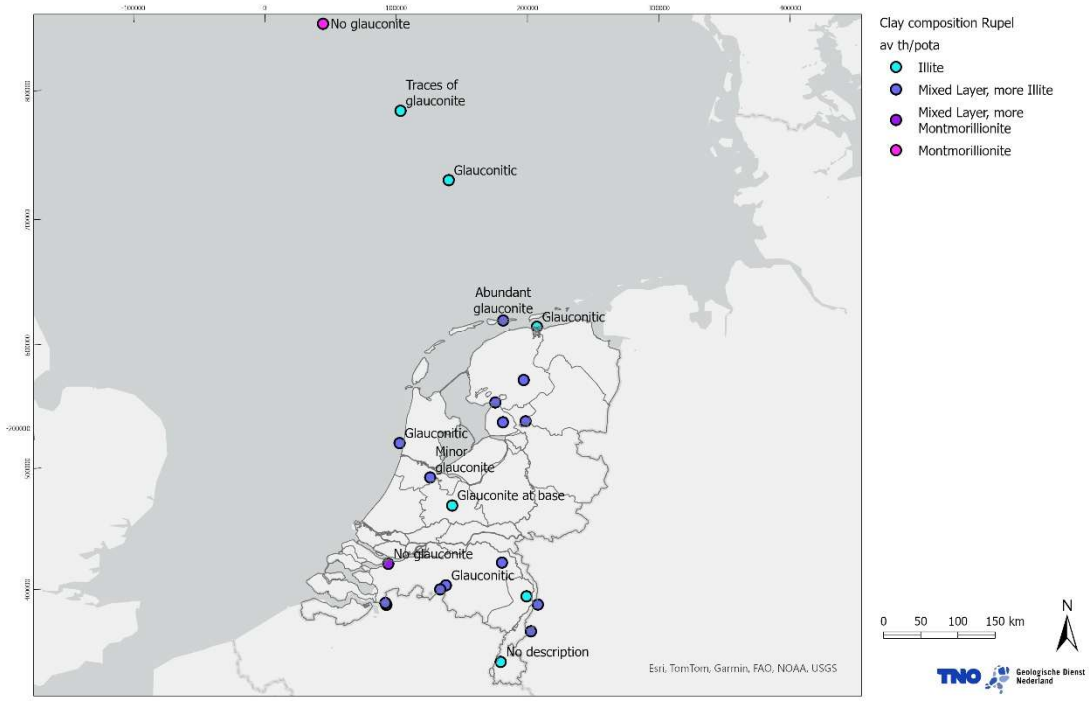

Figure 6.2. Spatial distribution of the description of glauconite in the lithological descriptions of the wells together with the clay composition from Chapter 3 for the Rupel Clays.

Many sandy formations in the North Sea Groups are known to be rich in glauconite (Keijzer, 2025), even more so than the clayey sediments. Since glauconite formation depends on K-influx which is related to fluid movement, it could be that in sandy deposits with higher permeability, the glauconite formation reaches more mature levels compared to silty or clayey deposits. Griffioen et al. (2025) show high smectite content present in marine sediments of the Dongen and Rupel Fm (Figure 13.14). It could be that some of the smectite in the Paleogene clays is the product of incomplete glauconitisation and thus also autochthonous: the average XRD compositions of the Boom Mb indicate 18% of glauconite-smectite (section 3.2) in addition to 32% smectite.

6.2 Comparison with previous studies

This study presents an update of previous studies (CORA 2001, OPERA – Verhoef et al., 2017) which focused on the Paleogene clay intervals of the North Sea Supergroup in the onshore of the Dutch subsurface. The mapping project within the CORA project was finalised in 1996 and focused on the distribution, thickness and depth of the same Paleogene clay intervals as this study (plus the Oosterhout Formation that was not included in the present study). Since the finalisation of the CORA study, these intervals have been characterised in more detail as well as an additional 1649 wells have been drilled in the on- and offshore since 1. Jan 1996. The country-wide mapping project of the deep subsurface (DGM-deep) has published version five of the Base of the Upper North Sea Group and Base of the Lower North Sea Group based on 2D and 3D seismic interpretation in 2019, marking the top and base of the Paleogene clays respectively. Also in 2019 an update of the stratigraphic interpretation of the units of the North Sea Supergroup was introduced, harmonizing the interpretations of the shallow and deep subsurface models.

The OPERA project included detailed studies on the Boom Member of the Rupel Formation (former Rupel Clay Member) and looked in detail at the development of a safety case for the disposal of radioactive waste, a detailed study on geological and geohydrological properties of the unit, its geomechanical behavior, geochemical composition and potential future burial scenarios. Since the focus of the present study is on all Paleogene clay units it does not attempt to reproduce the level of detail of the OPERA project for the Boom Member. The focus was mainly on the integration of newly available data for the Boom Member and considering newly available techniques and measurements with respect to the other clay units. The focus of the data collection and mapping was extended to also include the offshore area. With respect to newly available data, the results of the newly drilled SCAN wells are especially valuable for the interpretation of the Paleogene clay units due to their research approach and their focus on the medium depth interval relevant for nuclear waste disposal but also shallow geothermal energy and heat storage.

7 Conclusions and recommendations

7.1 Conclusions

In this study several parameters that can be derived from available oil and gas exploration data were investigated for their impact on permeability and their ability to ensure limited fluid flow into and within the geological unit (also called sealing capacity). Several different techniques (e.g., log analyses and seismic attributes) were tested to assess their possibilities for gathering new information. In addition a more regional approach was used by including data from the offshore, extending on the approach already adopted for the Boom Member in the OPERA project. Indirect indicators for sealing capacity from previous projects such as overpressure or drilling hazards were investigated as well and integrated with the results of this study allowing for a more comprehensive overview. The results of this study can be used to plan more detailed campaigns, focusing either on specific regions or stratigraphic units. The highlighted parameters can guide the direction of research or in the identification of missing information.

In the following these parameter are listed and their effect on sealing capacity rated as positive, ambiguous or negative. The ranking and reasoning behind the categories is explained per parameter/aspect. None of these parameters alone can be seen as an indicator for a good sealing layer or a bad sealing layer. Information on one parameter is not enough to interpret the sealing capacity of a layer, several parameters should always be seen together.

Mineralogy:
Positive:
- High smectite content (> 50 % of the clay fraction, Kariuki and van der Meer, 2004)

Smectite has swelling or sealing properties and has therefore a positive influence on the sealing capacity. Smectite content can be identified from (harmonised) logs, e.g., spectral gamma ray but needs to be calibrated to XRD analyses.
- High Vshale in general (> 0.8)

A high percentage of the clay sized fraction also has positive effect on the sealing capacity. Using logs, e.g., gamma ray in general the Vshale can be identified, however, this is sensitive to cutoffs used during the analysis. Calibration to available lithological descriptions as well as to grain size analyses is recommended.

Ambiguous:
- Intermediate Vshale (between 0.6 and 0.8)

If the Vshale is averaged across the whole units, lower Vshale values don't necessarily mean that the layer is not sealing. In heterogeneous clay units, individual intervals with a high Vshale can form intra-unit seals if these intervals are of similar thickness as the units with a high average Vshale. If the Vshale is structurally lower in the whole unit, this will lower the sealing capacity.

- High percentages of Mixed-Layer clays or other clay minerals like Illite or Chlorite (> 25 %, Kariuki and van der Meer, 2004)

Illite and Chlorite are nonswelling clay minerals. Due to their small grain size and structure they are generally considered to improve sealing of the layer, however, not to the degree Smectite would.

Negative:

- High amounts of glauconite

Glauconite has a generally higher grain size and therefore reduces the sealing capacity. In addition, the formation of glauconite suggests fluid migration through formation and can therefore be seen as an indicator for fluid flow. Glauconite content is difficult to identify from logs and XRD and needs to be linked to sedimentological descriptions of core or cuttings.

- Low Vshale (< ~0.6)

A lower percentage of clay sized particles usually increases the porosity and permeability, decreasing the sealing capacity in the sediments. Low average Vshale values can also suggest the presence of intercalated sand or silt layers within the formation. However, also these units need to be investigated for the presence of intervals with high Vshale that can serve as intra-unit seals.

Faults and fractures (on seismic resolution)

Positive:

- Absence of major structures and fractures

The absence of clearly delineated faults in clay layers (especially when visible in under- and overlying layers) can point to ductile behavior of the clay or absence of tectonic stress. Faults and fractures are generally seen as weak zones promoting fluid migration, their absence is therefore considered a positive sign for the sealing capacity of the layer.

Ambiguous:

- Presence of polygonal faults

Polygonal faults suggest the presence of fine grained, smectite or carbonate rich sediments, which is considered a positive indicator for sealing capacity. However, polygonal faults are the result of fluid flow and fluid escape from the layer and can increase the vertical permeability as well as act as potential weak zones for fault reactivation if they were not cemented or act as horizontal barriers due to clay smearing.

- Absence of polygonal faults

The absence of polygonal faults on the other hand can point to coarser grain size of the sediment or to a different mineralogical composition. This could have a negative effect on the sealing capacity. The absence could on the other hand also be related to a different direction of fluid flow and pressure dissipation.

Negative:

- Large scale faults through clay layer

Clearly delineated large scale faults through a clay layer can act as fluid pathways, especially when the fault throw is large enough to cause the clay layer to be juxtaposed with a more permeable sand or silt layer. In addition clear faults within clay layers can suggest brittle behaviour of the clay.

Overpressure, hydrocarbon fields, gas shows

Positive:

- Overpressure below or within the clay layer

The presence of overpressure below and within the clays is a clear sign for low permeability and high sealing capacity.

- Gas fields below the clay layer

Gas fields below a clay formation filled to spill indicate sealing capacity up to the point of minimum capillary entry pressure which can be derived from the gas column height.

- Significant gas shows in porous layers below clays

Similar to the gas fields, significant gas shows below the clay formation can also indicate sealing capacity in areas without trapping structures. However the minimum capillary entry pressure cannot be derived in this case.

Ambiguous:

- Gas fields not filled to spill

Gas fields not filled to spill can indicate a lower capillary entry pressure and potential leaking through the seal at higher pressures. However, these gas fields can also indicate insufficient charging from the source or recent tectonic changes which have no effect on the sealing capacity.

- Oil fields without gas cap

Similar to gas fields not filled to spill, oil fields without a gas cap can also indicate a potentially leaking seal for gas. It is, however, also possible that no gas was generated and accumulated in the structure.

- Gas shows within clay formations

Thermogenic gas shows within the clay formations suggest a migration pathway into the formation, suggesting fluid flow through it. Generally, however, gas shows within more permeable layers in the clay unit can also indicate a more sealing layer, impermeable for gas on top.

Negative:

- Gas shows throughout the column, pock marks at sea floor linked to deep gas sources and seismic chimneys, shallow gas fields above the clay formations linked to deep gas sources

All of these observations point at fluids moving through the subsurface and can be considered negative signs for sealing clay layers.

Thickness and depth (cut-offs based on feasibility studies of previous studies)

Positive:

- Thickness of sealing layer at least 100 m

A thickness of more than 100 m has been proven to be sealing for gas even with the presence of polygonal faults (de Wijk field, thickness Ieper ~ 120 m).

- Depth > 500 m

At depths greater than 500 m the compaction of the clay is usually enough to retain fluids. All shallow fields in the Paleogene clays examined in the context of this study are at least 500 m deep, suggesting that clays at this depth can be considered sealing.

Ambiguous:

- Thickness between 25 and 100 m

In the area of the IJsselmonde field the thickness of the sealing Ieper Member is between 25 and 100 m. However, no polygonal faults were interpreted in the area, a lower thickness could therefore be sealing in the absence of other permeability enhancing properties.

Negative:

- Thickness below 25 m

A layer with a thickness below 25 m is generally considered too thin to have significant sealing capacities.

- Depth above 200 m or deeper than 1000 m

Clays at depth above 200 m are usually uncompacted and have very high porosities and fluid content. Intervals below 1000 m are considered out of scope for this study due to technical considerations.

7.2 Recommendations

In addition to the above mentioned conclusions, several aspects which could be useful for a shale assessment could not be studied in detail in the context of this study. These aspects are listed as recommendations for future studies.

During the updates of the maps of the Paleogene clays it became evident, that in a large proportion of the “deep” hydrocarbon exploration and production wells the stratigraphy in the North Sea Supergroup is not well constrained. This is related to the fact that the main focus of these wells was on deeper formations and structures. However, with the new focus on the middle-deep intervals for geothermal energy, heat storage but also nuclear waste disposal, the stratigraphy in these wells need to receive, and partly already gets, structural update, harmonisation and reinterpretation of the Paleogene and younger units.

In addition new data from oil and gas operators that was previously excluded from the mining act is currently made available in the context of the GIP program line “Additional data operators”. It is expected that the amount of information on the subsurface that becomes publicly available will increase significantly, which can be used for similar studies and new updates.

Due to the current interest in Paleogene formations for geothermal heat production or heat storage, new information is expected to become available in the next few years, such as from the SCAN well SVG-01. Potential projects which could result in useful information are the MOOI DIAMETER[25] project, which investigates the application of Low Temperature Geothermal heat production and Warming^{UP}GOO[26] which focuses on characterisation of the North Sea Supergroup. Since for heat storage good seals are a requirement, research into this topic could provide additional information or data for updating the information in this report.

The important role of the Vsh on the permeability has been confirmed, however NMR data from the DAPGEO-02 well has highlighted why the Vsh is not the only controlling factor on the permeability as silty intervals with very low Vsh but also low permeability are present in DAPGEO-02. The characterisation of a silty facies should be considered for a full evaluation of the sealing potential of the Paleogene clays. More data are necessary for such analysis including additional porosity and permeability data from core samples from the different Paleogene clays within the country or in specific area of interest, and a sampling campaign focused on the calibration of the already available NMR data in DAPGEO-02.

Recent developments in machine learning could improve old methods: de Rijk et al. (2025) show how the application of machine learning algorithms has improved the estimation of hydraulic conductivity from particle size distributions. Using a dataset of 4600 samples, they showed that much better results can be obtained with ML than using the traditional empirical equations, also for silt and clay rich samples.

[25] MOOI DIAMETER - Topsector Energie
[26] WarmingUPGOO - WarmingUp

References

Alrefaee, H. A., Ghosh, S., & Abdel-Fattah, M. I. (2018). 3D seismic characterization of the polygonal fault systems and its impact on fluid flow migration: An example from the Northern Carnarvon Basin, Australia. *Journal of Petroleum Science and Engineering, 167*, 120–130. https://doi.org/10.1016/j.petrol.2018.04.009

Aertens, M., Weetjens, E., Govaerts, J., Maes, N., & Brassinnes, S. (2023). CP1 and Tribicarb-3D: Unique long-term and large-scale in situ migration tests in Boom Clay at the HADES Underground Research Laboratory. In X. L. Li, M. Van Geet, C. Bruggeman, & M. De Craen (Eds.), *Geological Disposal of Radioactive Waste in Deep Clay Formations: 40 Years of RD&D in the Belgian URL HADES*. https://doi.org/10.1144/SP536-2022-41

Levasseur, S., Collin, F., Daniels, K. A., Dymitrowska, M., Harrington, J. F., Jacops, E., Norris, S., Xavier, S., Talandier, J., Truche, L., & Wendling, J. (2021). EURAD Deliverable D6.1 – Initial state of the art on gas transport in clayey materials. Work Package Gas. EC Grant agreement no: 847593.

Bourg, I. C. (2015). Sealing shales versus brittle shales: A sharp threshold in the material properties and energy technology uses of fine-grained sedimentary rocks. *Environmental Science & Technology Letters, 2*, 255–259.

Bremmer, C. N., Simmelink, H. J., Heidema, A. H., Hoogendoorn, A., & Pagnier, H. J. M. (1996). Project 'CAR' – Fase 1. Kartering slecht-doorlatende laagpakketten van tertiaire formaties (in Dutch). Rijks Geologische Dienst, Heerlen, the Netherlands.

Cartwright, J. A. (1994a). Episodic basin-wide fluid expulsion from geopressured shale sequences in the North Sea basin. *Geology, 22*, 447–450. https://doi.org/10.1130/0091-7613(1994)022<0447:EBWFEF>2.3.CO;2

Cartwright, J. A. (1994b). Episodic basin-wide hydrofracturing of overpressured Early Cenozoic mudrock sequences in the North Sea Basin. *Marine and Petroleum Geology, 11*, 587–607. https://doi.org/10.1016/0264-8172(94)90070-1

Cartwright, J. A., & Lonergan, L. (1996). Volumetric contraction during the compaction of mudrocks: A mechanism for the development of regional-scale polygonal fault systems. *Basin Research, 8*, 183–193. https://doi.org/10.1046/j.1365-2117.1996.01536.x

Cartwright, J. (2011). Diagenetically induced shear failure of fine-grained sediments and the development of polygonal fault systems. *Marine and Petroleum Geology, 28*, 1593–1610. https://doi.org/10.1016/j.marpetgeo.2011.06.004

Clausen, J. A., Gabrielsen, R. H., Reksnes, P. A., & Nysæther, E. (1999). Development of intraformational (Oligocene–Miocene) faults in the northern North Sea: Influence of remote stresses and doming of Fennoscandia. *Journal of Structural Geology, 21*, 1457–1475. https://doi.org/10.1016/s0191-8141(99)00083-8

Commissie Opberging Radioactief Afval (CORA). (2001). *CORA eindrapport, Terugneembare berging, een begaanbaar pad?*Ministerie van Economische Zaken. www.covra.nl

Corina, A. N., Wollenweber, J., Kastelein, K., van der Valk, K., Moghadam, A., Heerens, G.-J., & Fisher, H. (2021). Application of bentonite as an alternative sealing material for deep hydrocarbon and geothermal wells. In *Proceedings of the 55th US Rock Mechanics/Geomechanics Symposium* (ARMA21–1330), Houston, Texas, USA.

Davies, R. J., Ireland, M. T., & Cartwright, J. A. (2009). Differential compaction due to the irregular topology of a diagenetic reaction boundary: A new mechanism for the formation of polygonal faults. *Basin Research, 21*, 354–359. https://doi.org/10.1111/j.1365-2117.2008.00389.x

De Bruin, G., Ten Veen, J., Wilpshaar, M., Versteijlen, N., Geel, K., Verweij, H., & Carpentier, S. (2022). Origin of shallow gas in the Dutch North Sea – Seismic versus geochemical evidence. *Interpretation, 10*(1), SB63–SB76.

De Jager, J., Van Ojik, K., & Smit, J. (2025). Geological development. In *Geology of the Netherlands* (pp. 20–50). https://doi.org/10.5117/9789463728362_ch01

De Keijzer, O. (2025). The impact of glauconite on petrophysical well logs in the Breda Subgroup and Oosterhout Formation (Master's thesis, Utrecht University).

De Rijk, V., Buma, J., Veldkamp, H., & Zech, A. (2025). Predicting saturated hydraulic conductivity from particle size distributions using machine learning. *Stochastic Environmental Research and Risk Assessment, 39*(2), 423–435.

Ding, X. J., Liu, G. D., Sun, M. L., & Wang, P. G. (2013). Origin of polygonal fault systems: A case from the Sanzhao Sag in the Songliao Basin, East China. *Petroleum Exploration and Development, 40*, 309–319. https://doi.org/10.1016/s1876-3804(13)60040-3

Ecclestone, M., ten Veen, J., Brussée, M., Korevaar, S., Nelskamp, S., Peeters, S., & Versteijlen, N. (2021). Play 1 Cenozoic. https://www.geodeatlas.nl/pages/play-1-cenozioc

Field development plan De Wijk Fase 2. (2016). NAM. https://www.nlog.nl/nlog-mapviewer/field/WYK?lang=en

Gaucher, E. C., Blanc, P., Bardot, F., Braibant, G., Buschaert, S., Crouzet, C., Gautier, A., Girard, J. P., Jacquot, E., Lassin, A., Negrel, G., Tournassat, C., Vinsot, A., & Altmann, S. (2006). Modelling the porewater chemistry of the Callovian-Oxfordian formation at a regional scale. *Comptes Rendus Geoscience, 338*, 917–930.

Gaucher, E. C., Tournassat, C., Pearson, F. J., Blanc, P., Crouzet, C., Lerouge, C., & Altmann, S. (2009). A robust model for pore-water chemistry of clayrock. *Geochimica et Cosmochimica Acta, 73*, 6470–6487.

Goulty, N. R. (2008). Geomechanics of polygonal fault systems: A review. *Petroleum Geoscience, 14*, 389–397. https://doi.org/10.1144/1354-079308-781

Goulty, N. R. (2002). Mechanics of layer-bound polygonal faulting in fine-grained sediments. *Journal of the Geological Society, 159*, 239–246. https://doi.org/10.1144/0016-764901-111

Goulty, N. R., & Swarbrick, R. E. (2005). Development of polygonal fault systems: A test of hypotheses. *Journal of the Geological Society, 162*, 587–590. https://doi.org/10.1144/0016-764905-004

Geel, C. R. (2016). Geological screening of ductile formations (Deliverable report D4.1 of TKI Plugging wells by enhanced formation ductility). TNO internal report TNO 2016 R10273.

Griffioen, J., Koenen, M., Meeussen, H., Cornelissen, P., Peters, L., & Jansen, S. (2017). Geochemical interactions and groundwater transport in the Rupel Clay. A generic model analysis. OPERA-PU-TNO522.

Griffioen, J., Felder, M., Molenaar, N., Spijker, J., & Hoving, A. (2025). Sediment mineralogy and geochemistry. In J. Veen, G.-J. Vis, J. de Jager, & T. Wong (Eds.), *Geology of the Netherlands* (2nd ed.). Amsterdam University Press.

Han, J., Leng, J., & Wang, Y. (2016). Characteristics and genesis of the polygonal fault system in southern slope of the Qiongdongnan Basin, South China Sea. *Marine and Petroleum Geology, 70*, 163–174. https://doi.org/10.1016/j.marpetgeo.2015.11.022

Hansen, D. M., Shimeld, J. W., Williamson, M. A., & Lykke-Andersen, H. (2004). Development of a major polygonal fault system in Upper Cretaceous chalk and Cenozoic mudrocks of the Sable Subbasin, Canadian Atlantic Margin. *Marine and Petroleum Geology, 21*, 1205–1219. https://doi.org/10.1016/j.marpetgeo.2004.07.004

Henriet, J. P., De Batist, M., Van Vaerenburgh, W., & Verschuren, M. (1988). Seismic facies and clay tectonic features of the Ypresian clay in the Southern North Sea. *Bulletin de la Société belge de Géologie, 97*, 457–472.

Henriet, J. P., De Batist, M., & Verschuren, M. (1991). Early fracturing of Paleogene clays southernmost North Sea: Relevance to mechanisms of primary hydrocarbon migration. *Special Publication - European Association of Petroleum Geologists Bulletin, 1*, 217–227.

Higgs, W. G., & McClay, K. R. (1993). Analogue sandbox modelling of Miocene extensional faulting in the Outer Moray Firth. *Geological Society, London, Special Publications, 71*, 141–162. https://doi.org/10.1144/gsl.sp.1993.071.01.07

Hoetz, G., & Nijhuis, I. (2019). Anticipating geo-drilling hazards by sharing geo-drilling events information nationwide. Contribution to SPE Annual Technical Conference and Exhibition 2019, 12 p.

Hoving, A. L., Geel, C. R., Wollenweber, J., Orlic, B., & Griffioen, J. (2019). TKI Geoenergy 2018 – A framework for the assessment of ductile shales for wellbore sealing and abandonment. TNO internal report TNO2019 R10900.

Houben, A. (2025). Biostratigraphy of Miocene strata in the Netherlands. WarmingUP GOO TNO Utrecht.

Kariuki, P. C., & Van der Meer, F. (2004). A unified swelling potential index for expansive soils. *Engineering Geology, 72*, 1–8.

Koenen, M., & Griffioen, J. (2014). Mineralogical and geochemical characterization of the Boom Clay in the Netherlands. OPERA-PU-TNO521-1.

Koenen, M., & Griffioen, J. (2016). Characterisation of the geochemical heterogeneity of the Rupel Clay Member in the Netherlands. *Netherlands Journal of Geosciences, 95*(2), 269–281. https://doi.org/10.1017/njg.2016.6

Li, J., Mitra, S., & Qi, J. (2020). Seismic analysis of polygonal fault systems in the Great South Basin, New Zealand. *Marine and Petroleum Geology, 111*, 638–649. https://doi.org/10.1016/j.marpetgeo.2019.08.052

Lonergan, L., Cartwright, J., & Jolly, R. (1998a). The geometry of polygonal fault systems in Tertiary mudrocks of the North Sea. *Journal of Structural Geology, 20*, 529–548. https://doi.org/10.1016/s0191-8141(97)00113-2

Lonergan, L., Cartwright, J., Laver, R., & Staffurth, J. (1998b). Polygonal faulting in the Tertiary of the central North Sea: Implications for reservoir geology. *Geological Society, London, Special Publications, 127*, 191–207. https://doi.org/10.1144/gsl.sp.1998.127.01.14

Lopez-Quiros, A., Sanchez-Navas, A., Nieto, F., & Escutia, C. (2020). New insights into the nature of glauconite. *American Mineralogist, 105*, 674–686. https://doi.org/10.2138/am-2020-7341

Mäder, U. (2009). Reference pore water for the Opalinus Clay and “Brown Dogger” for the provisional safety analysis in the framework of the sectoral plan – interim results (SGT-ZE). NAGRA Arbeitsbericht (2009), 1–45.

Munsterman, D. K., Donders, T. H., Houben, A. J. P., Ten Veen, J. H., & Wesselingh, F. P. (2025). Paleogene–Neogene. In *Geology of the Netherlands* (pp. 293–332). https://doi.org/10.5117/9789463728362_ch09

Nagra. (2024). Post-Closure Safety Report (NTB 24-10 Rev. 1). https://www.drbg.ch/rbg-gtl/zentrale-referenzberichte/post-closure-safety-report-ntb-24-10

Nelskamp, S., Verweij, J. M., & Witmans, N. (2012). The role of salt tectonics and overburden in the generation of overpressure in the Dutch North Sea area. *Netherlands Journal of Geosciences, 91*(4), 517–534.

Paul C. Rizzo Associates, Inc. (2013). Preliminary ground investigation report project KCB2 Borssele, The Netherlands (PGIR-for-COVRA-Complete).

Pytte, A. M., & Reynolds, R. C. (1989). The thermal transformation of smectite to illite. In N. D. Naeser & T. H. McCulloh (Eds.), *Thermal History of Sedimentary Basins* (pp. xx–xx). Springer. https://doi.org/10.1007/978-1-4612-3492-0_8

Schlumberger. (2009). Log interpretation chart (2009 Edition).

Seebeck, H., Tenthorey, E., Consoli, C., & Nicol, A. (2015). Polygonal faulting and seal integrity in the Bonaparte Basin, Australia. *Marine and Petroleum Geology, 60*, 120–135. https://doi.org/10.1016/j.marpetgeo.2014.10.012

Simmelink, H. J., Heidema, A. H., Hoogendoorn, A., & Pagnier, H. J. M. (1996). Project ‘CAR’ – Fase 1, Kartering slecht-doorlatende laagpakketten van Tertiaire formaties. RGD rapport GB 2514.

Sun, Q., Wu, S., Lü, F., & Yuan, S. (2010). Polygonal faults and their implications for hydrocarbon reservoirs in the southern Qiongdongnan Basin, South China Sea. *Journal of Asian Earth Sciences, 39*, 470–479. https://doi.org/10.1016/j.jseaes.2010.04.002

Ten Veen, J., Verweij, H., Donders, T., Geel, K., De Bruin, G., Munsterman, D., Verreussel, R., Daza Cajigal, V., Harding, R., & Cremer, H. (2013). Anatomy of the Cenozoic Eridanos Delta hydrocarbon system. TNO report TNO2013R10060, 217p.

Ten Veen, J. H., Vis, G.-J., De Jager, J., & Wong, T. E. (2025). Geology of the Netherlands (2nd ed.). Amsterdam University Press. https://doi.org/10.5117/9789463728362

Tewksbury, B. J., Hogan, J. P., Kattenhorn, S. A., Mehrtens, C. J., & Tarabees, E. A. (2014). Polygonal faults in chalk: Insights from extensive exposures of the Khoman Formation, Western Desert, Egypt. *Geology, 42*, 479–482. https://doi.org/10.1130/g35362.1

TNO. (2015). Integrated pressure information system for the onshore and offshore Netherlands. Final report. R10056.

Turrini, L., Jackson, C. A.-L., & Thompson, P. (2017). Seal rock deformation by polygonal faulting, offshore Uruguay. *Marine and Petroleum Geology, 86*, 892–907. https://doi.org/10.1016/j.marpetgeo.2017.06.038

Vandenberghe, N., De Craen, M., & Wouters, L. (2014). The Boom Clay geology, from sedimentation to present-day occurrence. A review. *Memoirs of the Geological Survey of Belgium, 60*, 76 p.

Velayatham, T., Holford, S. P., Bunch, M. A., & King, R. C. (2021). Fault controlled focused fluid flow in the Ceduna Sub-Basin, offshore South Australia; Evidence from 3D seismic reflection data. *Marine and Petroleum Geology, 127*, 104813. https://doi.org/10.1016/j.marpetgeo.2020.104813

Verhoef, E., Neeft, E., Chapman, N., & McCombie, C. (2017). Summary OPERA safety case. www.covra.nl

Veschuren, M. (2019). Outcrop evidence of polygonal faulting in Ypresian marine clays (Southern North Sea Basin) leads to new synthesis. *Marine Geology, 413*, 85–98.

Verweij, H., & Hegen, D. (2015). Integrated pressure information system for the onshore and offshore Netherlands, Final report. TNO report TNO2015R10056, 83 p.

Verweij, H., Nelskamp, S., Valstar, J., & Govaerts, J. (2016b). Definition of the future boundary conditions for the near-field model*2. OPERA-PU-TNO421*2.

Verweij, H., Vis, G.-J., & Imberechts, E. (2016a). Spatial variation in porosity and permeability of the Rupel Clay Member in the Netherlands. *Netherlands Journal of Geosciences, 95*(2), 253–268. https://doi.org/10.1017/njg.2016.2

Vis, G.-J., & Verweij, J. M. (2014). Geological and geohydrological characterization of the Boom Clay and its overburden. OPERA-PU-TNO411.

Vis, G.-J., Verweij, H., & Koenen, M. (2016). The Rupel Clay Member in the Netherlands: Towards a comprehensive understanding of its geometry and depositional environment. *Netherlands Journal of Geosciences, 95*(3), 221–251.

Watterson, J., Walsh, J., Nicol, A., Nell, P. A. R., & Bretan, P. G. (2000). Geometry and origin of a polygonal fault system. *Journal of the Geological Society, 157*, 151–162. https://doi.org/10.1144/jgs.157.1.151

Wemaere, I., Marivoet, S., & Labat, S. (2008). Hydraulic conductivity variability of the Boom Clay in north-east Belgium based on four core drilled boreholes. *Physics and Chemistry of the Earth, 33*, S24–S36.

Winthaegen, P. L. A., & Verweij, J. M. (2003). Estimating regional pore pressure distribution using 3D seismic velocities in the Dutch Central North Sea Graben. *Journal of Geochemical Exploration, 78–79*, 203–207.

Wiseall, A. C., Graham, S., Zihms, S., Harrington, J., Cuss, R., Gregory, S., & Shaw, R. (2015). Properties and behaviour of the Boom Clay formation within a Dutch repository concept. OPERA-PU-BGS615.

Wu, S. G., Sun, Q. L., Wu, T. Y., Yuan, S. Q., Ma, Y. B., & Yao, G. H. (2009). Polygonal fault and oil-gas accumulation in deep-water area of Qiongdongnan Basin. *Acta Petrolei Sinica, 30*, 22–26, 32. https://doi.org/10.7623/syxb200901005

Xia, Y., Yang, J., Chen, Y., Lu, S., Wang, M., Deng, S., Yao, Z., & Lu, M. (2022). A review of the global polygonal faults: Are they playing a big role in fluid migration? *Frontiers in Earth Science, 9*, 786915. https://doi.org/10.3389/feart.2021.786915

Yang, Y., & Aplin, A. C. (2004). Definition and practical application of mudstone porosity–effective stress relationships. *Petroleum Geoscience, 10*, 153–162.

Yang, Y., & Aplin, A. C. (2010). A permeability–porosity relationship for mudstones. *Marine and Petroleum Geology, 27*, 1692–1697.

Appendix A – H

Appendix A

Appendix A – Overview of publications on Paleogene clays

Appendix\Appendix A_Overview of publications on Paleogene clays.xlsx

Appendix B

Appendix B - Top, Base and Thickness maps

Appendix\Appendix B_Top, Base and Thickness maps

Appendix C

Appendix C – Petrophysical and mineralogical core and log data

Appendix\Appendix C_Petrophysical and mineralogical core and log data.xlsx

Appendix D

Appendix D – Maps of petrophysical and mineralogical results

Appendix\Appendix D_Maps of petrophysical and mineralogical results

Appendix E

Appendix E – High resolution figures seismic attributes

Appendix\Appendix E_High resolution figures seismic attributes

Appendix F

Appendix F - Maps of gas shows

Appendix\Appendix F_Maps of gas shows

Appendix G

Appendix G – Maps of drilling hazards

Appendix\Appendix G_Maps of drilling hazards

Appendix H

Appendix H - GIS project

Appendix\Appendix H - GIS Project of the project results, readme and shape file definitions

Energy & Materials Transition

Princetonlaan 6
3584 CB Utrecht
www.tno.nl

TNO innovation for life